

2016

Quantitative Analysis of Periodic Breathing and Very Long Apnea in Preterm Infants.

Mary A. Mohr
College of William and Mary

Follow this and additional works at: <https://scholarworks.wm.edu/etd>



Part of the [Physics Commons](#)

Recommended Citation

Mohr, Mary A., "Quantitative Analysis of Periodic Breathing and Very Long Apnea in Preterm Infants." (2016). *Dissertations, Theses, and Masters Projects*. Paper 1593092111.
<https://dx.doi.org/doi:10.21220/m2-njkk-9v07>

This Dissertation is brought to you for free and open access by the Theses, Dissertations, & Master Projects at W&M ScholarWorks. It has been accepted for inclusion in Dissertations, Theses, and Masters Projects by an authorized administrator of W&M ScholarWorks. For more information, please contact scholarworks@wm.edu.

**Quantitative Analysis of Periodic Breathing and Very Long Apnea in Preterm
Infants**

Mary A. Mohr

Grand Island, New York

**Master of Science, The College of William and Mary, 2012
Bachelor of Science, University at Buffalo, 2010
Associate in Science, Niagara County Community College, 2008**

**A Dissertation presented to the Graduate Faculty
of the College of William and Mary in Candidacy for the Degree of
Doctor of Philosophy**

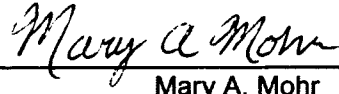
Department of Physics

**The College of William and Mary
January, 2016**

APPROVAL PAGE

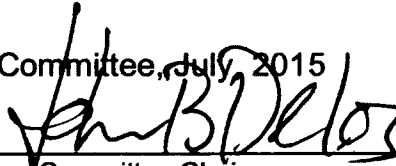
This Dissertation is submitted in partial fulfillment of
the requirements for the degree of

Doctor of Philosophy



Mary A. Mohr

Approved by the Committee, July, 2015

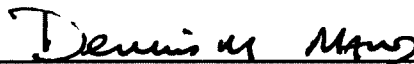


Committee Chair

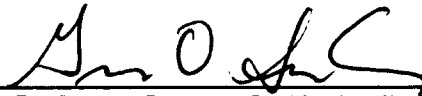
Professor John Delos, Physics
The College of William and Mary



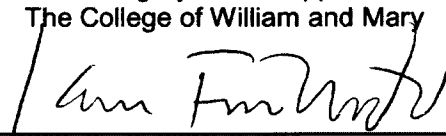
Professor William Cooke, Physics
The College of William and Mary



CSX Professor Dennis Manos, Physics and Applied Science
The College of William and Mary



Professor Gregory Smith, Applied Science
The College of William and Mary



Professor Karen Fairchild, Pediatrics
University of Virginia

COMPLIANCE PAGE

Research approved by

Protection of Human Subjects Committee

Protocol number(s): PHSC-2012-05-09-7958-jbdelo

Date(s) of approval: May 9, 2012

ABSTRACT

Electronic signals from bedside monitors in University of Virginia's Neonatal Intensive Care Unit (NICU) are routinely collected and stored. The overall goal of our research is predictive monitoring: we seek patterns in signals that give early warning of impending pathology. This work focuses on apnea (pauses in regular respiration), and on periodic breathing (regular cycles of breathing and apnea).

Our examination of apnea events revealed a disturbing number of cases in which the cessation of breathing lasted at least 60 seconds. These observations were validated, clinical correlations of these events were identified, and a theory was developed that partially explains how they occur.

Periodic breathing in neonates is a normal developmental phenomenon. It arises when there is instability in the respiratory control system. A mathematical model of periodic breathing was developed to analyze the stability of the control system in infants. Periodic breathing has long been thought to be benign, however, exaggerated durations of periodic breathing may be an indicator of pathology. Characterization of periodic breathing has previously been limited to short monitoring times in small numbers of infants. An automated system for measurement and characterization of periodic breathing was developed and applied to 5 years of data from the NICU. The amount of periodic breathing that infants had was found to increase with gestational age (up to 32 weeks). Also, times of excessive periodic breathing were recorded and clinical correlations were sought. A significant increase in periodic breathing in the 24 hours before diagnosis of necrotizing enterocolitis was found.

TABLE OF CONTENTS

Acknowledgements	ii
List of Tables	iii
List of Figures	iv
Chapter 1. Introduction and Collection of Data	1
Chapter 2. Very Long Apnea Events	16
Chapter 3. Wavelet Detection of Periodic Breathing	52
Chapter 4. A Model of Periodic Breathing	68
Chapter 5. Clinical Correlates of Excessive Periodic Breathing	95
Chapter 6. Future Directions	104
Appendix A Very Long Apnea data	107
Appendix B Periodic breathing data	108
References	111

ACKNOWLEDGEMENTS

I am sincerely grateful to my advisor, Dr. John Delos, for his guidance, counsel, and encouragement. It has been a great pleasure to be his Ph.D. student. His enthusiasm is a source of inspiration.

I wish to thank Dr. Karen Fairchild, Dr. Douglas Lake, Dr. Randall Moorman, Dr. John Kattwinkel, Dr. Robert Sinkin, and Dr. Manisha Patel for all that I learned from them. They made my introduction to clinical research truly enjoyable.

I owe my thanks to Dr. William Cooke, Dr. Dennis Manos, and Dr. Gregory Smith for their interest, insights, and penetrating questions. I am grateful for their willingness to review this dissertation.

This work was performed in part using the SciClone computational facilities at the College of William and Mary which were provided with the assistance of the National Science Foundation, the Virginia Port Authority, Sun Microsystems, and Virginia's Commonwealth Technology Research Fund. My thanks to Eric Walters and the rest of the SciClone staff for their patience, instruction, and help in managing the large amounts of data that made this work possible.

LIST OF TABLES

1. Characteristics of VLBW infants with and without validated VLA events	26
2. Clinical conditions in infants with VLAs	29
3. Apnea rates	30
4. Fits and correlation coefficients	36
5. Initial conditions and constants	46
6. Contingency table from validation of wavelet transformation analysis	64
7. Symbols used in the periodic breathing model	72
8. Values for partial pressures of gases in air and body used in model	74
9. Parameter values for oxygen dissociation	76
10. Time delays	83
11. Change in loop gain	93
12. Parameter values for loop gain analysis	94
13. <i>Clinical characteristics of infants with and without excessive periodic breathing</i>	98
14. Clinical events near the time of excessive periodic breathing	99
15. Infant IDs, start times, and durations of Very Long Apneas	107
16. Mean percent of time in periodic breathing by gestational age and postmenstrual age	108
17. Infant IDs and diagnosis times for infants with late onset sepsis	109
18. Infant IDs and diagnosis times for infants with necrotizing enterocolitis	110

LIST OF FIGURES

1. The EKG signal	8
2. The chest impedance	9
3. The pulse oximetry signal	9
4. Vital signals during an apnea event	11
5. An example of a very long apnea (VLA)	19
6. ABD tag starting early	20
7. ABD tag with low frequency fluctuations	20
8. Apnea and hypopnea combination	21
9. One ABD tag for two separate events	21
10. ABD tag with uninterpretable signal	22
11. Number of VLA events per infant	25
12. VLAs by gestational age and by chronological age	27
13. Respiratory support during VLAs	28
14. Bradycardia and apnea alarm histograms	32
15. Slow fall in heart rate and oxygen during VLAs	33
16. Methods for measuring severity of apneas	35
17. Oxygen falling in two stages	45
18. Wavelets for detecting periodic breathing	58
19. Wavelet coefficients at different ratios	59
20. Wavelet transformation of probability of apnea signal	61
21. Maximum value of periodic breathing index for clinician identified vs. no clinician identified periodic breathing	63
22. Examples of periodic breathing and clustered apnea	65

23. A model of periodic breathing	73
24. Calculated dissociation curves for oxygen	77
25. Lung compartment	79
26. Body tissue compartment	81
27. Brain compartment	82
28. Oscillatory behavior in model	28
29. Infants with data available for analysis and with periodic breathing detected	96
30. Mean percent of time in periodic breathing by gestational age and postmenstrual age	97
31. Percent periodic breathing and number of ABD10s per day	97
32. Periodic breathing in SIDS infant	100
33. Periodic breathing before diagnosis of late onset sepsis	101
34. Periodic breathing before diagnosis of necrotizing enterocolitis	102

Chapter 1

Introduction and Collection of Data

The University of Virginia's (UVA's) neonatal intensive care unit (NICU) has been collecting and storing bedside monitor data and clinical information continuously since January 2009. This large dataset provides us with the opportunity to analyze apnea and periodic breathing in large numbers of infants. Our goal is to find new ways to use the data that is routinely measured to predict the future state of the patient. We have focused on periodic breathing and Very Long Apnea events.

In this chapter we describe the data that is collected and stored. In chapter 2 we discuss apnea events that lasted for over 60 seconds (Very Long Apnea events). We present a mathematical model to describe these events. We show that two differential equations govern how the oxygen saturation falls during an apnea event and that the rate of the fall of oxygen saturation is determined by four constants and initial conditions.

Chapters 3 through 5 focus on periodic breathing. A new method of detecting periodic breathing is presented in chapter 3. In chapter 4 the model used to describe the fall of oxygen saturation is expanded to describe periodic breathing. Periodic breathing has often been modelled in the past, Models of periodic breathing help us to understand why periodic breathing occurs. Fitting the model to individual patient may allow us to determine values of physiological

parameters which are used in the model. Knowledge of these values may allow us to discover how parameter values change in an infant during illness which is accompanied by periodic breathing. It may also help us to identify infants who are at risk because of abnormal values. In chapter 5 we show possible correlates of excessive periodic breathing. Up until this time periodic breathing had not been quantized in a large number of infants. Our first task therefore is to use the method of detecting periodic breathing that is presented in chapter 3 to detect periodic breathing in the entire dataset and establish what normal amounts of periodic breathing are. Once that has been done we are able to determine which infants had excessively high amounts of periodic breathing. We looked at how periodic breathing changed before illness was diagnosed to see if rising amounts of periodic breathing could be used to detect illness earlier.

Clinical data

The UVa NICU is a quaternary care unit that admits approximately 500 newborns per year, about half of them preterm and a quarter very low birth weight (<1500 grams). The data from bedside monitors (GE Medical, models Solar 8000M and I, and Dash 3000, GE Healthcare, Milwaukee) is collected and stored via a BedMaster central network server (Excel Medical, Jupiter, FL). The UVa NICU had 45 beds when collection of data began. Eight beds were added in December 2013.

The clinical information includes birthdates, gestational ages, birth weight, gender, demographic information, admission and discharge times, bed assignments, diagnosis dates, respiratory support, and other information documented by clinicians.

The bed assignment record is particularly important. The bedside monitor data is stored by bed, not by patient. In order to find data for a particular patient it is necessary to know what bed that patient was in. Whenever there is ambiguity in the bed assignments (e.g. two patients assigned to the same bed at the same time or data for a bed that has no patient assigned to it at that time) we are unable to use that data.

There are three different ages that are used to describe a neonate. The gestational age (GA) is measured in weeks starting from the first day of the mother's last menstrual period. While the infant is in the womb the gestational age is increasing but it becomes fixed when the infant is born. Here we always use GA to mean the age of the infant at the time of birth, since we are always referring to infants after birth. The chronological age is the age of the infant since birth. Sometimes the chronological age is given as "days of life". The postmenstrual age (PMA) is the gestational age plus the chronological age. An infant that was born at 32 weeks and is one week old has a gestational age of 32 weeks, a chronological age of 1 week, and a postmenstrual age of 33 weeks.

Premature infants are defined as infants born at less than 37 weeks gestational age. Another important factor is the birth weight. Infants who weigh

less than 1000 grams at birth are extremely low birth weight (ELBW) infants, while those who weigh less than 1500 grams are very low birth weight (VLBW) infants. 90% of infants born at 37 weeks GA (full term) are over 2500 grams (Oken et al. 2003).

Respiratory support

There are three main types of respiratory support. The most extreme is ventilation. Mechanical ventilation delivers air to the patient through an endotracheal tube. The tube is inserted into the infant's trachea (intubation) when the infant is put on mechanical ventilation and removed (extubation) when the infant is taken off the ventilator. Continuous positive airway pressure (CPAP) is less extreme than ventilation. CPAP helps an infant breathe by applying positive pressure to prevent airway closure. The next step in the progression is a nasal cannula (NC). A nasal cannula is a lightweight tube that attaches to the patient's nose. The nasal cannula delivers oxygen to the patient but does not help the patient to breathe. Supplemental oxygen may also be administered on any of the three types of support. The patient could also be breathing room air without assistance.

Diseases in the NICU

The diseases which are of greatest concern in the NICU are: sepsis, necrotizing enterocolitis, intraventricular hemorrhage, bronchopulmonary dysplasia, and retinopathy of prematurity.

Sepsis is a blood infection, typically bacterial, but also viral or fungal, which can be diagnosed by a blood test. Neonatal sepsis occurs in infants less than 90 days old. Early onset sepsis (infection before or during delivery) occurs in the first week of life, while late onset sepsis (infection after delivery) occurs in infants from day of life 8 to 89. Sepsis is diagnosed by a blood test. In a study in 2002 of 6215 VLBW infants, 21% developed late onset sepsis, these infants had longer NICU stays (mean length of stay: 79 vs 60 days) and a higher mortality rate (18% vs 7%) (Stoll et al. 2002). Often the immune response to sepsis can be as damaging as the infection itself. In our studies late onset sepsis (LOS) was defined as signs of sepsis after three days of birth, together with a positive blood culture and a minimum of five days antibiotic therapy.

Necrotizing enterocolitis (NEC) is a condition which involves tissue death in the intestines. Infants with NEC typically display immature intestinal lining, low perfusion, feeding intolerance, abdominal distention, and bloody stools (Neu, Walker 2011). NEC is diagnosed by an x-ray which reveals air in the intestines when NEC is present. 1-5% of all infants admitted to the NICU develop NEC and 7-14% of VLBW infants are affected (Schnabl et al. 2008). NEC typically appears in the first three months of life, especially in ELBW infants born at less than 28

weeks GA (Schnabl et al. 2008). The mortality rate associated with NEC is 20 to 30% (Neu, Walker 2011).

Intraventricular hemorrhage (IVH) is bleeding into the brain ventricles. IVH is classified as grade I, II, III, or IV. Grades III and IV are defined as severe IVH. Bronchopulmonary dysplasia (BPD), abnormal growth of lung tissue, is a chronic respiratory condition which primarily affects infants born at less than 28 weeks GA (Strueby, Thebaud 2014). Infants were defined as having BPD if they required supplemental oxygen at 36 weeks PMA. Retinopathy of prematurity (ROP) affects the infant's eyes and can cause blindness. ROP can be caused when oxygen levels are too high in neonates.

Bedside monitor data

The data collected from the bedside monitors falls into three categories: alarms, waveform data, and vital sign data.

The time, duration, and type of each alarm is recorded. These alarms include bradycardia, desaturation, and apnea alarms. Bradycardia alarms activate when the heart rate falls below a set limit, typically 90 beats per minute, for at least 8 heartbeats. Desaturation alarms activate when the oxygen saturation falls beneath a set limit, typically 85%, for at least 5 seconds. These alarms continue to sound until the heart rate or oxygen saturation rise above the set limit. Apnea alarms activate after 15 seconds of no monitor-detected breaths and continue until the monitor detects a breath.

The waveform data consists of three channels of electrocardiogram (EKG) waveforms (sampled at 240 Hz), the chest impedance waveform (sampled at 60 Hz), and the pulse oximetry (photoplethysmographic) waveform (sampled at 120 Hz).

The beating of the heart causes electric currents to flow in the body. Three leads are attached to the patient to record the EKG. These leads are typically placed on the upper right chest, the upper left chest, and above the lower left hip. Lead I measures the EKG using the leads on the upper right and left chest. Lead II uses the leads on the right chest and above the left hip. Lead III uses the leads on the left chest and above the left hip. The 3 EKGs record different voltages because the leads are placed in different positions.

The basic pattern of the EKG is a p wave, which appears during depolarization before the atria contract, a QRS complex, which also occurs during depolarization before the ventricles contract, and a t wave, which occurs during repolarization as the ventricles recover after contraction (Figure 1). We are mainly concerned with detecting the R peaks. The distance between two R peaks is called the RR interval. The heart rate is calculated by taking $1/(\text{RR interval})$. We detect the R peaks and use them to calculate the instantaneous heart rate.

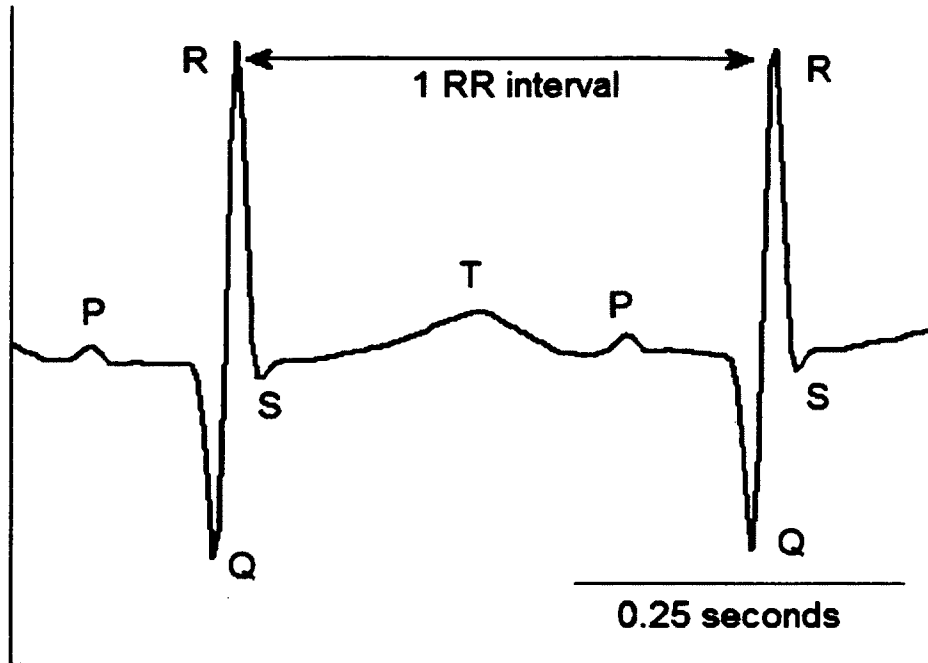


Figure 1: The EKG signal showing the p, q, r, s, and t waves.

The chest impedance is measured using the two leads that are placed across the chest for the EKG. A small high frequency (52.6 kHz, outside the EKG range) voltage is applied across the chest. This creates a current. The current is measured and the chest impedance is calculated by dividing the voltage that is applied by the current that is measured. The basic impedance, due to the skin, muscles, other tissues, blood, and the lead contacts is on the order of several hundred ohms. Air has poor conductivity. The impedance rises as the lungs fill with air and falls as the lungs empty (Figure 2). In this way the chest impedance signal shows the infant's breaths. Often the beating of the heart can also be seen in the chest impedance as the blood, which has high conductivity, is pumped in

and out of the heart. The chest impedance is the most important signal for our research. Unfortunately, this signal is full of artifact.

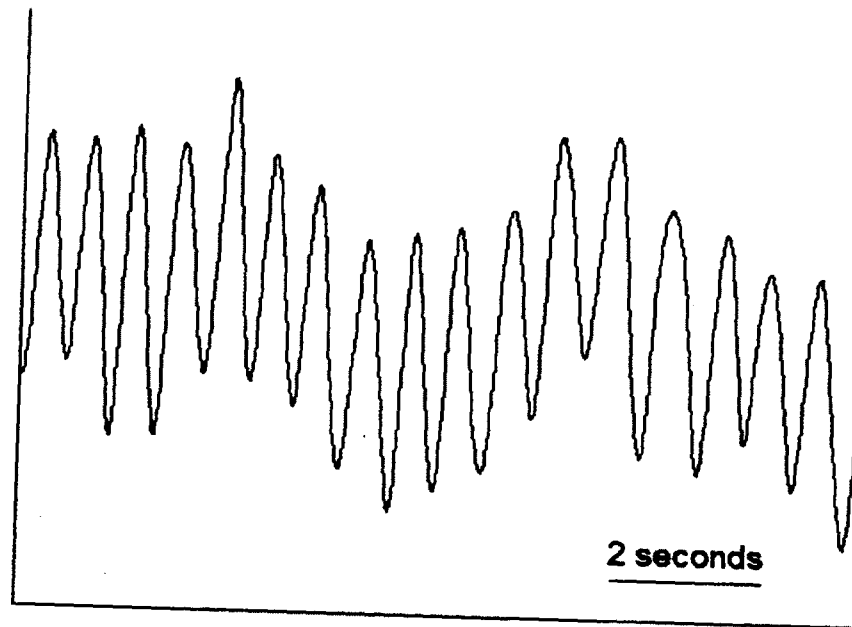


Figure 2: The chest impedance

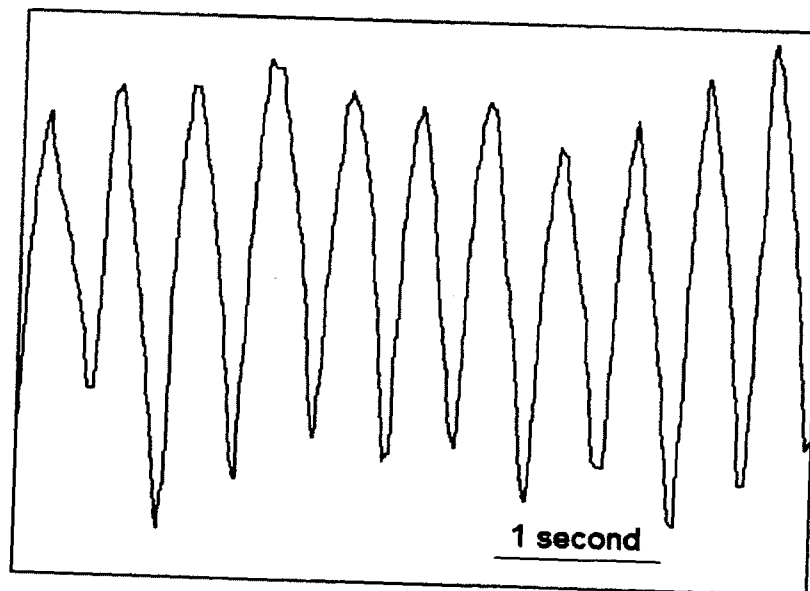


Figure 3: The pulse oximetry signal

The pulse oximetry (Figure 3) is measured using a probe which wraps around the infant's hand or foot. On one side is a light emitter and on the other side is a light detector. The probe emits two wavelengths of light (red and infrared) which are detected after passing through the hand or foot. The amount of light transmitted depends on the wavelength and also on the amount of oxygen in the hemoglobin. The signal is pulsed because the volume of blood in the arteries increases when the heart beats. The pulse oximetry signal recorded by the bedside monitors, and collected by the BedMaster system, is the measured amount of red light that is absorbed by the blood. Little information can be extracted from this signal. It gives a second measure of heart rate and also, when compared with the EKG, a measure of the propagation time of the pulse from the heart to the detector. Neither one of these measures are often used. However, this signal, together with the corresponding measurement from the infrared wavelength, is used to obtain the oxygen saturation of hemoglobin in the blood (SpO_2), as described below.

The vital sign data includes heart rate, oxygen saturation (percent of saturated hemoglobin), respiration rate, and a second measure of heart rate which is calculated from the pulse oximetry (Figure 4). All four signals are recorded at 0.5 Hz. The vital sign signals are all averages, typically of the previous eight seconds. The heart rate is calculated from the EKG signal. Because this is an average heart rate, if an instantaneous heart rate is needed it

must be obtained from the EKG signal. The additional heart rate from the pulse oximetry is measured using the frequency of the pulses in that signal.

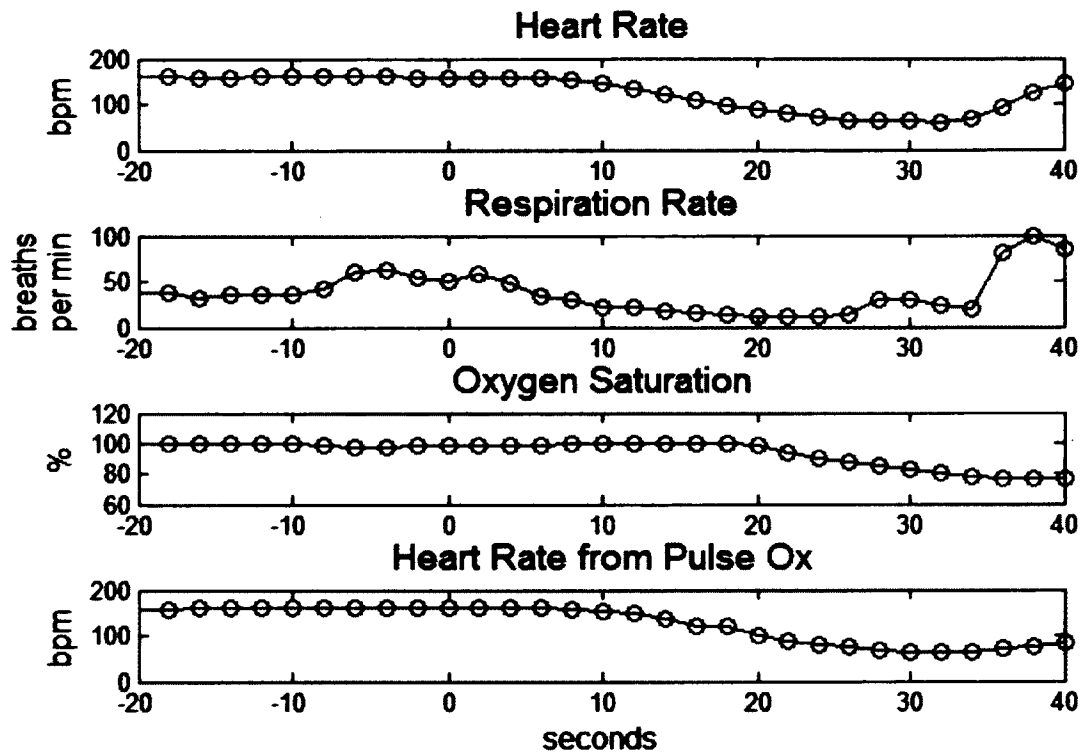


Figure 4: Vital signals during an apnea event (from 0 to 30 seconds).

Oxygen saturation is the percent of binding sites in the hemoglobin that are filled by oxygen molecules. The oxygen saturation is calculated from the absorption of red and infrared light measured by the pulse oximeter. When the hemoglobin is oxygenated it absorbs more red light, otherwise it absorbs more infrared light. The ratio of light absorbed by the two wavelengths is calculated and the monitor converts this to a measure of oxygen saturation. Unlike the pulse oximetry signal, the pulse does not appear in the oxygen saturation.

The respiration rate is derived from the chest impedance. This respiration rate is often incorrect. When the infant is breathing normally the fluctuations in the chest impedance signal due to the air flowing in and out of the lungs are much greater than those that are due to the blood being pumped in and out of the heart. But when the infant stops breathing the fluctuations due to the blood (cardiac artifact) are often mistaken by the monitor for breathing. This is more likely to happen when the heart rate falls during apnea. A slower heart rate allows more blood to fill the heart during each beat. The increased volume of blood in the heart results in greater changes in the chest impedance. These changes are more pronounced during apnea because the changes due to breathing are absent.

Apnea detection

A new algorithm for detecting central apnea was previously developed by Hoshik Lee and validated by clinicians at UVa (Lee et al. 2012). The algorithm filters the chest impedance signal (this includes removing the cardiac artifact), analyzes the residual fluctuations, and produces, at quarter-second intervals, the probability that the infant is having a central apnea event at that moment. Careful validation indicated that the algorithm agrees with expert opinion of clinicians in about 90% of central apnea events.

The algorithm uses the chest impedance and the EKG waveforms. A 4 minute window of the chest impedance is Fourier transformed to remove the

cardiac artifact. If the Fourier transform is taken with a time steps of equal length, then the cardiac artifact is a broad peak. Instead, the EKG (with the fewest missed beats) is used to determine the time between each heartbeat (the RR intervals). The chest impedance is resampled (with 30 points between every heartbeat) and the Fourier transform is taken with the unit of time equal to one RR interval. Now the cardiac artifact appears as isolated peaks at integer frequencies. The peaks are removed and the signal is transformed back. This signal is the single filtered chest impedance signal. Next, variations slower than 4 seconds are removed. These variations are often caused by the infant moving and are too slow to be due to breathing. This signal is normalized by dividing it by the envelope function of the original chest impedance signal over a 16 minutes centered on the 4 minute window. At this point we have the double filtered chest impedance signal.

The double filtered chest impedance signal is used for apnea detection. The standard deviation of the signal is taken over a 2 second window every quarter second. The standard deviation is high when the infant is breathing and low when the infant is not. We use the thresholding function

$$P = \frac{1}{1 + e^{12(\sigma - 0.44)}}$$

to convert from the standard deviation, σ , to the probability, P , that the infant is having an apnea event at that moment. The constants in the thresholding function were obtained through validation of hundreds of samples by clinicians at

UVa. Application of the thresholding function to the standard deviation signal gives the unprocessed probability of apnea signal. This signal has a minimum value of zero (when the infant is breathing) and a maximum value of one (during apnea). We define the apnea as starting when the signal crosses above 0.1 and ending when the signal crosses below 0.1. The signal is processed by removing all apnea events that are less than 2 seconds. All apnea events that are less than 5 seconds are also removed unless there is another apnea within 10 seconds of it. The resulting signal is called the processed probability of apnea signal.

This processed signal was used to detect all apnea events lasting for at least 10 seconds. Any apnea events that were separated by less than 3 seconds were joined together. The processed apnea signal was also used to detect all apnea events lasting for at least 10 seconds and accompanied by bradycardia and desaturation, presumably due to the apnea. The events are categorized as ABD_n (Apnea Bradycardia Desaturation), with “n” signifying the minimum length of cessation of breathing in seconds (e.g. ABD₆₀ means cessation of breathing was 60 seconds or more, and ABD₃₀₋₄₀ means cessation of breathing was between 30 and 40 seconds). The algorithm's threshold for bradycardia is heartrate <100 beats per minute, and for oxygen desaturation is SpO₂ <80%, for any duration. The heartrate must pass below the threshold within 50 seconds after the start of the apnea or before 25 seconds after the end of the apnea. The oxygen saturation must pass below the threshold within 55 seconds after the start of the apnea or before 38 seconds after the end. We remind the reader that

the heartrate and oxygen saturation are both averages roughly over the past 8 seconds. Additionally, the oxygen saturation is measured at the hand or foot and there is a delay due to the time it takes for the desaturated blood to travel from the lungs to where it is measured. For all infants in our database, we have recorded the date, time, and apnea duration of every ABD10 event (10 seconds or more).

We used this apnea detection method with 5 years of bedside monitor and clinical data to study very long apnea events and periodic breathing in a large number of infants.

Chapter 2

Very Long Apnea Events

Application of the apnea detection method to the bedside monitor data resulted in an unpleasantly large amount of ABD60 tags. We sought to determine whether these were truly cases where breathing ceased for over 60 seconds and, if so, to explain physiologically why this happens.

More than two decades ago, Southall, et al. reported prolonged apnea and bradycardia events in preterm infants in neonatal intensive care units (NICUs) (Southall et al. 1983). In their study of 14 babies observed for 24 hour periods, the authors were disturbed to report cessations of breathing as long as 213 seconds and that extended apnea events were often not detected or recorded. Present practices (Darnall et al. 1997, Finer et al. 2006, Martin, Abu-Shaweesh & Baird 2004) hold that any cessation of breathing longer than 10 seconds, if accompanied by bradycardia and oxygen desaturation, is an event that should be recorded (as is any apnea longer than 20 seconds regardless of bradycardia or desaturation). Most events last less than half a minute, either self-resolving or terminating when a caregiver stimulates the infant in response to a monitor alarm. Apnea events lasting over a minute may reflect abnormal physiology, impending illness, alarm failure, and/or failure of bedside clinicians to rescue infants from prolonged apneic spells.

Nearly all very low birthweight infants (VLBW, <1500 grams) experience apnea due to inherent brainstem and peripheral chemoreceptor immaturity, and pathologic processes such as sepsis, respiratory failure, intracranial hemorrhage, and seizures may increase the number or severity of apnea events. Apnea events may lead to tissue hypoxemia and, especially if prolonged, severe, or frequent, might contribute to adverse short and long-term outcomes, including neurodevelopmental impairment. Preventing or minimizing bradycardia and desaturation related to apnea should therefore be a priority in NICU care. Steps toward this goal include understanding physiologic associations with severe apnea, and optimizing monitor alarm systems and caregiver responses.

Much has changed in NICUs since the early reports of prolonged apnea events. Bedside monitors have better alarm systems, automated data collection and analysis is now possible, and continuous positive airway pressure (CPAP) and caffeine to treat apnea are nearly universal for VLBW infants. It may be surprising, then, that very long apnea events are still present in NICUs. We evaluated the ABD60 tags resulting from the apnea detection method to establish that apnea events lasting longer than 60 seconds are still occurring.

Long apnea in the UVa NICU

All waveform, vital sign, and alarm data from NICU bedside monitors were collected and stored for all 1263 patients in the UVa NICU from January 2009 to March 2011. For the current analysis, we focused on central apnea events

associated with bradycardia and desaturation. Our previously developed and validated algorithm for detecting central apnea (Lee et al. 2012), presented in chapter 2, tagged all detected central apnea events lasting for at least 10 seconds and associated with bradycardia and desaturation. In 782 of these events the apnea lasted for 60 seconds or longer. These events were evaluated to determine their validity. Those ABD60 events that survived the validation described below are called Very Long Apnea events (VLAs).

After validation we chose to study only very low birth weight infants (VLBW). Two reasons made this a sensible choice: VLBWs have respiratory support data recorded, while non-VLBWs do not, and there was only one non-VLBW infant who had a validated VLA.

Validation of ABD60 events in the UVa database

782 ABD60 events were tagged in 1263 infants (461 in VLBW infants when all waveform signals were available). All tags were subjected to a pre-validation process which uses the weighted apnea duration, defined as the area under the probability of apnea signal divided by the apnea duration, and the power in the breathing band to calculate the probability that the tag represents a true apnea event. 113 events failed this pre-validation (including 3 tags when the infant was being ventilated). An additional 105 tags had waveform data missing from the database. All 229 tags that either occurred when the infants was on a

ventilator, failed the pre-validation process, or had waveform data missing were excluded from the clinical validation.

553 ABD60 tags were subjected to clinical validation by four clinicians who are experts on interpretation of the signals. Clinicians assigned each tag to one of the following categories: definite ABD lasting at least 60 seconds (VLAs) (Figure 5), ABD lasting less than 60 seconds (Figure 6), low frequency fluctuations (the source of these fluctuations is unknown) (Figure 7), combination of apnea and hypopnea (slow or shallow breathing) (Figure 8), one ABD for multiple apnea events (Figure 9), uninterpretable signal (Figure 10), or no central apnea. All events categorized as VLAs were assigned a start and end time by the clinicians.

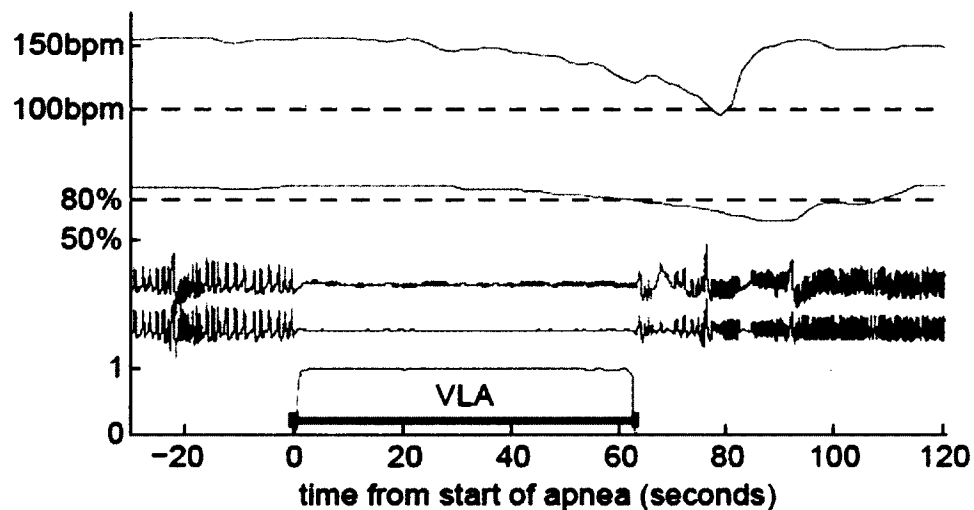


Figure 5: An example of a very long apnea (VLA). Shown are raw and processed electronic signals collected from bedside monitors. From top to bottom: heart rate from monitor, 100 beat per minute threshold for bradycardia, oxygen saturation and 80% threshold for desaturation, raw chest impedance, filtered chest impedance (removing cardiac artifact and slow fluctuation). Bottom curve is probability that the infant is having an apnea at each moment. This VLA lasts slightly more than 60 seconds. (Reproduced from Mohr et al. 2015b.)

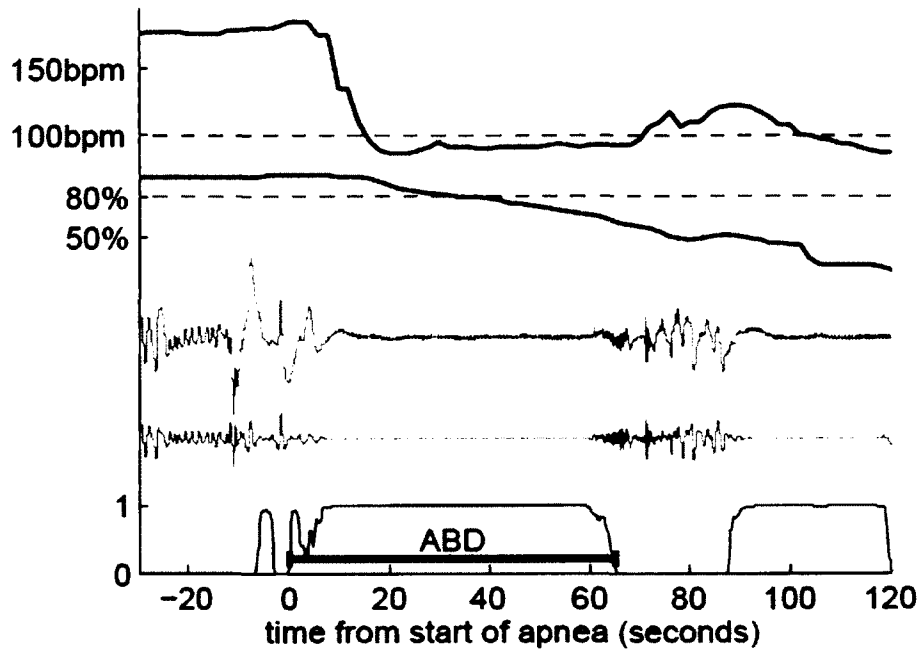


Figure 6: ABD tag starting early. This apnea lasts less than 60 seconds. Signals from top to bottom are: heart rate, oxygen saturation, raw chest impedance, filtered chest impedance, and probability of apnea.

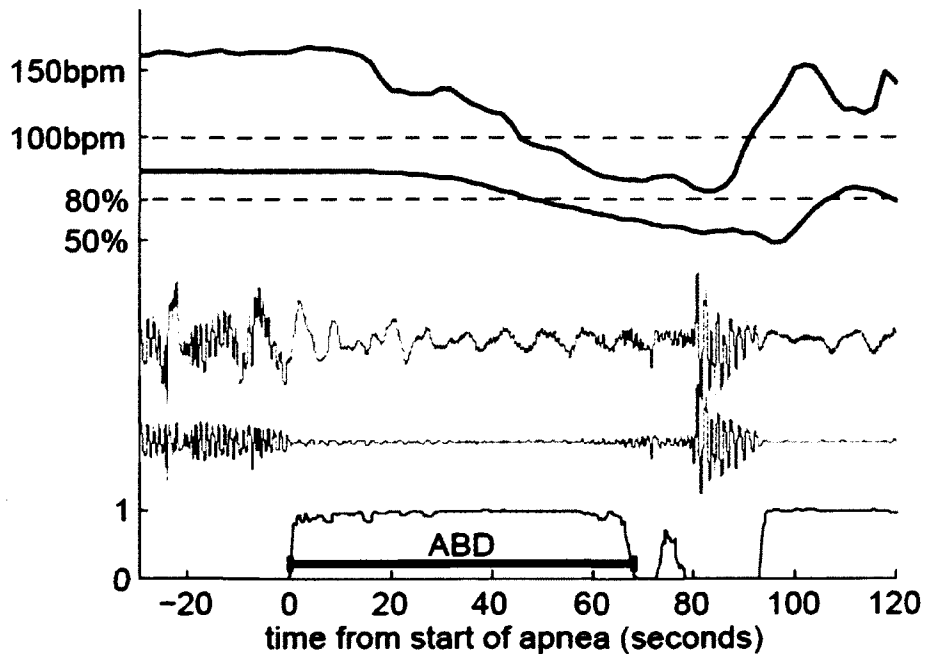


Figure 7: ABD tag with low frequency fluctuations in chest impedance. Signals from top to bottom are: heart rate, oxygen saturation, raw chest impedance, filtered chest impedance, and probability of apnea.

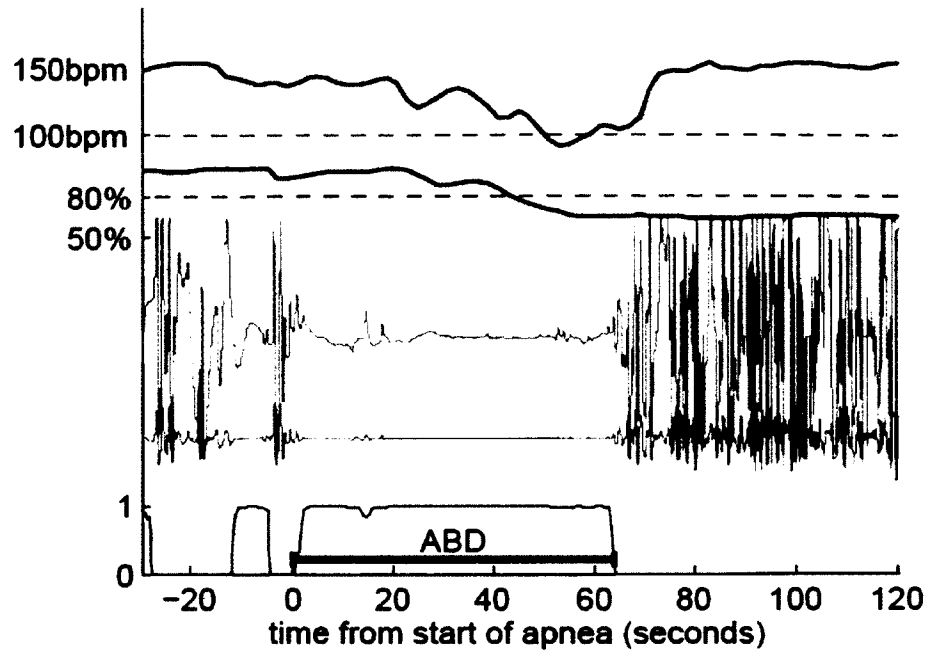


Figure 8: VLA with combination of apnea and hypopnea. Signals from top to bottom are: heart rate, oxygen saturation, raw chest impedance, filtered chest impedance, and probability of apnea. (Reproduced from Mohr et al. 2015b.)

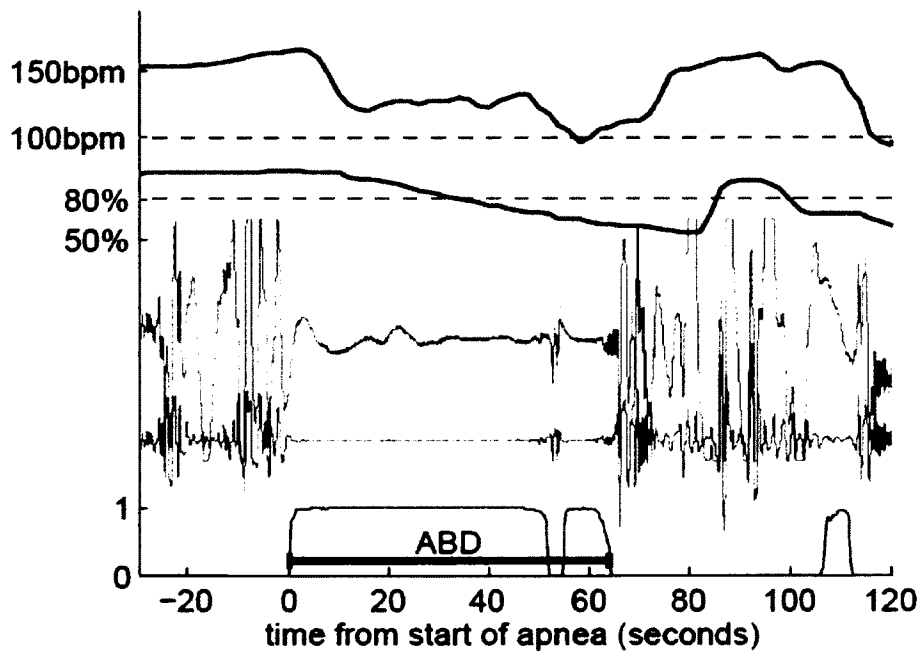


Figure 9: One ABD tag for two separate apnea events. Signals from top to bottom are: heart rate, oxygen saturation, raw chest impedance, filtered chest impedance, and probability of apnea.

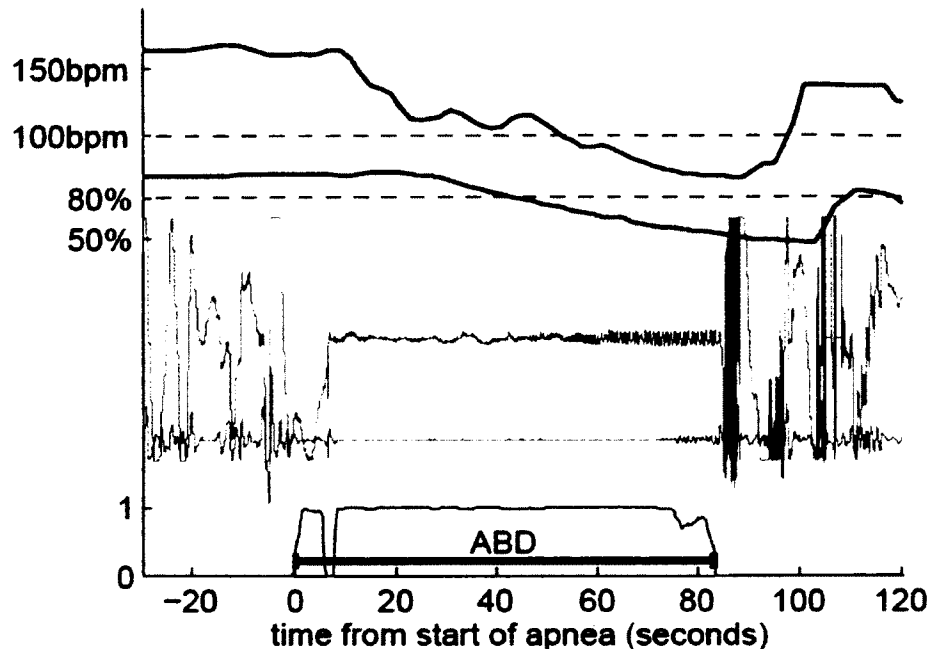


Figure 10: ABD tag with uninterpretable chest impedance signal before and after the apnea. Signals from top to bottom are: heart rate, oxygen saturation, raw chest impedance, filtered chest impedance, and probability of apnea.

The following conditions had to be met in order for a tag to qualify as VLA: the chest impedance had to be acceptably flat for at least 60 seconds; there could be no apparent breaths within the 60 seconds; the event must have been accompanied by any duration of bradycardia (<100bpm) and desaturation (< 80%); the cessation of breathing had to last at least 60 seconds; the filtered chest impedance could have no artifacts, no indication of shallow breaths, and no twitches in chest impedance which had an associated increase in heart rate; there could be no low frequency fluctuations for which there was any apparently related increase in heart rate; any episodes of increased heart rate could not be associated with a breath or low frequency fluctuations; there had to be acceptable breathing in the chest impedance signal before and after the event.

Samples were reviewed by four clinicians in groups of two. The two clinicians in each group validated events separately. If a sample was categorized as a VLA by one clinician and not the other, then all four reviewers discussed the sample until a consensus agreement was reached. Through this process, 90 events were categorized as VLAs. 86 of these occurred in 29 VLBW infants, 3 occurred in a single non-VLBW infant, and 1 occurred in an unidentified infant (no patient assigned to that bed at the time of the event). We focus our evaluation of VLAs on the 86 events that occurred in identified VLBW infants. This decision allowed us to include respiratory support data for all evaluated events, since only VLBW infants had respiratory support data available.

Our requirements for VLA were very stringent, because our goal was to show indisputably that ABD60 events do truly exist. Many tagged ABD60s that did not meet these requirements may still be true ABD60 events. Of the 461 ABD60 events in VLBW infants for which all waveform signals were available, 20 had poor and uninterpretable signals and 38 were recognized as apnea events of less than 60 seconds duration. These 58 events were excluded. The remaining 317 events can be considered “questionable” ABD60 events. We consider these “questionable” cases to be examples of failure of respiratory regulation lasting at least 60 seconds, but we do not include them in our category of indisputable VLAs. Using our stringent requirements we estimate that VLAs occur at a rate of 1 per 70 infant-days, while the estimate if we include questionable events is over four times larger, 1 per 16 infant-days.

Shorter apnea samples

We collected random samples of 10-20 second and 30-40 second ABD events. 100 ABD10-20s and 100 ABD30-40s were collected from infants who also had VLAs. The rate of fall of heart rate and oxygen saturation (SpO₂) during these shorter events were compared to the rates of fall during VLAs. 100 ABD10-20s and 100 ABD30-40s were also collected from infants who never had an ABD60 tag and whose post-menstrual age (PMA) at the time of the event was less than 34 weeks. These events were compared to the shorter events in VLA infants. An additional requirement was that the shorter ABDs did not occur during periodic breathing, as periodic breathing could affect pre-apnea heart rate and oxygen saturation.

Patient characteristics and clinical associations

As stated above, ABD60 events in 335 VLBW infants were subjected to the validation process (described previously). 86 events in 29 infants were determined to be Very Long Apnea events. The estimated frequency of these VLAs is 1 per 70 infant-days. The number of events per infant ranged from 1 to 19 (Figure 11).

In most respects, infants with VLAs were not significantly different from other VLBW infants (Table 1). Infants with VLA events had significantly longer NICU stays than those without, and their average gestational age was slightly lower ($p=0.09$) (Table 1). Over half of the VLA infants fell in the GA range of 25-

27 weeks (Figure 12a) and 84% of VLAs occurred less than 4 weeks from birth (Figure 12b). 79% of the VLAs occurred while infants were on continuous positive airway pressure (CPAP), usually with supplemental oxygen (Figure 13). All 29 infants were on caffeine therapy at some time during their NICU stay, one VLA occurred 4 days after caffeine was discontinued. Two infants had VLA on the day of birth, prior to caffeine being initiated. No VLA events occurred within 10 days of NICU discharge.

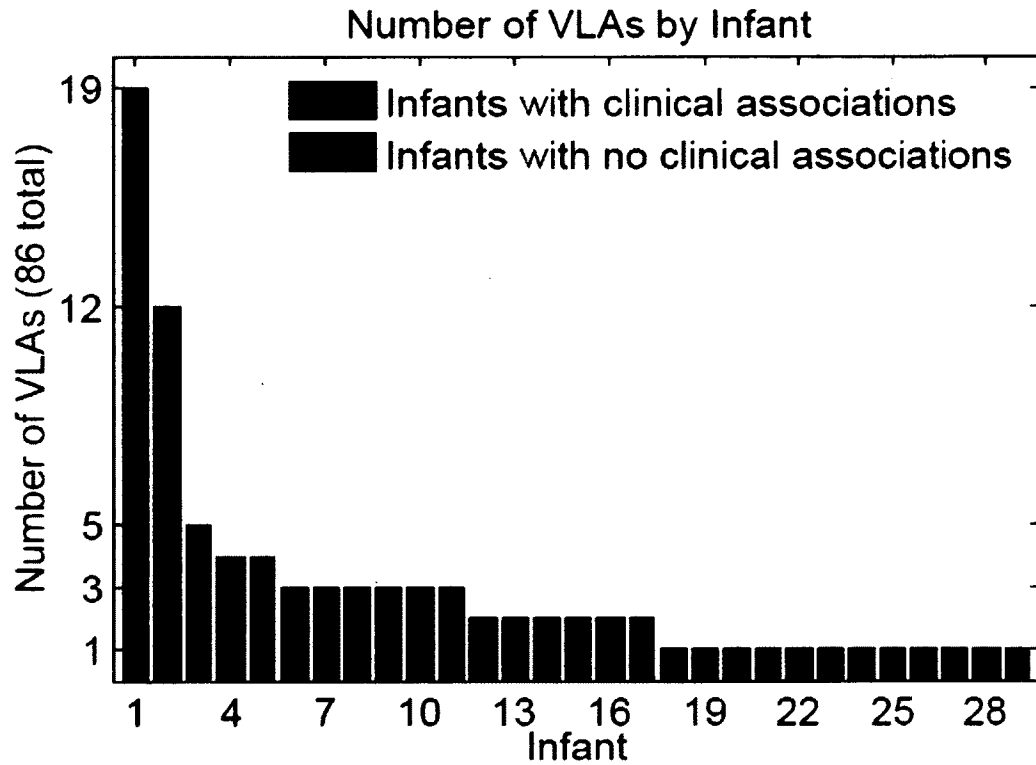


Figure 11: Number of VLA events per infant (Infant 1 had 19 events, and 29 infants had at least 1 event). (Reproduced from Mohr et al. 2015b.)

Table 1: Characteristics of VLBW Infants with and without validated VLA events
(Reproduced from Mohr et al. 2015b.)

	VLA (n=29)	No VLA (n=306)	P=
Gestational age (weeks)	26.5 ± 1.9	27.5 ± 3.1	0.09
Birth weight (grams)	952 ± 249	988 ± 299	0.53
ELBW	19 (66%)	150 (49%)	0.12
Male	14 (48%)	154 (50%)	0.85
Mechanical ventilation at any time	23 (79%)	214 (70%)	0.39
Death before NICU discharge	1 (3%)	31 (10%)	0.34
Length of NICU stay (days)	78 ± 27	63 ± 42	0.02

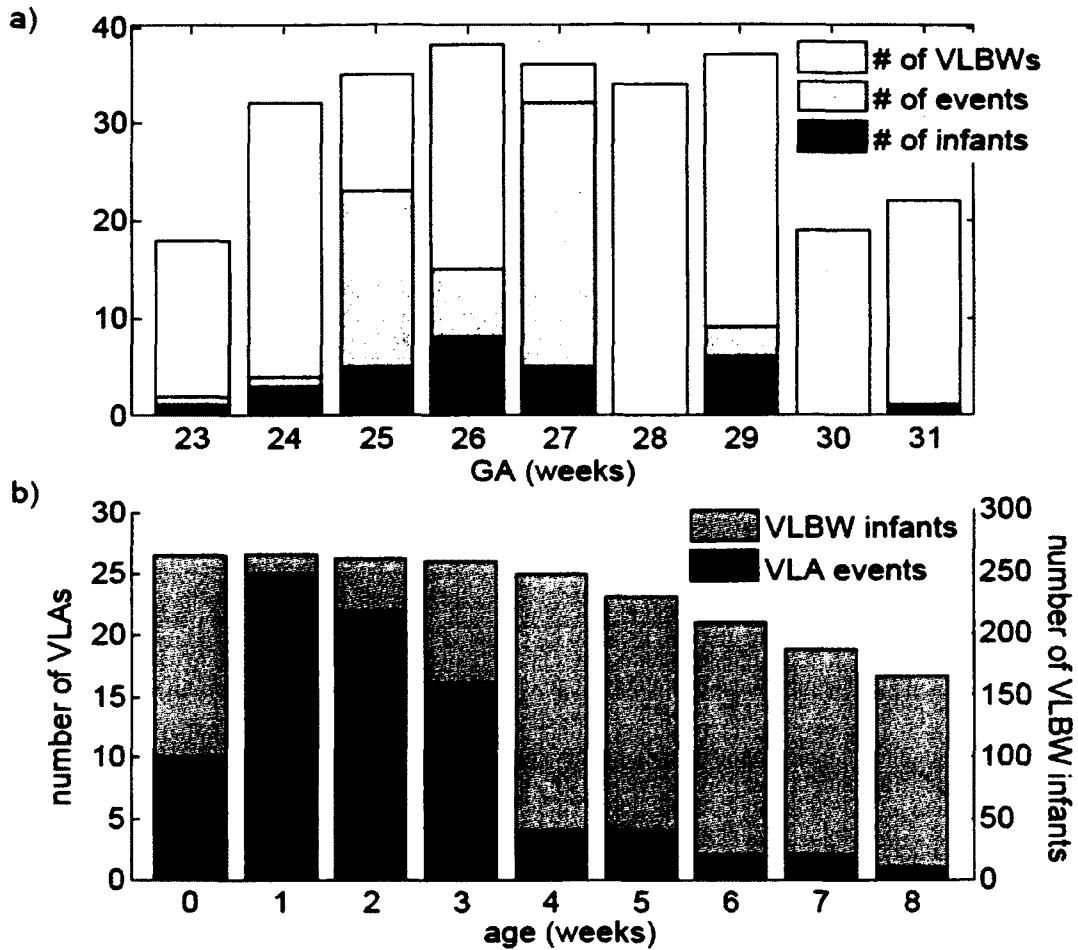


Figure 12: (a) Histogram of number of VLA events and number of VLA infants versus gestational age (GA) at birth. For comparison the number of infants versus GA for the entire population of Very Low Birth Weight (VLBW) infants in our database is also shown. For example, among 26-week GA infants, eight of the 37 VLBW infants had at least one event, and there were 15 total events. (b) Histogram of number of VLA events versus chronological age (CA) at time of event for those infants having one or more VLAs (left scale). For comparison the number of VLBW infants who were in the UVa NICU at that CA is also shown (right scale). For example, at one week of age, there were 25 VLAs among 266 VLBW infants. (Reproduced from Mohr et al. 2015b.)

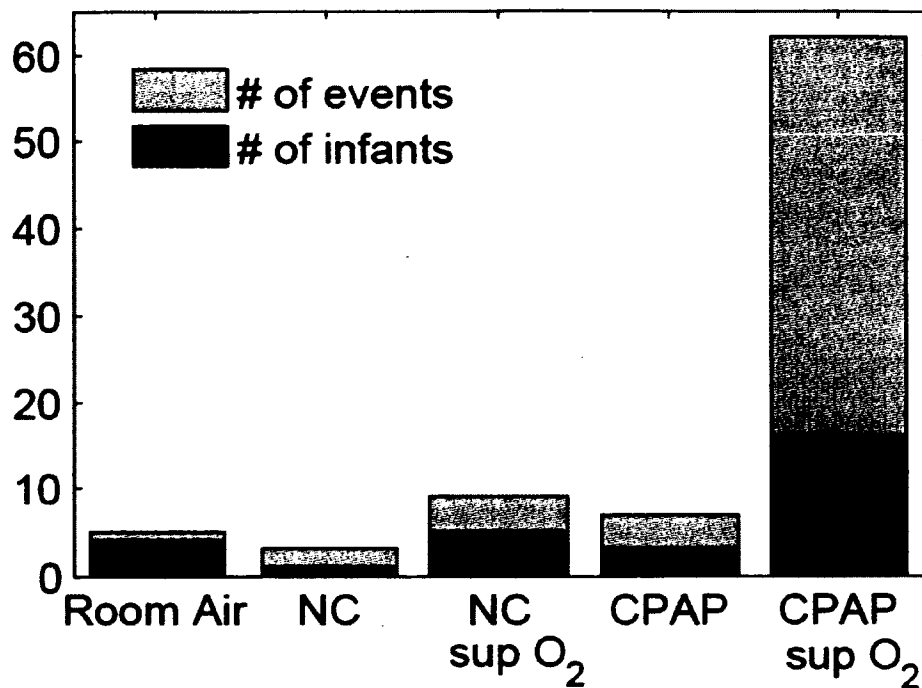


Figure 13: Histogram showing respiratory support of VLA infants at the times of their events. From left to right: room air, nasal cannula without supplemental oxygen, nasal cannula with supplemental oxygen, CPAP without supplemental oxygen, and CPAP with supplemental oxygen. Most VLA events occurred while infants were on CPAP with supplemental oxygen. (Reproduced from Mohr et al. 2015b.)

In 18 of the 29 infants with VLAs, medical record review identified clinical conditions (separate from prematurity which was present in all subjects) that were possibly associated with apnea (Table 2). Ten infants were receiving antibiotics at the time of the VLA, four were started on antibiotics within 24 hours of the VLA for suspected sepsis (although none had proven septicemia), seven were intubated within 12 hours of the VLA, and six had other conditions. The infant with the greatest number of events (nineteen) died suddenly and unexpectedly for unclear reasons. He was stable on full feeds, CPAP and caffeine at the time of death, and autopsy was declined. The other infant with a

large number of events (12 VLAs at 2-3 weeks of age) was on erythromycin for severe gastroesophageal reflux. No VLAs occurred beyond 18 days of age and he was discharged home at 78 days of age. We could see no systematic differences in the characteristics of the VLAs associated with these different clinical situations.

Table 2. Clinical conditions in infants with VLAs
(Reproduced from Mohr et al. 2015b.)

# of infants	Clinical association	GA	#VLAs	PMA
1	Died 48h after last VLA	27	19	28-32
1	Post-hemorrhagic hydrocephalus, ventricular tap performed prior to VLA cluster	26	3	31
1	Grade IV intraventricular hemorrhage	26	2	30
1	On prostaglandins for congenital heart disease	29	3	31
2	On medication for severe GE reflux	25	3-12	27-29
4	Antibiotics started for suspected sepsis within 24h of VLA	23-29	1-19	26-31
10	Receiving antibiotics at time of event	25-30	1-19	25-32
7	Intubated within 12h of VLA	23-29	1-4	24-31
11	None identified, other than prematurity	24-31	1-5	27-34

For the other 11 infants (38% of the VLA infants), we could not identify a clinical condition that appeared to be a cause or effect or to have an association

with the VLA. These 11 differ only slightly from the 18 with clinical associations. The infants without clinical associations had slightly higher GAs, but the difference was not significant ($p=0.16$). Not surprisingly, these 11 infants also had shorter stays in the NICU than the other 18 infants did ($p=0.02$). There were no differences in the rate of fall of heart rate and oxygen saturation between VLA infants with clinical associations and those without.

Table 3. Apnea rates
(Reproduced from Mohr et al. 2015b.)

Groups	number of ABD10 tags	number of infants	% of all VLBW babies	Tags per baby-day of data
Group I: Infants with Indisputable 60 second VLAs	6,617	29	9	4.29
Group N: Infants who Never had a ABD 60	6,300	199	59	1.52
Infants who never had a computer-detected ABD10 (included in Group N)	0	62	19	0
All VLBW Infants:	30,793	335	100	2.94

Apnea rates in study group and comparison group

The 29 infants who had VLAs formed our study group. All infants who never had an ABD60 tag formed our comparison group. The total numbers of ABD10 tags for the study group and the comparison group of VLBW infants are in Table 3. Infants who had VLAs also had many ABD10 events. The majority of

infants never had any ABD60 events; these infants also had a lower rate of ABD10 events.

Bedside monitor alarms in VLA events

Bedside monitor apnea alarms are designed to sound 15 seconds after cessation of breathing. Apnea alarms sounded in 66% of VLAs, but failed to do so in 34%. Bradycardia alarms activated in 57% of VLAs, and low oxygen alarms activated in 81%. At least one alarm activated in 97% of VLAs. The monitors use slightly different criteria than the apnea algorithm for bradycardia and desaturation, so it is not surprising that these alarms did not go off during all VLA events.

For the cases in which the bedside monitor sounded an apnea or bradycardia alarm, Figure 14 shows histograms of the time from the start of the computer-detected apnea to the alarm, and of the time from the alarm to the end of the detected apnea.

If the bedside apnea alarm sounded, it did so rather promptly, typically less than 25 seconds from the beginning of the computer-detected apnea. If the bedside bradycardia alarm sounded, it usually occurred long after the cessation of breathing (Figure 14), consistent with the slow fall of heart rate in these events. Shortly after the bradycardia alarm sounded (but frequently quite long after the apnea alarm), the apnea ended.

It appears that bedside caregivers respond quickly to bradycardia alarms, which are “crisis” alarms on the monitors in the UVa NICU (in contrast to apnea

“warning” alarms), but as a result of the slow fall of heart rate these alarms are delayed. More reliable apnea alarms, with fewer false negatives and false

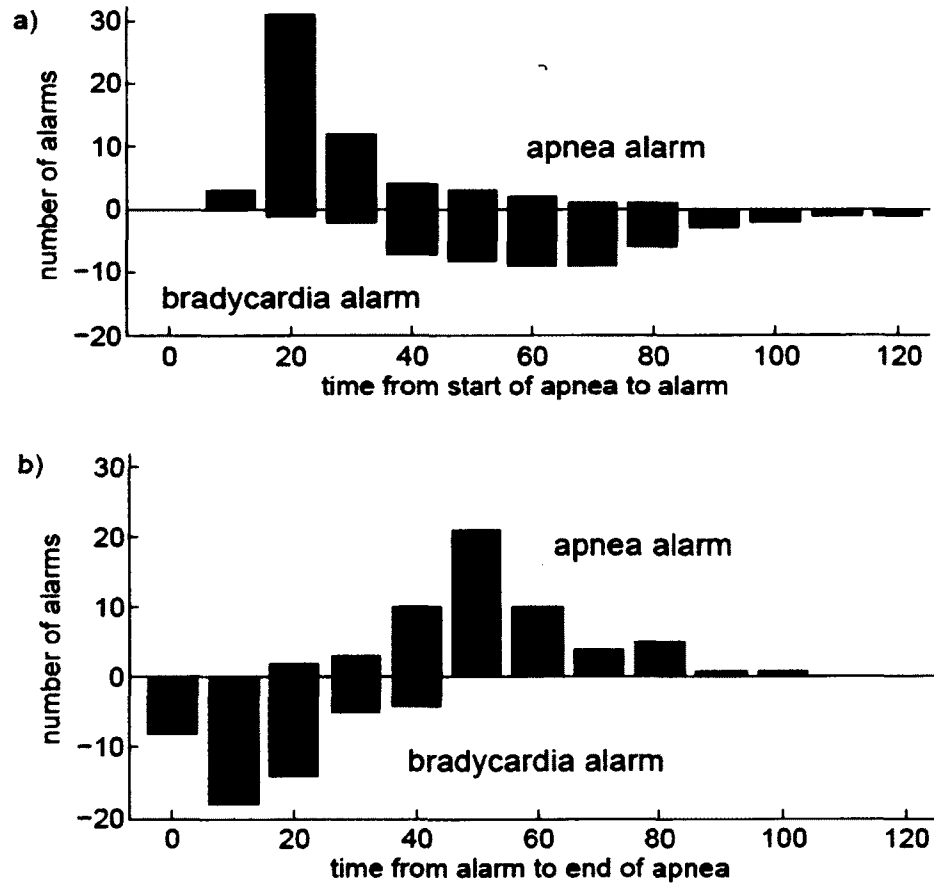


Figure 14: (a) Time from cessation of breathing to bedside apnea or bradycardia alarm, and (b) time from alarm to end of apnea for VLAs. If the apnea alarm sounds, it usually does so within about 20 seconds after the beginning of the apnea. In VLA events, the heart rate falls slowly, so the bradycardia alarm is much delayed, typically sounding 60 to 70 seconds after the apnea begins. Apneas usually end a short time after the bradycardia alarm. (Reproduced from Mohr et al. 2015b.)

positives, would be helpful to NICU personnel and might have a significant beneficial effect on the health of infants by reducing hypoxemia and bradycardia.

Short and long apnea events in VLA Infants

A striking characteristic of VLAs is that heart rate and oxygen saturation fall later and more slowly than they do during shorter ABD events. This can be seen in Figure 15.

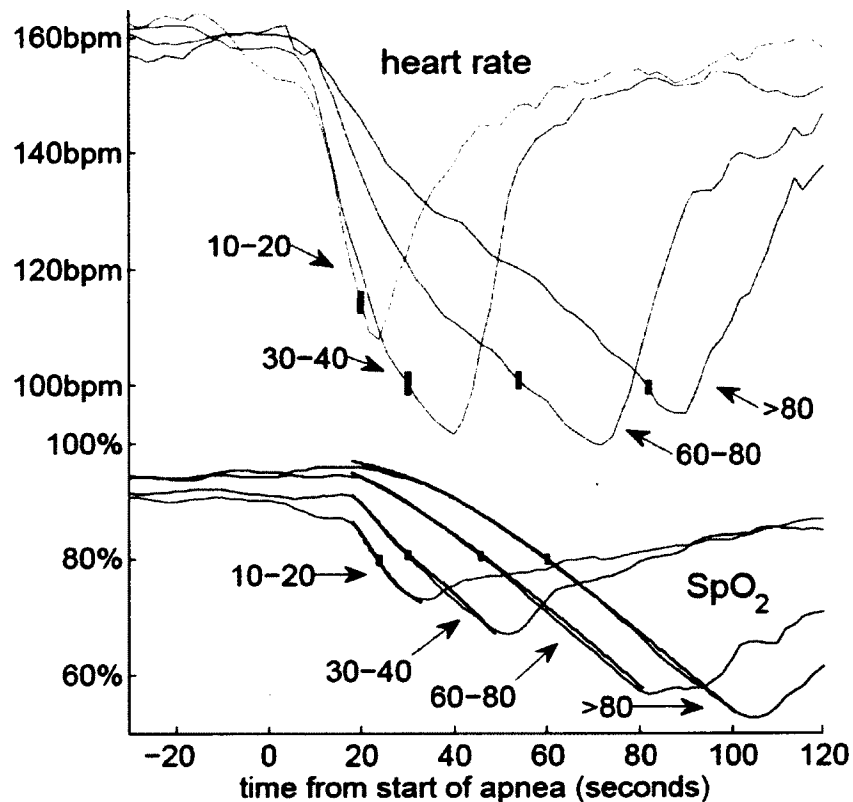


Figure 15: In VLAs oxygen saturation and heart rate fall slowly. We show the average heart rate and oxygen saturation (SpO_2) for all of the VLAs (ABD60-80, $n=46$, and ABD80, $n=40$). For the shorter events we took a random sample of ABD10-20 ($n=100$) and ABD30-40 ($n=100$) from this same group of infants. The start of the computer-detected apnea is $t=0$. The black curves, barely distinguishable from the observed SpO_2 curves, are based on the theory from equations 2.1 – 2.5 with constants given in Table 4. Vertical lines indicate ± 1 standard error of the mean. (Reproduced from Mohr et al. 2015b.)

100 ABD 10-20 and 100 ABD 30-40 events were randomly selected from infants who had VLAs. The events were chosen such that the infant's PMA was less than 31 weeks at the time of the event. The average of multiple events is plotted, and the standard error of the mean is marked. (The heart rate fell below 100 BPM and the oxygen saturation fell below 80% in every individual event. However, these thresholds were crossed at different times in different events, so the averages do not necessarily fall below the thresholds.)

Measures of severity

One difficulty in assessing the impact of a VLA arises from the slow fall of SpO₂. Because of this slow fall it is not clear that the duration of the event is a good measure of its severity.

Another measure that can be used to determine the severity of the VLA is the area between the SpO₂ curve and a chosen threshold. This area is related to the oxygen deficit in the blood. For example, if normal oxygen transport is M ml/minute, and the area between the SpO₂ curve and the baseline value is A %-minutes, then $M \cdot A / 100$ is the oxygen deficit resulting from the apnea. We can also make a similar measurement with heart rate.

The area measured depends upon the threshold that is chosen. Measures were made with two different thresholds in order to determine if the results were consistent. The first threshold was chosen to be the lesser of 92% or the measured pre-apnea baseline (PAB). The PAB was obtained by evaluating the

mean μ and standard deviation σ of SpO_2 over an interval prior to the apnea event, $PAB = \mu - 2\sigma$. The interval was chosen to be within 120 seconds of the beginning of the VLA, but not containing another desaturation with an area greater than 2%-minutes. An example is shown in Figure 16a, with an area of

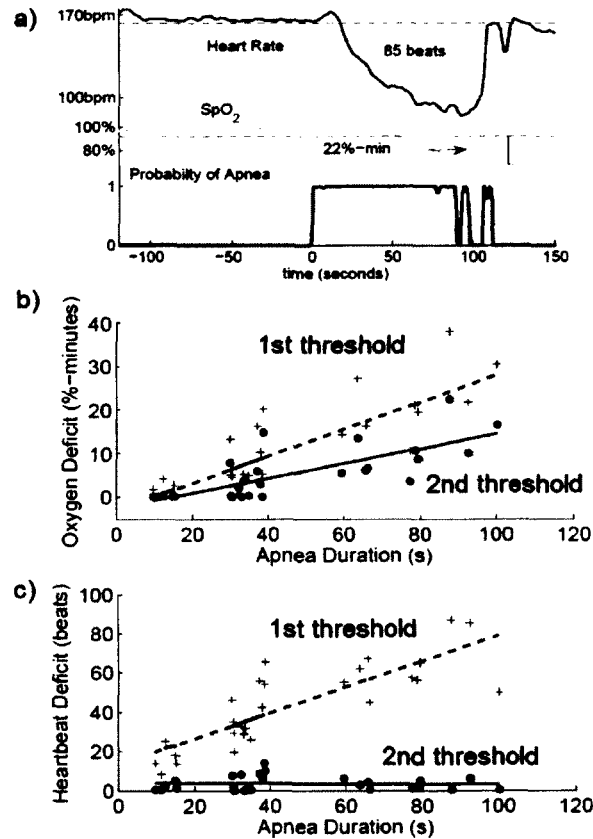


Figure 16: Methods for measuring severity of apneas. (a) For each signal, a baseline is chosen. For heart rate the mean minus two standard deviations in an interval before the apnea that contains no significant deceleration is chosen as a baseline. For SpO_2 the lower of a similar baseline or 92% is used. The areas between the chosen baseline and the signal are computed. In this case the VLA is followed by short events, and after reaching a minimum, SpO_2 rises and falls again. We include only the area up to the marked boundary, at the local max of SpO_2 . (b) Heartbeat deficit (HR) vs. apnea duration for one infant, with linear fits using the least squares method. (b) Oxygen deficit (O_2) vs. apnea duration. Linear fits and correlation coefficients are given in Table 4. (Reproduced from Mohr et al. 2015b.)

22 %-minutes. The second threshold was chosen to be 80%, the desaturation threshold in our ABD definition.

We choose to limit the impact of confounding variables by carrying out these measurements on data from one patient. We chose the patient who had the largest number of long apnea events. Random sets of ABD10-20 and ABD30-40 events from this infant were collected and the measurements were made on both long and short apnea events. The results of these measurements are shown in Figure 16b. The 80% threshold gives a slope that is about half of the slope for the first threshold, but in both cases the correlation coefficients are comparable (see Table 4).

Table 4. Fits and correlation coefficients between Duration (T) and Area (A)

	Linear fit	Correlation Coefficient
Oxygen, 1 st threshold	$A = 0.31T - 3.0$	0.81
Oxygen, 2 nd threshold	$A = 0.17T - 2.58$	0.75
Heartbeats, 1 st threshold	$A = 0.66T + 13.08$	0.82
Heartbeats, 2 nd threshold	$A = -0.0053T + 3.65$	-0.04

The depth and duration of an associated bradycardia are relevant measures of the severity of an apnea event, but again, an area measure is more appropriate. For each event, a baseline was chosen from the heart rate prior to the apnea. Again, two different thresholds were chosen and the results were compared. The first threshold is the mean minus two standard deviations over an interval within 120 seconds from the cessation of breathing, but not containing a drop of more than 10 beats per minute. The area between that baseline and the actual heart rate while the heart rate is below the baseline was calculated. This

area is the heartbeat deficit – the number of heartbeats that the infant would have had if its heart rate continued at the baseline value minus the actual number of beats. In Figure 16a this baseline is shown and the area below the baseline in this case amounts to a deficit of 85 beats. The second threshold was chosen to be 100bpm (the bradycardia threshold in our ABD definition).

The results of these measurements can be seen in Figure 16c. In this case there is a marked difference between the results from the two different thresholds. The 100bpm threshold shows no difference between long and short apnea events. This result is consistent with our observation that NICU personnel respond quickly to bradycardia alarms. In contrast the first threshold shows a greater heartbeat deficit in longer apnea events.

The graphs in Figures 16b and 16c show measures of the relative significance of VLAs vs. short apnea events. The roughly linear trend suggests that a 90 second apnea results in about three times the oxygen deficit and three times the heartbeat deficit of a 30 second apnea. (This fact is not obvious *a priori*, because heart rate and oxygen saturation decrease slowly in long apnea events.) Such deficits could be reduced by earlier and more accurate identification of apnea events.

Oxygenation before VLAs

A possible reason for elevated oxygen saturation before a VLA is that infants are breathing more rapidly before a VLA than they are before a short apnea.

The respiration rate reported by monitors is notoriously unreliable because of artifacts in the CI signal. Our filtered CI, from which most artifacts have been removed, was used to locate zero-crossings of the filtered CI, and maxima and minima between each zero-crossing. Breath length was defined as the time between two successive minima. To prevent residual fluctuations around zero to be mistakenly interpreted as breaths, two additional criteria were applied: The probability of apnea was required to be less than 0.5 at the times of the minima and consecutive maxima and minima had to be at least 0.1 times the standard deviation of the signal.

Apnea events in VLA infants were examined. The respiration rate for 100 breaths preceding each of the 86 VLAs, and also for 100 breaths preceding 100 randomly selected apnea events of duration 10-20 seconds in the same infants were obtained. The breath durations leading up to a VLA are generally shorter than those leading up to a 10-20 second apnea. The median SpO₂ also rises gradually in the 5 minutes leading up to a VLA.

A mathematical model for the rate of decline of SpO₂

Presented here is the theory represented by the theoretical curves in Figure 15 showing oxygen saturation as a function of time. The most striking fact about VLAs is that oxygen saturation falls more slowly in these events than in shorter apnea events (Figure 15). Why is this? We propose that the explanation of the slow fall of oxygen saturation is that both arterial and venous oxygenation are unusually high at the start of the event. The high value of venous saturation, S_v , causes the partial pressure of oxygen in the alveoli to drop rather slowly. (The alveoli are the air sacs in the lungs where gas exchange takes place.) The high initial values of oxygen saturation correspond to values at which the oxygen dissociation curve (which gives the oxygen saturation as a function of the partial pressure of oxygen and is determined by the dissociation constants for oxygen and hemoglobin) is flat, a small change in oxygen saturation is a large change in partial pressure. As oxygen is absorbed from alveoli into blood, and the partial pressure of oxygen in the alveoli falls, the associated drop in arterial oxygen saturation is small. The following quantitative model shows this effect.

An excellent study of the theory of arterial oxygen desaturation during apnea in preterm infants was carried out by Sands et al. (Sands et al. 2009), following a long train of similar studies. This is the basis for the following theory which we compare with our observations. In Chapter 4 this model will be expanded to give a description of periodic breathing. The following assumptions and approximations are used: (1) Applying the principles of conservation of

matter we find that during an apnea the only loss of oxygen in the lungs arises from diffusion into the blood. In the tissues oxygen is received from the blood and consumed by the metabolism. (2) In each heartbeat, gaseous oxygen in the alveoli equilibrates with oxygen in pulmonary capillaries so that the oxygen in the alveolar air is in equilibrium with the oxygen in the arteries. (3) Venous blood is homogeneous, with uniform SpO_2 . (4) The oxygen saturation in the pulmonary vein leaving the lungs is equal to the oxygen saturation measured by the pulse oximeter a few seconds later, in the hand or foot. (5) All oxygen in the blood is carried by hemoglobin. (6) During the apnea, the cardiac output does not change significantly. This is a reasonable assumption because of the Frank-Starling mechanism whereby the heart contracts with greater force when it is stretched more during filling (Hall, Guyton 2011). (7) SpO_2 is related to partial pressure of oxygen in the alveoli. In this model we use an equation first given by Hill (Hill 1910) and quoted (with a slight change) by Delivoria-Papadopoulos and McGowan (Delivoria-Papadopoulos, McGowan 2011) to describe this relationship

$$SpO_2 = 100kP_{O_2}^n / (1 + kP_{O_2}^n) \quad (2.1)$$

In this equation, we took $n = 2.9$ (Delivoria-Papadopoulos, McGowan 2011), and calculated k from reasonable values of P_{50} , the value of pressure at which $SpO_2 = 50\%$.

In this model we are assuming that all oxygen in the blood is carried by the hemoglobin. (In chapter 4 we will not make this assumption.) The

concentration of oxygen in the blood, C_{O_2} , depends on the amount of oxygen that is bound to the hemoglobin and the amount that is dissolved in the blood plasma. Each molecule of hemoglobin has four binding sites for oxygen and at 100% saturation each gram of hemoglobin carries 1.36 ml of oxygen. The concentration of oxygen in the blood is given by $C_{O_2} = 1.36Hb \cdot SpO_2 + 0.000031P_{O_2}$, where Hb is the number of grams of hemoglobin per ml of blood and P_{O_2} is the partial pressure of oxygen in the blood. The second term is negligible and in this chapter we ignore it, thus we have $C_{O_2} = 1.36Hb \cdot SpO_2$.

By applying conservation of matter we find that in the lungs the amount of oxygen coming in equals the rate of blood flow, \dot{Q} , times the concentration in the veins, C_v . (The veins are assumed to be in equilibrium with the pulmonary arteries.) The amount of oxygen leaving the lungs equals the rate of blood flow times the concentration in the arteries, C_a . (The arteries are assumed to be in equilibrium with the pulmonary veins.) The rate of change of oxygen in the lungs is the rate of change of the fraction of oxygen in the lung air, F_A , times the volume of air in the lungs. In the tissues the rate of change of oxygen is the rate of change of the concentration of oxygen in the blood times the volume of blood in the tissues. The amount of oxygen coming into the tissues equals the rate of blood flow times the concentration in the arteries. The amount of oxygen leaving the tissues equals the amount of oxygen being consumed metabolically, MR_{O_2} , plus the rate of blood flow times the concentration in the veins. (Figures 25 and

26 in chapter 4 show the lung compartment and the tissue compartment in the expanded model.)

The equation for the rate of change of oxygen in the lungs is:

$$\frac{dF_A}{dt} V_L = \dot{Q}(C_v - C_a)$$

The fraction of oxygen in the lung air is proportional to the partial pressure of oxygen in the lung air, P_a , (according to assumption 2 the oxygen in the alveolar air is in equilibrium with the oxygen in the arteries).

$$\frac{dP_a}{dt} \propto \frac{1.36Hb\dot{Q}(S_v - S_a)}{V_L}$$

where we used $C_{O_2} = 1.36Hb \cdot SpO_2$ to convert concentrations to oxygen saturation in the arteries, S_a , and oxygen saturation in the veins, S_v .

Changing from a rate of change of partial pressure to a rate of change of

saturation using $\frac{dP_a}{dt} = \frac{dP_a}{dS_a} \frac{dS_a}{dt}$ we get $\frac{dS_a}{dt} \propto \frac{dS_a}{dP_a} \frac{1.36Hb\dot{Q}(S_v - S_a)}{V_L}$.

$$\frac{dS_a}{dt} \propto \frac{dS_a}{dP_a} \frac{1.36Hb\dot{Q}(S_v - S_a)}{V_L}$$

which we write as

$$\frac{dS_a(t)}{dt} = D(S_a)C \cdot (S_v(t) - S_a(t)) \quad (2.2)$$

where C is a constant which is proportional to $\frac{Hb \cdot \dot{Q}}{V_L}$ and $D(S_a) = \frac{dS_a}{dP_a}$. The value

of $D(S_a)$ can be obtained from equation 2.1

The equation for the rate of change of oxygen in the tissues is:

$$\frac{dC_v}{dt} V_t = \dot{Q}(C_a(t - T_a) - C_v) - MR_{O_2}$$

where we have introduced the arterial transit time T_a , which is the time it takes the blood to go from the lungs to the tissues.

Using $C_{O_2} = 1.36Hb \cdot SpO_2$ to convert concentrations to oxygen saturations we have

$$\frac{dS_v}{dt} V_t = \dot{Q}(S_a(t - T_a) - S_v) - MR_{O_2}$$

which we write as

$$\frac{dS_v(t)}{dt} = \begin{cases} 0 & t \leq T_a \\ d \cdot (S_a(t - T_a) - S_v) - e & t > T_a \end{cases} \quad (2.3)$$

where e and d are constants and $e = \frac{MR_{O_2}}{V_t}$ and $d = \frac{\dot{Q}}{V_t}$.

Equation 2.2 is equivalent to equation 10 of Sands et al. (Sands et al. 2009), and equation 2.3 can be derived from equation 6 in Sands et al. $S_a(t)$ is the oxygen saturation leaving the lungs, which by assumption is equal to the oxygen saturation measured a few seconds later in the hand or foot. S_v is the venous oxygen saturation. C is a constant, proportional to hemoglobin concentration in the blood and to the cardiac output, which is the rate of blood flow \dot{Q} , and inversely proportional to lung volume, V_L . T_a is the arterial transit time, d is equal to cardiac output divided by venous blood volume, and e is the rate at which oxygen is utilized by the tissues. We treat C , T_a , d , and e as constants, independent of time, and independent of the duration of the apnea event. From

their values, and from the initial conditions $S_a(t = 0)$ and $S_v(t = 0)$, the above equations determine the evolution of $S_a(t)$.

These four constants and the initial conditions were determined by first obtaining preliminary estimates and then refining by fitting to the observations. The preliminary estimates were obtained by the following process. Sands et al. (Sands et al. 2009) showed that oxygen saturation during an apnea frequently follows a two-stage pattern. In the first stage ($t \leq T$) $S_a(t)$ drops rapidly, while in the second stage, it drops more slowly and at a constant rate (Figure 17). In cases where the two stages can be easily identified on a graph of $S_a(t)$, the arterial transit time T can be determined from the graph. Also, in the first stage $S_v(t)$ is constant. Hence in this stage, equation 2.2 contains two unknowns: S_v and C . These can be determined by choosing two points in time early in the apnea, $t_j = (t_1, t_2)$, extracting $S(t_j)$ and $\left. \frac{dS_a}{dt} \right|_{t_j}$ from the observations, and then solving the two equations for C and S_v .

To obtain estimates of d and e we set $t = T_a$ in equation 2.3 and find

$$d \cdot (S_a(0) - S_v(T_a)) - e = d \cdot (S_a(0) - S_v(0)) - e = 0 \quad (2.4)$$

In the second stage, the arterial oxygen saturation falls linearly with time at a rate approximately equal to (Sands et al. 2009)

$$\frac{dS_a(t)}{dt} \approx \frac{-e}{1 + d \cdot T_a} \quad (2.5)$$

From the observed rate of decline $\frac{dS_a(t)}{dt}$ in the second stage, and with $S_v(0)$ determined as above from stage 1, we have two equations for d and e with two unknowns.

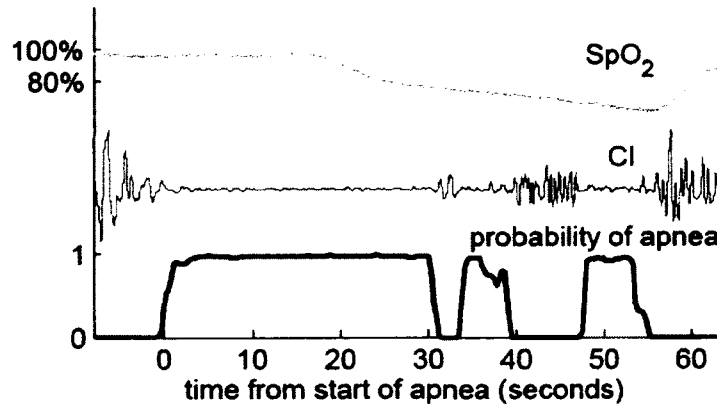


Figure 17: An example of oxygen saturation falling in two stages. SpO_2 (measured in the arteries, S_a) filtered CI, and the probability of apnea are shown. (Reproduced from Mohr et al. 2015b.)

Two issues remain. (1) There is a time delay between oxygen leaving the lungs and oxygen detected in the hand or foot. Part of this time delay is related to circulation time of blood and part of it is related to the averaging time of the oxygen monitor. A time delay of 20 seconds was chosen for all of the average curves in Figure 15, and gave satisfactory results. (2) The average saturation curves do not show any clear division between stage 1 and stage 2. Therefore, individual apnea events that show this distinction were used to obtain estimates of T_a , d , and e . There are several such cases, one of which is shown in Figure 17.

Finally, the values of these parameters were adjusted to fit the observations.

It is important to note that we used the same constant values of C , T_a , d , and e for short and long apnea events. We adjusted only the initial conditions $S_a(0)$ and $S_v(0)$ to fit the individual curves.

Table 5 lists the constants (except e , which can be found using equation 2.4) and the initial conditions. The resulting theoretical curves are shown in Figure 15. The agreement with the average SpO_2 curves is remarkable: over the whole of each of the ranges where SpO_2 is falling, the theoretical curves are only barely discernible from the observed ones, and differ from them by less than the standard error of the means of the observations.

Table 5. Initial conditions and constants

(uncertainty values in parenthesis were obtained by adjusting the parameters one at a time) (Reproduced from Mohr et al. 2015b.)

parameter	ABD 10-20	ABD 30-40	ABD 60-80 (VLAs)	ABD 80 (VLAs)
S_a	0.870 (0.005)	0.915 (0.007)	0.950 (0.005)	0.970 (0.003)
S_v	0.70 (0.01)	0.74 (0.01)	0.800 (0.005)	0.825 (0.005)
C	13.3 (0.6)			
d	0.2 (0.6)			
T_a	12 (1)			

In parentheses in Table 5 we report the uncertainty in the values of the parameters. These were obtained by finding the standard deviation of the mean of each set of observations, and adjusting parameters one at a time to find

values where the theoretical curves would disagree with observations by more than one standard error of the mean.

The theory given by Sands et al. (Sands et al. 2009) leads to remarkable agreement with our observations. It provides a credible explanation of why $SpO_2(t)$ falls slowly in long apnea events. Two factors are at work. At high oxygen saturations, the curve relating oxygen saturation to partial pressure of oxygen $SpO_2(P_{O_2})$ is flat, and the function $D(S)$ is near zero. In the alveoli and in the arteries, a large change in partial pressure of oxygen gives only a small change in SpO_2 . As a result, SpO_2 falls very slowly near the beginning of an apnea when oxygen saturation is high. In this regard the slow fall of SpO_2 from high levels is a natural consequence of well-known physiology. The second factor is the inferred somewhat elevated oxygen saturation in the veins. We have no direct measurements of venous oxygen saturation, it is obtained only by fitting to the observations. However this is consistent with the rise of SpO_2 in the 5 minutes prior to VLAs.

To understand the limits of the theory (Sands et al. 2009) as we apply it, let us re-examine some of the approximations. During an apnea, CO_2 concentration and pH of the blood may change, and these shift the hemoglobin saturation curve, $SpO_2(P_{O_2})$. This shift can be characterized by a changed value of P_{50} , the pressure at which hemoglobin is 50% saturated. This change, however, turns out to have only a small effect on the time dependence $SpO_2(t)$. One can include the effect approximately by changing the value of k in equation

2.1 for the time before S_v changes. However, when calculating $SpO_2(t)$ as described above using equations 2.1 and 2.2, the value of k exactly cancels (for fixed C and S_v), so at this level of approximation, P_{50} has no effect. (In a more accurate treatment, again holding C and S_v fixed, P_{50} would have a nonzero but small effect; Sands et al. (Sands et al. 2009), who used the Severinghaus formula (Severinghaus 1979) instead of equation 2.1, found that a change of P_{50} by 6-12 mmHg gave significant changes to $SpO_2(t)$, but part of the change they obtained resulted from changed initial values of SpO_2 and S_v .)

Another effect we neglected is extrapulmonary right-to-left shunt (blood which does not get oxygenated in the lungs as it travels from the right heart to the left heart). Since we find that the median oxygen saturation before a VLA is 96-98%, it appears that shunted blood is a small fraction of arterial blood, and would have little effect on the calculation of $SpO_2(t)$. Sands et al. (Sands et al. 2009) also note that shunt fraction affects the starting value of $SpO_2(t)$ but has little effect on its rate of change.

Cardiac output was assumed to be approximately constant. This approximation is commonly used in models of short apnea events and models of periodic breathing (Khoo et al. 1982, Milhorn, Guyton 1965, Tehrani 1997), and it can be justified as a manifestation of the Frank-Starling mechanism (Hall, Guyton 2011), which is now known to be present in neonates (Anderson et al. 1998, Girling 1972, Kirkpatrick et al. 1976, Price 2011).

Further study of assumption (3), that venous blood is well-mixed and homogeneously oxygenated, would be beneficial. This should be accurate in steady state, but it is not clear that it would hold during the rapid changes of oxygenation that occur during apnea.

This theoretical method might turn out to provide useful physiological information. C and d are both proportional to cardiac output, e is proportional to metabolic rate, and S_v is the venous oxygen saturation, none of which are continuously available in NICU monitoring. By fitting the time course of SpO_2 in individual apnea events to the theory, it may be possible to get estimates of these parameters during each apnea.

Conclusion

While apnea is a normal developmental phenomenon in preterm infants, very long apnea is an important problem that may reflect or lead to adverse events or outcomes. These events are interesting from a physiologic perspective and important from a patient safety perspective.

We found that very long apnea events are not rare. We used stringent criteria to define a VLA. We found that infants show no evidence of breathing for durations of up to 132 seconds. These events occur with a frequency of 1 per 70 infant-days in our population.

We also found that VLA infants differ from non-VLA infants in that they have a much higher rate of short apnea events and presumably have less

developed respiratory control. We found short apnea events in VLA infants to be indistinguishable from short apnea events in non-VLA infants.

It is difficult to establish the effect of VLAs on the short-term or long-term health of infants. Despite the slow drop of SpO₂ in VLAs, the available measure of deficit in oxygen transport is approximately proportional to the duration of the cessation of breathing, i.e. 90 second apnea events result in approximately 3 times the oxygen transport deficit of 30 second apnea events. Our information on clinical consequences leads to ambiguous results. On one end of the VLA spectrum, an apparently healthy preterm infant had 19 events over a 3 week period, and eventually died following a respiratory arrest from which he could not be resuscitated. However, other VLA infants had normal courses in the NICU. Lacking post-discharge objective neurodevelopmental follow-up testing on infants, we can only say that, with the possible exception of the infant who died, no clinical consequences could be proved to be caused by VLAs. Nevertheless, VLAs cannot be good for infants, and their frequency is disturbing.

Part of the explanation of why VLAs occur is that apnea alarms fail to activate in about one-third of these events. In addition, we previously showed that about two-thirds of all apnea alarms are false alarms (Lee et al. 2012), so alarm fatigue or alarm distrust may also be a factor (Vergales et al. 2014). Clinical experience and our data suggest that bedside caregivers respond quickly to bradycardia alarms, which are “crisis” alarms on the monitors in the UVa NICU (in contrast to apnea “warning” alarms), but as a result of the slow fall of heart

rate these alarms are delayed. We believe that more reliable apnea alarms, with fewer false negatives and false positives, would be helpful to NICU personnel and might have a significant beneficial effect on the health of infants by reducing hypoxemia and bradycardia.

The respiration rate was found to be somewhat elevated and SpO_2 to gradually rise in the 5 minutes prior to a VLA. Accordingly, SpO_2 is unusually high at the commencement of the event. Combining this observation with the hypothesis that venous oxygen is also somewhat elevated leads to a quantitative description of the average rate of fall of SpO_2 with time.

Prolonged apnea events should be preventable. Since these events could have detrimental consequences and are often not noticed and/or not recorded in the medical record, improvements in bedside monitor apnea detection, alarm systems, and caregiver responses are key to providing a safer environment for hospitalized preterm infants.

Chapter 3

Wavelet Detection of Periodic Breathing

Periodic breathing, characterized by regular, repeated cycles of apneic pauses and breathing, has generally been considered to be a normal respiratory pattern in most if not all newborn infants (Rigatto 2003). However, several decades ago, excessive amounts of periodic breathing were observed in infants who had “near-miss sudden infant death syndrome” and in siblings of infants that died of sudden infant death syndrome (SIDS) (Kelly, Shannon 1979, Kelly et al. 1980). A recent case of SIDS in a preterm infant discharged home from the University of Virginia (UVa) Neonatal Intensive Care Unit (NICU) led to an unexpected finding: on retrospective review of the UVa database, we found that this infant spent a strikingly large proportion of time in periodic breathing compared to other preterm infants, despite having almost no episodes of classical apnea of prematurity (AOP). To our knowledge this is the first time that excessive periodic breathing has been observed in a NICU patient who subsequently died of SIDS. Can such exaggerated periodic breathing be pathologic in newborn infants? To answer this question a new method of identifying and quantifying periodic breathing was developed.

The UVa dataset provides us with the ability to quantify periodic breathing on a larger scale than has previously been done. Here we describe a new method of detecting periodic breathing. Our object is to use this method to

calculate the amount of time that infants spend in periodic breathing. We seek to establish what normal amounts of periodic breathing are for infants based on gestational and postmenstrual age. These results are used to identify infants that had extreme amounts of periodic breathing. The clinical records of these infants are examined and clinical correlations with periodic breathing are sought to determine whether periodic breathing can give advanced warning of these conditions.

A widely accepted definition of periodic breathing has at least 3 cyclical apneas of at least 3 seconds duration with less than 20 seconds of breathing in between (Barrington, Finer 1990). As we will show, our detector recognizes such events, but we have reason to believe that this definition is too broad to provide a useful warning of impending pathology. First, we and others have observed that such brief episodes are very common, even in the absence of any indications of pathology. Second, physiological models of periodic breathing contain a natural distinction between transient oscillations and sustained oscillations. According to these models, periodic breathing represents high gain in the respiratory control system (Milhorn, Guyton 1965, Hall, Guyton 2011, Batzel, Tran 2000, Ben-Tal, Smith 2010, Cherniack, Longobardo & Evangelista 2005, Fowler, Kalamangalam 2000, Khoo et al. 1982, Levine, Hathorn & Cleave 2004, Rapoport, Norman & Goldring 1993, Berger et al. 2000, Norman et al. 2006, Takahashi, Doi 1993, Tehrani 1997, Verma, Katiyar & Singh 2009). In neonates, high gain appears to result from hypersensitivity of the chemoreceptors that trigger breaths in

response to changes in blood gases (Cherniack, Longobardo 2006, Al-Matary et al. 2004, Edwards, Sands & Berger 2013). Peripheral chemoreceptors are desensitized at birth, with the acute increase in blood oxygen content during fetal to neonatal transition, then are gradually reset by about one week of age at which time periodic breathing emerges (Barrington, Finer 1990). Hypersensitivity of chemoreceptors to changes in blood oxygen and carbon dioxide levels leads to self-sustained oscillations between breathing and apneic pauses, especially during quiet sleep (Pereira et al. 1995, Rigatto 2003).

In contrast to newborn infants, healthy adults rarely exhibit significant periodic breathing, except with acute exposure to hypoxia at high altitude (Ainslie, Lucas & Burgess 2013, Fowler, Kalamangalam 2002). Acute and chronic diseases can, however, lead to periodic breathing patterns such as Cheyne-Stokes respiration associated with heart failure (Dowell et al. 1971, Francis et al. 2000, Lange, Hecht 1962, Manisty et al. 2006, Vielle, Chauvet 1993a, Vielle, Chauvet 1993b, Vielle, Chauvet 1998, Lieber, Mohsenin 1992). Cheyne-Stokes respiration is characterized by a regular pattern of respiration and apnea; the cycle time in adults ranges from 30 seconds to two minutes, and during the respiratory phase, both the amplitude and the frequency of breathing wax and wane in a regular crescendo-decrescendo pattern. Heart failure may cause excessive time delay in the control loop, which can also lead to high loop gain, resulting in periodic breathing. A similar pattern was seen in a small number of stroke patients (Hermann et al. 2007). A distinction between the patterns of

neonatal periodic breathing and adult Cheyne-Stokes breathing is that the cycle time in the former has an average of about 15 seconds, while in the latter the average is about a minute. Both cases are apparently associated with high loop gain, but the physiological causes may be distinct: chemoreceptor hypersensitivity in infants vs. excessive time delay in heart failure.

There are several other types of abnormal respiration that are easily confused with periodic breathing, and the distinctions among them are not sharp. An excellent review is given by Richerson and Boron (Richerson, Boron 2005), who identify, besides Cheyne-Stokes respiration, Biot breathing, ataxic breathing, cluster breathing and gasping. During a study of Cheyne-Stokes respiration, Biot (Wijdicks 2007) came across a distinct pattern in patients with meningitis: there were irregular pauses lasting 10-30 seconds, and the breathing was irregular and rapid, without the crescendo-decrescendo pattern. Similar to Biot breathing are patterns called cluster breathing or ataxic respiration, which can occur as a result of lesions in the pons or medulla. It appears that there are not precisely defined differences among these.

Physiological models of periodic breathing involve a control system in which parameters have changed so that it has gone from a stable steady state to a stable limit cycle. For values of parameters between those leading to steady state and those leading to a limit cycle, one finds oscillatory decay to the steady state. In contrast, Biot breathing, cluster breathing, and ataxic breathing seem to involve more profound failure of the control system. To construct a pattern-

recognition algorithm for periodic breathing, we focus not on the breathing, but on the apneas, and we ask whether the apnea events are occurring with a regular rhythm and, if so, is that rhythm sustained or does it stop after a short time?

Wavelet Detection

A wavelet transformation method was developed to identify and quantify periodic breathing. Two functions are used in the wavelet transformation: the wavelet and another function. The wavelet is shifted through the function and at every point the integral of the product of the two functions is taken, this gives the area overlap. Wavelets are designed with equal area above and below zero, thus the wavelet transformation with a constant function will give zero. The wavelet transformation begins with a mother wavelet, $\psi(t)$. From this mother wavelet a family of wavelets are calculated, $\psi_{s,\tau}(t) = |s|^{-p}\psi(\frac{t-\tau}{s})$ (Kaiser 1994). These wavelets have a size that depends on the scale, s , and a position that depends on the translation, τ . Wavelet coefficients are calculated using $\gamma(s, \tau) = \int_{-\infty}^{\infty} f(t)\bar{\psi}_{s,\tau}(t)dt$, where $\bar{\psi}$ is the complex conjugate of ψ . (Our wavelet has no imaginary part so $\psi = \bar{\psi}$.) These coefficients, $\gamma(s, \tau)$, are a function of time and scale. Wavelet coefficients calculated at lower scales give information about the finer details of the function. The term $|s|^{-p}$ in $\psi_{s,\tau}(t)$ is a scaling factor. p is commonly chosen to be either 0, 1/2, or 1 (Kaiser 1994). We choose to set $p = 1/2$ as this choice leaves the maximum value of the wavelet coefficients unaffected by the scale.

The wavelet transformation is uniquely suited to detect periodic breathing. Unlike the Fourier transformation, the wavelet transformation is localized, this means that the length of the signal segment that is being evaluated depends on the cycle length.

The Haar wavelet is a commonly used wavelet, developed by Alfréd Haar in 1909. A wavelet transformation of the apnea signal using a Haar wavelet detects individual apnea events, but gives no additional information about periodicity of the apnea events. To detect periodicity it was necessary to use a wavelet that was itself periodic. Such wavelets already exist, but in this case it was advantageous to create a wavelet that was uniquely suited to its purpose.

Our previously developed probability of apnea signal (Lee et al. 2012) was used for periodic breathing detection. The unprocessed signal which contains apneic pauses as short as 2 seconds was used, after filtering out all times where the probability of apnea was non-zero due to a dropped signal.

Generous definitions of periodic breathing include as few as three apnea events (Barrington, Finer 1990). The appropriateness of such a definition can be debated. However, it may be beneficial to detect three repetitive apnea events even so. We then have the option of choosing a threshold value for the wavelet coefficient values that will exclude those short events when we choose not to consider them.

For periodic breathing detection a wavelet with six cycles was designed (Figure 18). This design allowed for detection of as few as three repeated apnea

events. The wavelet was designed to resemble periodic breathing in the apnea signal, with six “apnea” phases and six “breathing” phases. There is a gradual transition between the breathing and apnea states. The wavelet is centered on zero and multiplied by a sine window. The gradual transition gives less weight to the signal at the transition time. Multiplication by the sine wave gives less weight to the beginning and end of the segment. (Three periodic apnea events give higher value than three events that are periodic but with a missing apnea between them). The wavelet was normalized so that the absolute value of the wavelet coefficient has a maximum value of 1 when the transformation of the apnea signal, which has a range of 0 to 1, is taken.

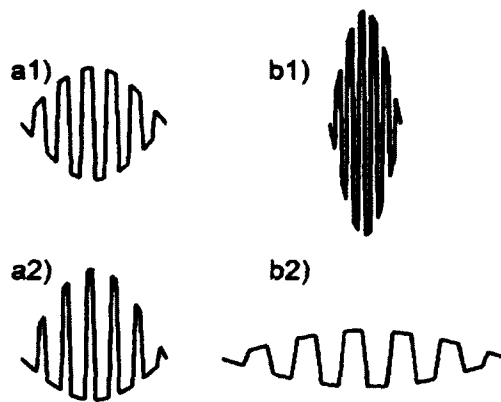


Figure 18: Mother wavelets and scaled wavelets for detecting periodic breathing. The two mother wavelets are modeled after the appearance of the probability of apnea signal during periodic breathing, with multiplication by a sine window to weight the middle of the wavelet more heavily. a1) Mother wavelet with two phases (apnea and breathing) of equal duration. a2) Mother wavelet with one phase twice as long as the other, created to detect a wide range of time ratios. b1, b2) Mother wavelets are scaled to different sizes (compressed or stretched along the horizontal axis), giving a family of wavelets that detect periodic breathing with cycle lengths ranging from 10-40 seconds. (Reproduced from Mohr et al. 2015a.)

Two such mother wavelets were used. One had an apnea:breathing ratio of 1:1, the other had an apnea:breathing ratio of 2:1. Because we use the absolute value of the wavelet coefficients, an apnea:breathing ratio of 2:1 gives the same results as using an apnea:breathing ratio of 1:2. These two wavelets allow for the detection of periodic breathing with duty cycles of 1:4 to 4:1 (Figure 19). (Giving less weight to the transition time improves the detection of periodic breathing at all ratios in this range.) The value of the wavelet coefficients is highest when the ratio is the same as the ratio of either of the two mother wavelets. However, Figure 19 shows that so long as the periodicity is sufficiently high periodic breathing will still be detected.

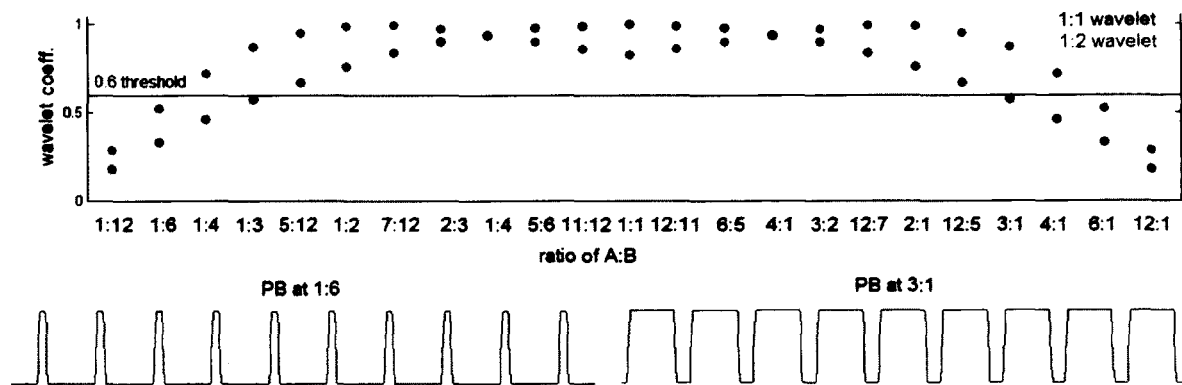


Figure 19: Wavelet coefficients at different apnea:breathing (A:B) ratios. Also shown is periodic breathing with an A:B ratio of 1:6 and with an A:B ratio of 3:1.

The two mother wavelets are used to calculate a family of wavelets

$$\psi_{s,\tau}(t) = |s|^{-p} \psi\left(\frac{t-\tau}{s}\right).$$

These wavelets have a cycle length (related to the scale s) (Figure 18b) and a position (τ). A wavelet coefficient, $\gamma(s, \tau)$, is calculated every quarter second as the wavelet is shifted through the apnea signal. The wavelet

coefficient is highest at the positions where the wavelet is most closely aligned with the apnea signal. During a segment of periodic breathing as the wavelet is shifted through the apnea signal the wavelet coefficients rise and fall. For periodic breathing detection we are only interested in the maximum values of the wavelet coefficients. The longest cycle length that we seek to detect is 40 seconds. For this reason we choose to take the maximum value of the wavelet coefficients in a 40 second window across all scales. This is done every 20 seconds. The result is our periodic breathing index. The periodic breathing index remains high during the entirety of the periodic breathing event.

The periodic breathing index is a continuous signal that is calculated throughout the entire apnea signal. To detect periodic breathing an appropriate threshold value is chosen. An episode of periodic breathing is defined as starting when the index first rises above the threshold and ending at the last point that is still above the threshold value. A higher threshold includes only the most periodic episodes of repeated apnea events. A lower threshold is useful when considering episodes of repeated apnea events that are less periodic. A preliminary analysis of the periodic breathing index suggested a threshold near 0.6 to distinguish periodic breathing. All times when this index was ≥ 0.6 were marked as periodic breathing events. After a threshold value is chosen the collection of periodic breathing episodes may be further refined by specifying that they last for a minimum length of time. When making these choices one should bear in mind that raising the threshold for the periodic breathing index often results in one

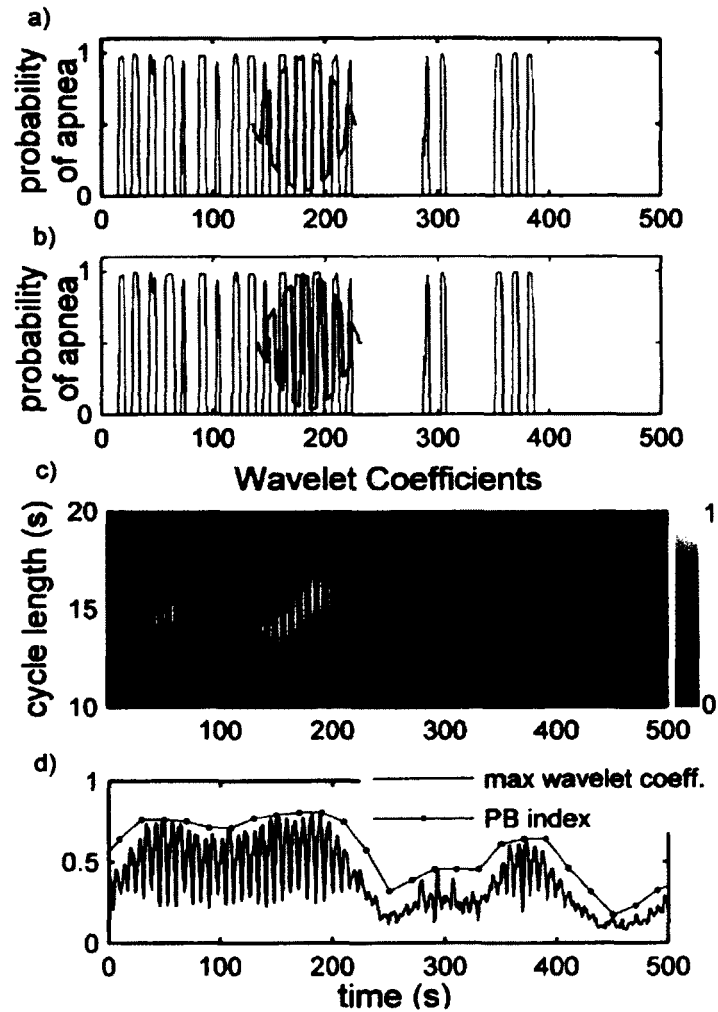


Figure 20: Wavelet transformation of probability of apnea signal to derive wavelet coefficients and periodic breathing index. a and b) 500 second window of the probability of apnea signal in a preterm infant, with shifted wavelet. At quarter second intervals, a wavelet coefficient is calculated that corresponds to the convolution of the wavelet and the probability of apnea signal. The absolute values of the coefficients range from 0 to 1 with a higher value indicating better alignment. Periodic breathing is identified when the coefficient meets or exceeds the threshold value of 0.6. In (a), the oscillations in the wavelet match those of the signal, giving a large wavelet coefficient, while in (b), the oscillations are out of phase, and the coefficient is small. Thus the coefficients oscillate rapidly as the wavelet is translated through the signal. c) Wavelet coefficients for scales corresponding to cycle lengths from 10 to 20 seconds. Lighter shades indicate higher values. d) The maximum of the absolute values of the wavelet coefficients across all scales at each point is shown along with the periodic breathing index, which is the maximum in a 40 second window calculated every 20 seconds. (Reproduced from Mohr et al. 2015a.)

periodic breathing episode being split up into multiple shorter episodes due to slight dips in the periodic breathing index that drop below the higher threshold value.

Validation

For validation of the periodic breathing detection algorithm 200 four minute windows of raw and filtered chest impedance, EKG, heart rate, oxygen saturation, and apnea signal data centered on an ABD10 tag were collected. 100 windows were randomly chosen from the set of all four minute windows centered on an ABD10 tag where the periodic breathing index met the threshold value of 0.6 at some point during the four minutes. The other 100 were randomly chosen from all four minute windows centered on an ABD10 tag where the periodic breathing index did not exceed 0.6 during the entire 4 minutes.

These 200 windows were examined by clinicians. They had no knowledge of how the windows were chosen. They were told to evaluate the windows and decide if they considered there to be any periodic breathing in the window. Four clinicians first reviewed the samples independently. All cases in which there was not 100% agreement were subjected to group discussion. Consensus was reached for 180 of the samples. These 180 samples were used to evaluate the reliability of the periodic breathing detection algorithm. The clinicians determined that 73 of the samples included periodic breathing and 107 did not, 20 were disputed. Based on this result we tested the predictive capability of a periodic

breathing index ≥ 0.6 for detecting clinician-identified undisputed periodic breathing. The maximum values of the periodic breathing index in the four-minute windows were 0.74 ± 0.03 (mean \pm 95% CI) for 73 windows with clinician-identified undisputed periodic breathing, 0.40 ± 0.02 for 107 windows with no clinician-identified periodic breathing, and 0.66 ± 0.02 for the 20 disputed windows (Figure 21). Of the 73 windows that contained clinician-identified definite periodic breathing, the computer-derived periodic breathing index was ≥ 0.6 for 70 (96% sensitivity). Other diagnostic utility measures are shown in Table 6. Calculation of the ROC curve (area under the curve = 0.98) showed that the

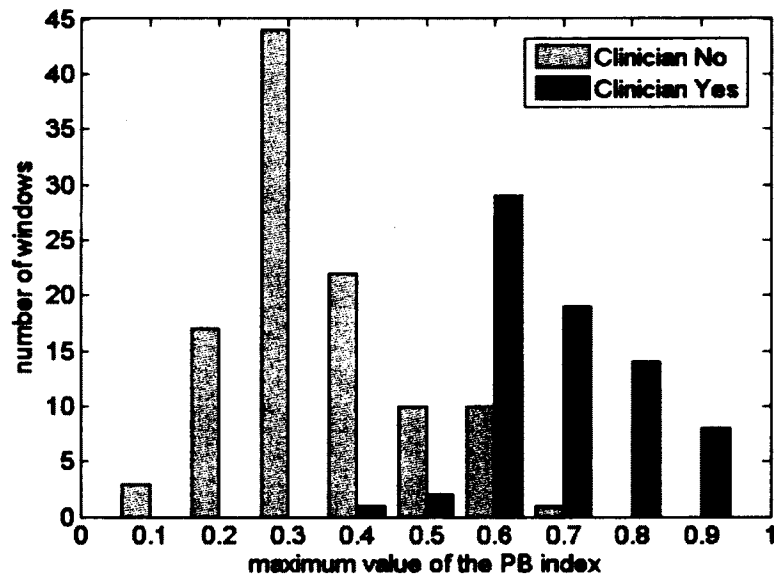


Figure 21: Superimposed histograms of the maximum value of the periodic breathing index (PB index) for the groups of clinician-identified periodic breathing (clinician yes) and no clinician identified periodic breathing (clinician no). The windows are classified according to the maximum value of the periodic breathing index in that window. The maximum periodic breathing index is at least as great as the value shown on the x-axis. (For example, there are 3 windows with a maximum periodic breathing index ≥ 0.1 and < 0.2 .) (Reproduced from Mohr et al. 2015a.)

product of sensitivity and specificity was maximized at the threshold of 0.6, confirming the appropriateness of this value.

Table 6: Contingency table from validation of wavelet transform analysis
(Reproduced from Mohr et al. 2015a.)

		Clinician			
		Yes	No	Total	
Computer	Yes	70	11	81	positive predictive value 86%
	No	3	96	99	negative predictive value 97%
	Total	73	107	180	
		sensitivity 96%	specificity 90%		

Discussion

Research on periodic breathing in infants has been limited, in part because this breathing pattern is transient and considered to be benign, and in part due to lack of methods to characterize and quantify periodic breathing in large numbers of infants over long periods of time. Our finding that a former NICU patient that died of SIDS had an inordinate amount of periodic breathing led to the development of an automated method to quantitate periodic breathing in all UVa NICU patients, a first step toward being able to quantify and characterize both normal and excessive, potentially pathologic periodic breathing in NICU patients.

An important feature of our wavelet method is its ability to distinguish irregular clusters of AOP from periodic breathing (Figure 22). Two questions

were asked: (1) Are the apnea events brief and occurring with a regular rhythm?
 (2) Is this regular apnea/breathing rhythm sustained for at least 3 cycles? Making this distinction is important. While periodic breathing can be described by physiological models with a well-behaved control system, in which the system can be in a stable steady state (normal respiration) or a stable limit cycle

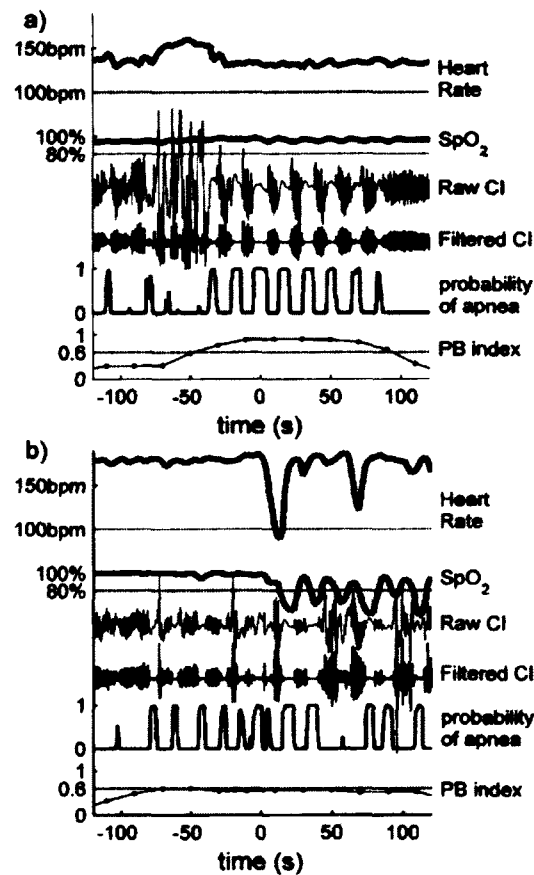


Figure 22: Periodic breathing versus clustered apnea. Four-minute window of heart rate, oxygen saturation (SpO₂), raw and filtered chest impedance (CI), probability of apnea signal, and periodic breathing index. Periodic breathing is identified by the wavelet method when the periodic breathing index meets or exceeds the threshold value of 0.600. a) Regular, repetitive apnea/breathing oscillations (maximum wavelet coefficient=0.905) identifying true periodic breathing. b) Cluster of irregular apnea/breathing. The computer did not identify this as definite periodic breathing since the wavelet coefficient was always below the threshold value (maximum wavelet coefficient=0.598). (Reproduced from Mohr et al. 2015a.)

(periodic breathing) (Cherniack, Longobardo 2006, Khoo et al. 1982), entirely different mechanisms may be responsible for clustered apnea. AOP and periodic breathing are distinct in character, gestational age predilection, and timing of onset and resolution (Barrington, Finer 1990). AOP is uncommon in infants >34 weeks' gestation, whereas periodic breathing is very common in both late preterm and term infants (Glotzbach et al. 1989, Oliveira et al. 2004). AOP begins within 1-2 days after birth and usually resolves between 36 and 42 weeks postmenstrual age (Eichenwald, Aina & Stark 1997), whereas periodic breathing typically starts after the first week and often persists beyond NICU discharge, for up to several months past term-corrected age (Wilkinson et al. 1995). The timing of onset of periodic breathing coincides with the time that peripheral arterial chemoreceptors, silenced at birth with the acute rise in blood oxygen levels, become highly sensitive to small fluctuations in blood gases (Pereira et al. 1995, Khan et al. 2005).

Periodic breathing typically includes apneic pauses of less than 10 seconds and may entrain only small or no decline in heart rate and oxygen saturation (Poets, Southall 1991, Razi, DeLauter & Pandit 2002), rarely low enough to reach the threshold to trigger bedside monitor alarms, whereas AOP is often prolonged and associated with significant bradycardia and oxygen desaturation (Finer et al. 2006). Hypoxia may trigger or exacerbate AOP or periodic breathing (Al-Matary et al. 2004), and administering oxygen to preterm infants can minimize both (Weintraub et al. 1992, Simakajornboon et al. 2002).

Advantages of the method

Past studies of periodic breathing have been limited to short monitoring times in small numbers of infants, often with visual inspection of respiratory impedance or inductance waveforms for characteristic apnea/breathing cycles. Our automated apnea algorithm gives a reliable measure of central apneic pauses, which can be used to quantify periodic breathing in large numbers of patients over long periods of time. This wavelet method distinguishes periodic breathing from apnea clusters where the durations of apnea and breathing are irregular. With increasing availability of high-speed data processing it is likely that this method could ultimately be applied in near-real-time to assess for immature breathing patterns that may have important clinical implications.

Chapter 4

A Model of Periodic Breathing

Mathematical models of periodic breathing give a quantitative description of the respiratory control system. Such models have been used to show under what conditions breathing is stable and regular, and under what conditions the respiratory control system goes into oscillations, representing periodic breathing. We would like to connect these models to properties that are measured and observed in the NICU. These properties include: respiration rate, depth of respiration, phase of breathing, oxygen saturation, and heart rate. Our studies have shown that periodic breathing can increase during times of illness, as discussed in chapter 5. We would like to use periodic breathing models to discover how and what physiological parameters are changed during illnesses where periodic breathing increases. We would also like to show how parameters change in healthy infants when they experience periodic breathing.

Previous models of periodic breathing have described the respiratory control system and shown the conditions under which breathing is stable and also the conditions for instability. These models start with simple principles and well established facts from which a set of differential equations are derived which model the respiratory control system. In 1954 Grodins et al. applied methods of control theory to the respiratory system's regulation of carbon dioxide (Grodins et al. 1954). This paper gave rise to a number of others on the chemical control of

respiration. Periodic breathing was seen in models which described carbon dioxide regulation only under unrealistic conditions. However, when oxygen regulation was included, periodic breathing was seen under more realistic conditions. As the complexity of these models increased, they were more helpful in understanding the causes of periodic breathing (Carley, Shannon 1988, Edwards, Sands & Berger 2013, Cherniack, Longobardo 2006, Batzel, Tran 2000, Levine, Hathorn & Cleave 2004, Norman et al. 2006, Rapoport, Norman & Goldring 1993, Takahashi, Doi 1993, Tehrani 1997). In 1982 Khoo et al. introduced a model which analyzed the stability of the respiratory system in adults (Khoo et al. 1982). This model is the basis for the one we give here with modifications for infants based on the work of Batzel and Tran (Batzel, Tran 2000).

The set of differential equations in periodic breathing models have a steady state which represents steady breathing. When parameter values change the system can go from a stable steady state to a stable limit cycle. Linearizing the equations about this steady state shows whether it is stable or unstable. The unstable case can lead to oscillations. Exact solutions to the differential equations show the transition from steady state to oscillations.

We present here a mathematical model of periodic breathing in infants. Stability analysis is applied to show that infants are more susceptible to periodic breathing during sleep. We also show that high controller gain, increased arterial

oxygen, decreased arterial carbon dioxide, and decreased lung storage volume for oxygen increase the infant's susceptibility.

This model contains many parameters that can be estimated from known values for infants, but these values are not measured for individual infants in the NICU, therefore we are unable to directly connect these parameters to observations.

We would like to use this model of periodic breathing to study the effect that illness has on periodic breathing. However, essentially no information is available about the effect of pathogens, or the immune response to them, on the parameters which govern the transition of the respiratory control system to oscillations.

Essential concepts

The model of periodic breathing presented here includes peripheral chemoreceptors for carbon dioxide and oxygen and central chemoreceptors for carbon dioxide. There is one lung compartment, one body tissue compartment, and one brain tissue compartment. We assume constant temperature, pressure, and humidity in well-mixed (homogenous) compartments. We neglect extrapulmonary right-to-left shunt, as we did in chapter 2.

The central and peripheral chemoreceptors regulate breathing. The oxygen and carbon dioxide peripheral chemoreceptors are located mainly in the carotid bodies in the bifurcations of the common carotid arteries (in the neck),

some are also located in the aortic bodies in the aortic arch (just above the heart) (Hall, Guyton 2011). The central carbon dioxide receptors are located in the medulla oblongata (in the brain). The central chemoreceptors regulate carbon dioxide, while the peripheral chemoreceptors respond mainly to oxygen but also to carbon dioxide. The peripheral chemoreceptors have a quicker, but less powerful response than the central chemoreceptors. In general it is the central receptors that are responsible for the long term response while the peripheral receptors are mainly responsible for periodic breathing.

In chapter 2 we presented a list of assumptions and approximations from which we derived a model of oxygen desaturation. Here we modify that list to extend the model to apply to periodic breathing. The following principles and approximations are used to derive the periodic breathing model (Figure 23): (1) Matter is conserved. The oxygen entering the body during inhalation equals the amount exiting during exhalation plus the amount that is consumed metabolically. Similarly for carbon dioxide. (2) The blood that passes through the pulmonary capillaries in the lungs comes to equilibrium with the alveolar gas. Therefore the arterial blood is in equilibrium with the alveolar gas. Also, the partial pressures of oxygen and carbon dioxide in the body tissues are in equilibrium with the partial pressures in the veins. (3) The peripheral detectors are in direct contact with the arterial blood and measure the partial pressures of oxygen and carbon dioxide in the arterial blood where they are located. The central chemoreceptors are not in direct contact with the arterial blood and measure the partial pressure of carbon

dioxide which arrives at their location after a diffusion process. (4) The respiratory controller integrates information from the central and peripheral chemoreceptors and adjusts the ventilation rate towards steady state accordingly. (5) There are time delays in the system which can destabilize the system. The blood at the body tissues and the chemoreceptors is the blood

Table 7: Symbols used in the periodic breathing model

C_a (C_{aCO_2} , C_{aO_2}) = arterial concentration (ml of gas/ml of blood)
 C_v (C_{vCO_2} , C_{vO_2}) = venous concentration (ml of gas/ml of blood)
 $C_{b_{vCO_2}}$ = venous concentration of CO₂ in brain (ml of gas/ml of blood)
 F_A = alveolar mole fraction
 F_I = inspired mole fraction
 G_C = central control gain (liters/min/mmHg)
 G_P = peripheral control gain (liters/min/mmHg)
 H_b = hemoglobin content (grams of hemoglobin/ml of blood)
 I_C = central apneic threshold (mmHg)
 I_P = peripheral apneic threshold (mmHg)
 P_a (P_{aCO_2} , P_{aO_2}) = arterial blood partial pressure (mmHg)
 P_I (P_{ICO_2} , P_{IO_2}) = partial pressure of inspired air (mmHg)
 $P_{b_{CO_2}}$ = partial pressure of CO₂ in brain (mmHg)
 MR (MR_{CO_2} , MR_{O_2}) = metabolic rate of CO₂ production/O₂ consumption (liters of gas/second)
 $MR_{b_{CO_2}}$ = metabolic rate of CO₂ production in brain (liters of gas/second)
 \dot{Q} = cardiac output (liters of blood/second)
 \dot{Q}_b = cerebral blood flow (liters of blood/second)
 S = oxygen saturation
 V_A = total lung volume (liters of gas)
 \dot{V}_A = alveolar ventilation (liters of gas/second)
 \dot{V}_D = dead space ventilation (liters of gas/second)
 \dot{V}_E = minute ventilation (liters of gas/second)
 V_L (V_{LCO_2} , V_{LO_2}) = effective lung volume (liters of gas)
 V_t (V_{tCO_2} , V_{tO_2}) = total tissue volume (liters of gas)
 V_T (V_{TCO_2} , V_{TO_2}) = effective tissue volume (liters of gas)
 V_b = total brain volume (liters of gas)

which was in the lungs at an earlier time and has the properties of the blood in the lungs at that earlier time. The blood returning to the lungs was in the body tissues at an earlier time.

In the periodic breathing model we do not neglect the oxygen that is dissolved in the blood plasma. Also, in the periodic breathing model we use a different equation to approximate the oxygen dissociation curve.

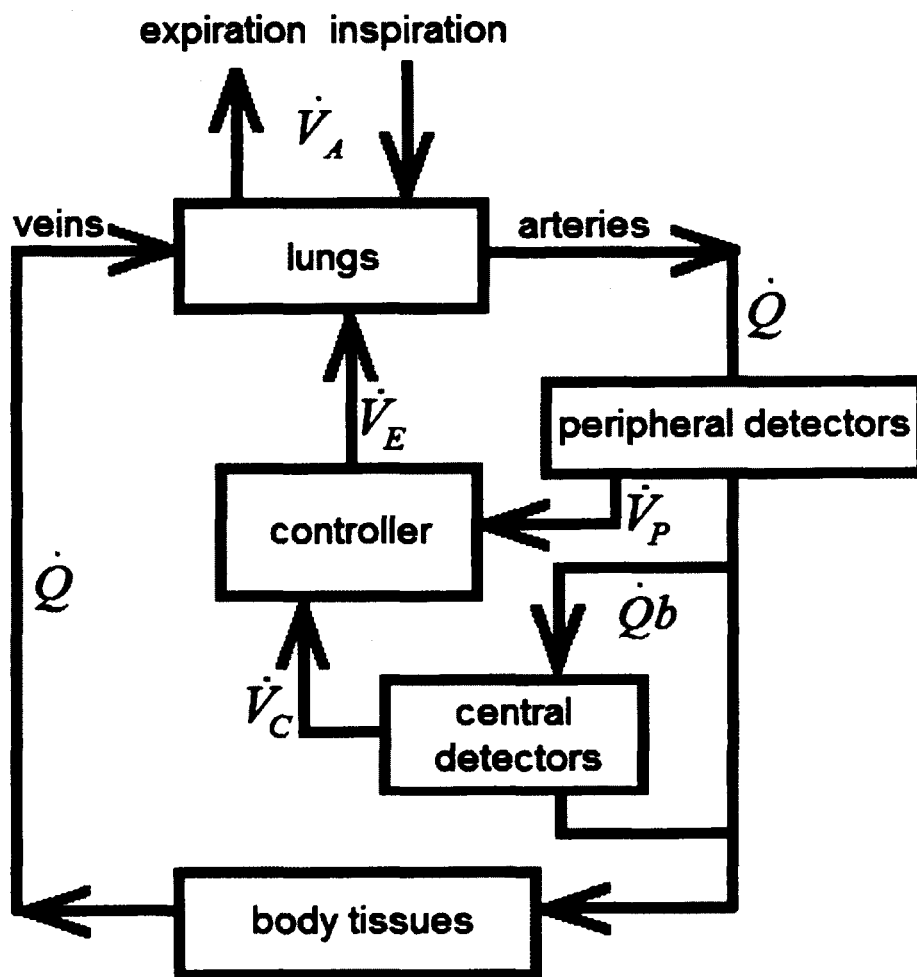


Figure 23: A model of periodic breathing

Minute ventilation

Minute ventilation (\dot{V}_E) is the rate at which air is inspired. Not all the air that is inspired makes it to the lungs. The air that remains in the respiratory passages is called dead space air (Hall, Guyton 2011). Alveolar ventilation is equal to minute ventilation minus dead space ventilation $\dot{V}_A = \dot{V}_E - \dot{V}_D$.

Measuring oxygen and carbon dioxide in the body

The amount of carbon dioxide or oxygen in air is measured in terms of partial pressure. Standard atmospheric pressure is 760 mmHg. The air that is inhaled is humidified in the respiratory passages. The air that reaches the alveoli in the lungs is completely humidified (Hall, Guyton 2011). Water vapor has a partial pressure of 47mmHg at body temperature (310.15 K). If the glottis is open the total pressure of air remains at 760 mmHg inside the body. Thus, the humidification of the inhaled air dilutes all the gases in the air lowering their partial pressures as shown in Table 8 (Batzel, Tran 2000, Hall, Guyton 2011).

Table 8: Values for partial pressures of gases in air and body used in model (for 4 month old awake infant)

	Carbon dioxide	Oxygen	Water vapor
Atmospheric air	0 mmHg	150 mmHg	3.7 mmHg
Humidified air	0 mmHg	141 mmHg	47 mmHg
Alveolar air	34 mmHg	96 mmHg	47 mmHg
Arteries	34 mmHg	96 mmHg	-
Tissues	36 mmHg	48 mmHg	-
Veins	36 mmHg	48 mmHg	-

How are carbon dioxide or oxygen measured blood? When we have a solution of liquid that is in equilibrium with air, the partial pressure of a gas in that air depends on the concentration of the gas in the solution. We say that the partial pressure of a gas in the solution is the partial pressure that we would see in air that is in equilibrium with the solution.

We can convert between concentrations of gases in the blood and partial pressures using dissociation curves which give the relationship between concentration and partial pressure. We assume that the values of the carbon dioxide dissociation curve are the same in infants as in adults (Batzel, Tran 2000). The oxygen dissociation curve in infants shifts with maturation.

We assume that the dissociation curves are the same in all compartments.

The carbon dioxide dissociation curve is represented by the following linear equation:

$$C_{CO_2} = K_{CO_2} \cdot P_{CO_2} + K_{1CO_2}$$

where $K_{CO_2} = 0.0065$ and $K_{1CO_2} = 0.244$ (Khoo et al. 1982).

The oxygen dissociation curve was approximated by Severinghaus and further modified by Sands et al. for better accuracy

$$S = \frac{1}{\frac{P_{50}^3 + k_1 P_{50}}{P_{O_2}^3 + k_1 P_{O_2}} + 1}$$

where $k_1 = \frac{9P_{50}^3 - P_{90}^3}{P_{90} - 9P_{50}}$ and P_{50} and P_{90} are the partial pressures of oxygen at 50%

and 90% saturation respectively (Sands et al. 2009). The relationship between oxygen saturation and concentration is given by:

$$C_{O_2} = 1.36Hb \cdot S + 0.000031P_{O_2}$$

One molecule of hemoglobin has four binding sites for oxygen. At 100% oxygen saturation each gram of hemoglobin carries 1.36 ml of oxygen, this gives the first term. The second, and much smaller, term comes from the amount of oxygen dissolved in the blood plasma.

Parameter values are given in Table 9 (Delivoria-Papadopoulos, Roncevic & Oski 1971). Figure 24 shows the dissociation curves that are calculated this way.

Table 9: Parameter values for oxygen dissociation

	P_{50} (mmHg)	P_{90} (mmHg)	Hb (g/ml)
Day One	19.4	42.5	0.178
Day Five	20.6	45.5	0.162
3 weeks	22.7	50.2	0.120
6-9 weeks	24.4	53.5	0.105
3-4 months	26.5	58.5	0.102

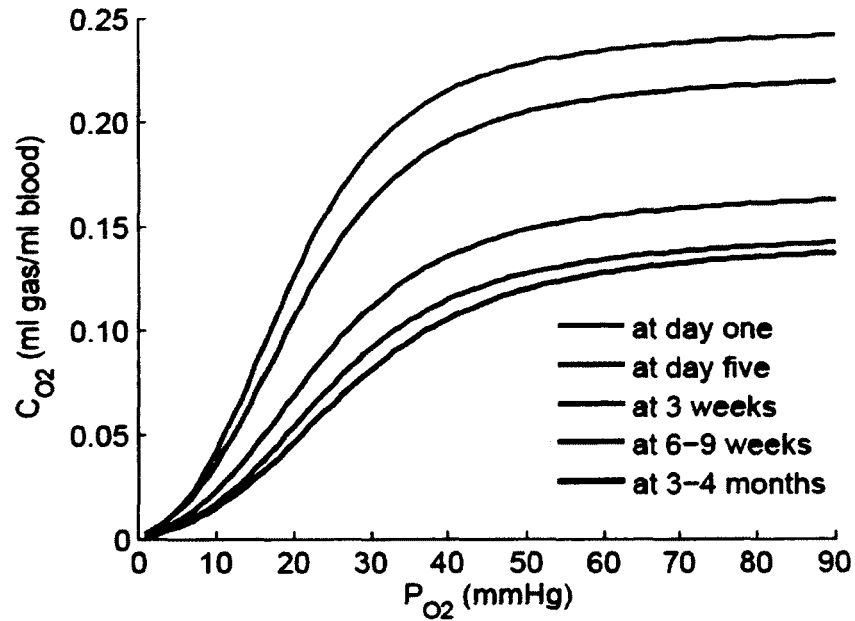


Figure 24: Calculated dissociation curves for oxygen

Development of the periodic breathing model

Equations for the lung, body tissue, and brain compartments are derived using conservation of mass. In the lungs the rate of change of oxygen or carbon dioxide is equal to the rate inhaled minus rate exhaled plus rate coming in from veins minus the rate leaving in arteries. The rate of oxygen or carbon dioxide inhaled or exhaled is equal to the alveolar ventilation rate \dot{V}_A times the fraction of oxygen or carbon dioxide in the air, humidified air for inspiration, alveolar air for exhalation. The fraction we use is the mole fraction, the number of moles of oxygen or carbon dioxide per the total number of moles of air.

In the body tissues the rate of change of oxygen is equal to the rate in from the arteries minus the rate out through the veins minus the rate of metabolic

consumption of oxygen. The rate of change of carbon dioxide in the body tissues is equal to the rate in through the arteries minus the rate out through the veins plus the rate of metabolic production of carbon dioxide. The rate of oxygen coming in through the arteries is equal to the rate that the blood is being pumped, called cardiac output, times the concentration of oxygen in the blood. Similarly, for oxygen out through the veins and carbon dioxide in the arteries and veins.

The rate of change of carbon dioxide in the brain where the central chemoreceptors are located is equal to the rate of carbon dioxide in through the arteries minus the rate out through the veins plus the rate of metabolic production of carbon dioxide in the brain. The blood flow in the brain is smaller than the total blood flow in the arteries and veins. The rate of carbon dioxide in through the arteries is equal to the cerebral blood flow times the concentration of carbon dioxide in the arteries. The rate of carbon dioxide out through the veins is equal to the cerebral blood flow times the venous concentration of carbon dioxide in the brain. Note that while the concentration of carbon dioxide in the arteries of the brain is the same as the concentration in the arteries elsewhere, the concentration in the veins of the brain is not the same as the concentration in the veins elsewhere.

The respiratory controller uses the input received from the chemoreceptors to set the ventilation rate. Periodic breathing arises because of the delay in the time it takes blood from the lungs to reach the chemoreceptors. The controller responds to the amount of carbon dioxide and oxygen at the

chemoreceptors which was the amount at the lungs at some earlier time. During periodic breathing we see the controller responding to low carbon dioxide at the chemoreceptors, but by this time the carbon dioxide at the lungs has already returned to normal. This causes the system to overshoot and by the time the blood with a normal level of carbon dioxide has reached the chemoreceptors and the controller responds to it, the level of carbon dioxide at the lungs has already increased above the normal level. The peripheral control gain and the central control gain govern the intensity of the response to high or low levels of carbon dioxide or oxygen. The ventilatory response is proportional to the control gain times the difference between the detected partial pressure of carbon dioxide and the apneic threshold. If the partial pressure is higher than the apneic threshold the ventilatory response is positive, otherwise it is zero. Higher gains result in a greater change to the ventilation rate increasing the likelihood of periodic breathing.

Mathematical formulation of the periodic breathing model

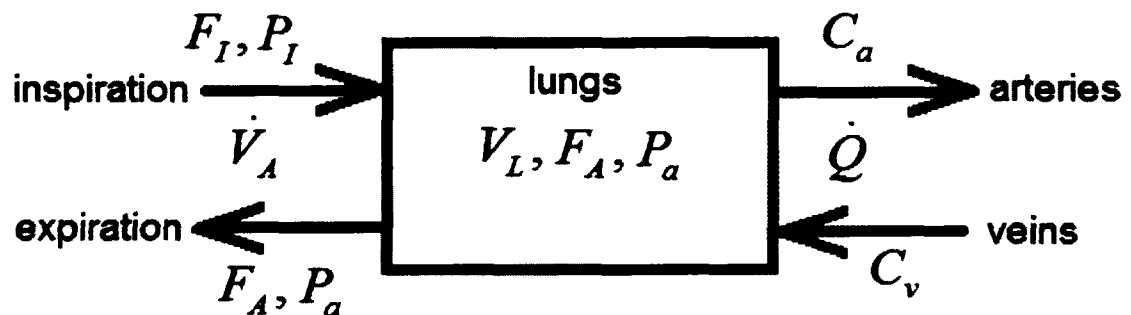


Figure 25: Lung compartment

Conservation of mass gives the following equation for the lung compartment (Figure 25):

$$\frac{dV_A}{dt} = \dot{Q}(C_v - C_a) + \dot{V}_A(F_I - F_A) \quad (4.1)$$

Concentrations are defined as the effective volume of the gas divided by the total storage volume of the gas. Partial pressures and ventilation rates are typically measured at BTPS (body temperature and pressure, saturated with water vapor) while concentrations are measured at STPD (standard temperature and pressure, dry). Giving equation 4.1 with concentration in STPD and all other terms in BTPS introduces a conversion factor of (body temperature) / (standard temperature) = 310.15K / 273.15K.

Equation 4.1 now becomes:

$$\frac{dV_A}{dt} = \left(\dot{Q}(C_v - C_a) \cdot \frac{310.15}{273.15} + \dot{V}_A(F_I - F_A) \right) \quad (4.2)$$

To put equation 4.2 in terms of partial pressures we use

$$F_I = \frac{P_I}{P_B}, \text{ where } P_B \text{ is barometric pressure (760 mmHg), and}$$

$$F_A = \frac{P_a}{P_B} = \frac{V_A}{V_L}, \text{ the second equality gives } \frac{dP_a}{dt} = \frac{dV_A}{dt} \cdot \frac{P_B}{V_L}.$$

Finally we have:

$$\frac{dP_a}{dt} = \left(\frac{\dot{Q}(C_v - C_a)}{V_L} \cdot 863 \text{ mmHg} + \frac{\dot{V}_A(P_I - P_a)}{V_L} \right) \quad (4.3)$$

Equation 4.3 applies to both oxygen and carbon dioxide:

$$\frac{dP_{aCO_2}}{dt} = \left(\frac{\dot{Q}(C_{vCO_2} - C_{aCO_2})}{V_{LCO_2}} \cdot 863 \text{ mmHg} + \frac{\dot{V}_A(P_{iCO_2} - P_{aCO_2})}{V_{LCO_2}} \right) \quad (4.4)$$

$$\frac{dP_{aO_2}}{dt} = \left(\frac{\dot{Q}(C_{vO_2} - C_{aO_2})}{V_{LO_2}} \cdot 863 \text{ mmHg} + \frac{\dot{V}_A(P_{iO_2} - P_{aO_2})}{V_{LO_2}} \right) \quad (4.5)$$

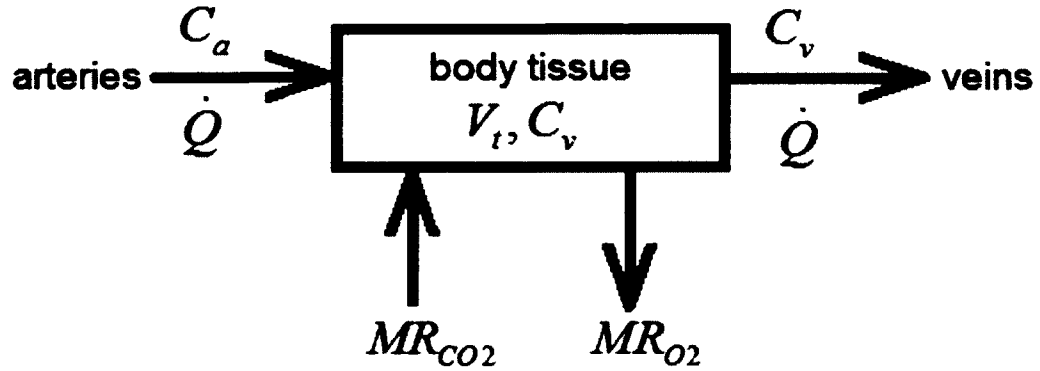


Figure 26: Body tissue compartment

Applying conservation of mass to the body tissue compartment (Figure 26) gives:

$$\frac{dV_{tCO_2}}{dt} = \dot{Q}(C_{aCO_2} - C_{vCO_2}) + MR_{CO_2}$$

Using $V_T = C_v V_t$, we have:

$$\frac{dC_{vCO_2}}{dt} = \frac{\dot{Q}(C_{aCO_2} - C_{vCO_2})}{V_{tCO_2}} + \frac{MR_{CO_2}}{V_{tCO_2}} \quad (4.6)$$

Similarly, for oxygen we have:

$$\frac{dC_{vO_2}}{dt} = \frac{\dot{Q}(C_{aO_2} - C_{vO_2})}{V_{tO_2}} - \frac{MR_{O_2}}{V_{tO_2}} \quad (4.7)$$

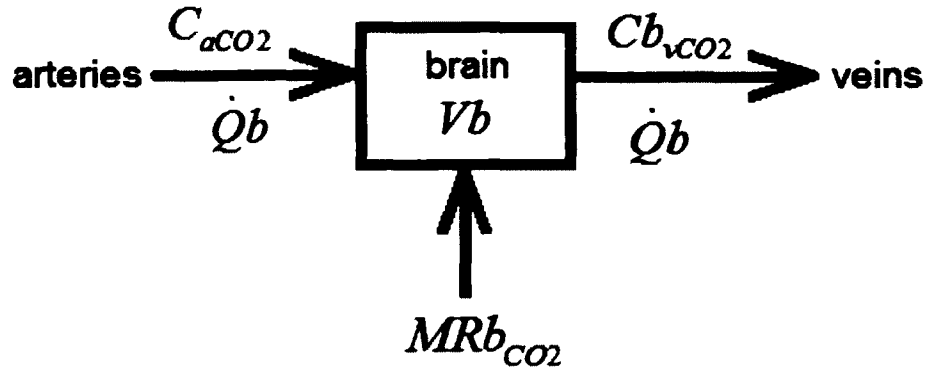


Figure 27: Brain compartment

Applying conservation of mass to the brain compartment (Figure 27) gives:

$$\frac{dCb_{vCO_2}}{dt} = \frac{\dot{Q}b(C_{aCO_2} - Cb_{vCO_2})}{Vb} + \frac{MRb_{CO_2}}{Vb}$$

Using the linear approximation of the carbon dioxide dissociation curve yields:

$$\frac{dPb_{CO_2}}{dt} = \frac{\dot{Q}b(P_{aCO_2}^C - Pb_{CO_2})}{Vb} + \frac{MRb_{CO_2}}{K_{CO_2} \cdot Vb} \quad (4.8)$$

The response of the chemoreceptors takes the form:

$$\dot{V}_P = G_P e^{-0.05P_{aO_2}} (P_{aCO_2}^P - I_P) \quad (4.9)$$

$$\dot{V}_C = G_C (P_{aCO_2}^C - I_C) \quad (4.10)$$

where $\dot{V}_E = \dot{V}_P + \dot{V}_C$ (Khoo et al. 1982, Severinghaus, Crawford 1978, Rebeck,

Slutsky & Mahutte 1977). A negative ventilatory response has no physiological

meaning. If $G_P e^{-0.05P_{aO_2}} (P_{aCO_2}^P - I_P) < 0$, then we say $\dot{V}_P = 0$, and if

$G_C (P_{aCO_2}^C - I_C) < 0$, then we say $\dot{V}_C = 0$.

It has been shown that the central controller responds to carbon dioxide in the brain compartment, Pb_{CO_2} . We can rewrite equation 4.10 in terms of Pb_{CO_2} by using equation 4.8 at steady state.

$$\overline{P_{aCO_2}} = \overline{Pb_{CO_2}} - \frac{MRb_{CO_2}}{K_{CO_2}\dot{Q}b} \quad (4.11)$$

$$\dot{V}_C = G_C \left(Pb_{CO_2} - \frac{MRb_{CO_2}}{K_{CO_2}\dot{Q}b} - I_C \right) \quad (4.12)$$

Time delays

To account for the time it takes for the blood to travel through the arteries and veins, we put the time delays from Table 10 into our set of equations.

Table 10: Time delays

τ_t	lung to tissue delay	8 seconds
τ_v	tissue to lung delay	9 seconds
τ_b	lung to brain delay	4 seconds
τ_p	lung to peripheral receptors delay	3 seconds

With time delays our set of equations becomes:

$$\frac{dP_{aCO_2}(t)}{dt} = \left(\frac{\dot{Q}(C_{vCO_2}(t-\tau_v) - C_{aCO_2}(t))}{V_{lCO_2}} \cdot 863 \text{mmHg} + \frac{\dot{V}_A(P_{lCO_2} - P_{aCO_2}(t))}{V_{lCO_2}} \right) \quad (4.13)$$

$$\frac{dP_{aO_2}(t)}{dt} = \left(\frac{\dot{Q}(C_{vO_2}(t-\tau_v) - C_{aO_2}(t))}{V_{lO_2}} \cdot 863 \text{mmHg} + \frac{\dot{V}_A(P_{lO_2} - P_{aO_2}(t))}{V_{lO_2}} \right) \quad (4.14)$$

$$\frac{dC_{vCO_2}(t)}{dt} = \frac{\dot{Q}(C_{aCO_2}(t-\tau_t) - C_{vCO_2}(t))}{V_{iCO_2}} + \frac{MR_{CO_2}}{V_{iCO_2}} \quad (4.15)$$

$$\frac{dC_{vO_2}(t)}{dt} = \frac{\dot{Q}(C_{aO_2}(t-\tau_t) - C_{vO_2}(t))}{V_{iO_2}} - \frac{MR_{O_2}}{V_{iO_2}} \quad (4.16)$$

$$\frac{dPb_{CO_2}(t)}{dt} = \frac{\dot{Q}b(P_{aCO_2}(t-\tau_b) - Pb_{vCO_2}(t))}{Vb} + \frac{MRb_{CO_2}}{K_{CO_2} \cdot Vb} \quad (4.17)$$

$$\dot{V}_A = \dot{V}_E - \dot{V}_D = G_P e^{-0.05 P_{aCO_2}^P} (P_{aCO_2}^P - I_P) + G_C \left(Pb_{CO_2}(t) - \frac{MRb_{CO_2}}{K_{CO_2} \dot{Q}b} - I_C \right) - \dot{V}_D \quad (4.18)$$

$$P_{aCO_2}^C = P_{aCO_2}(t - \tau_b) \text{ and } P_{aCO_2}^P = P_{aCO_2}(t - \tau_p)$$

Running the model

When a disturbance is added to the system, equations 4.13 – 4.18 give the oscillatory behavior shown in figure 28. Although we included time delays in the periodic breathing model, we did not include the effects of the mixing of blood in the arteries and veins. The partial pressures and the ventilatory rate shown in figure 28 have a wide range. Including the effects of mixing would smooth out these oscillations and give a smaller. Furthermore, the measured SpO2 is an average over several seconds, so that would further reduce the amplitude of the oscillations.

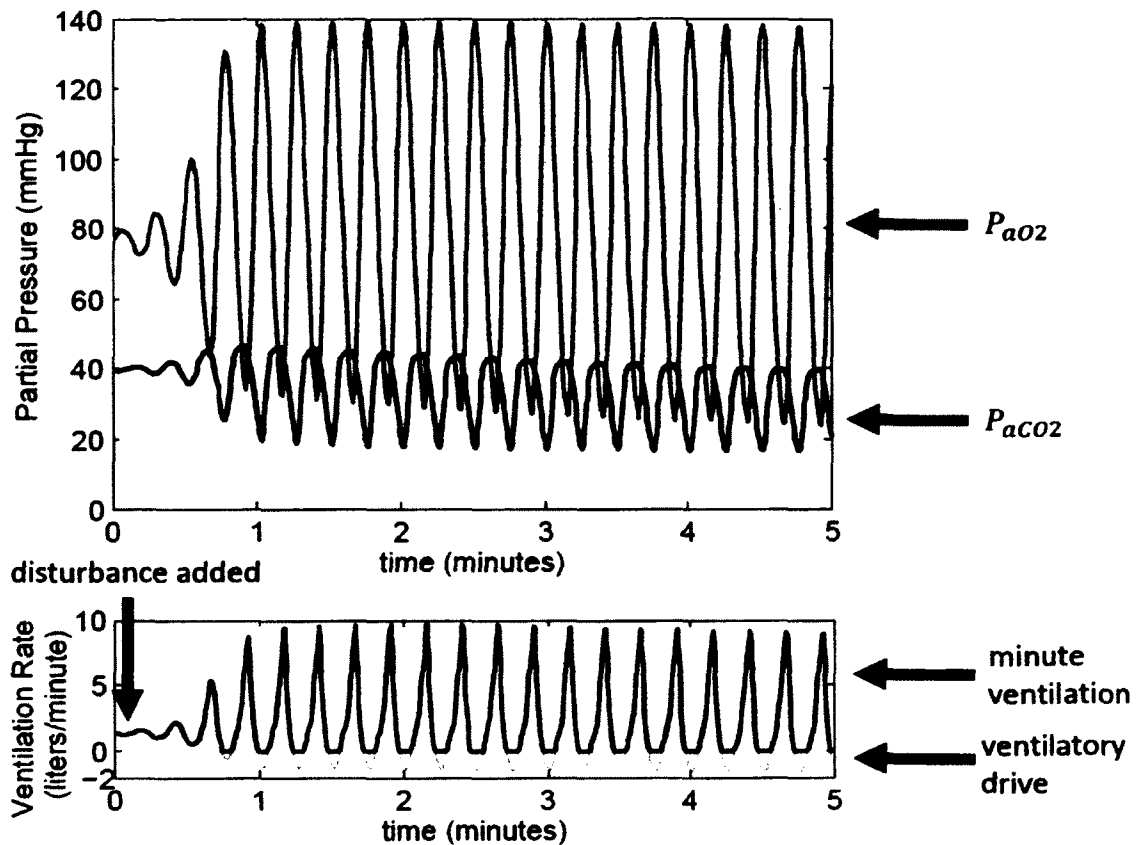


Figure 28: Equations 4.13 – 4.18 give the oscillatory behavior when a small disturbance is added. The disturbance that was added here lasted for the first five seconds. Although the minute ventilation is forced to be positive, the ventilatory drive, which was used in running the model, was allowed to be negative. The values used were for the asleep 2 case given in table 12.

Linearizing the equations

Equations 4.13, 4.14, and 4.18 are nonlinear. To evaluate the model we linearize these equations using a Taylor series expansion. We can use the linearized equation to analyze the model analytically around a steady state. The linear equations give a good approximation as long as we stay close to the steady state. If we move too far away then our linearized equations will no longer apply.

Using a Taylor series expansion to linearize equation 4.13 we get:

$$\frac{dP_{aCO_2}(t)}{dt} = \left(\frac{\dot{Q}(C_{vCO_2}(t - \tau_v) - C_{aCO_2}(t))}{V_{LCO_2}} \cdot 863 \text{ mmHg} + \frac{\dot{V}_A P_{ICO_2} - \bar{\dot{V}}_A P_{aCO_2}(t) - \dot{V}_A \bar{P}_{aCO_2} + \bar{\dot{V}}_A \bar{P}_{aCO_2}}{V_{LCO_2}} \right)$$

We have used the bar above a variable to represent the steady state value.

Equation 4.14 becomes:

$$\frac{dP_{aO_2}(t)}{dt} = \left(\frac{\dot{Q}(C_{vO_2}(t - \tau_v) - C_{aO_2}(t))}{V_{LO_2}} \cdot 863 \text{ mmHg} + \frac{\dot{V}_A P_{IO_2} - \bar{\dot{V}}_A P_{aO_2}(t) - \dot{V}_A \bar{P}_{aO_2} + \bar{\dot{V}}_A \bar{P}_{aO_2}}{V_{LO_2}} \right)$$

Equation 4.18 becomes:

$$\begin{aligned} \dot{V}_A = \bar{\dot{V}}_P - 0.05 G_P e^{-0.05 \bar{P}_{aO_2}^P} \left(\bar{P}_{aCO_2}^P - I_P \right) \left(P_{aO_2}^P - \bar{P}_{aO_2}^P \right) + G_P e^{-0.05 \bar{P}_{aO_2}^P} \left(P_{aCO_2}^P - \bar{P}_{aCO_2}^P \right) \\ + G_C \left(P_{bCO_2}(t) - \frac{MRb_{CO_2}}{K_{CO_2} \dot{Q}_b} - I_C \right) - \dot{V}_D \end{aligned}$$

Loop gain and stability analysis

To evaluate the stability of our system we will introduce a small sinusoidal disturbance. This disturbance could represent an infant yawning or sighing, which could give rise to periodic breathing if the system is unstable. The ratio of the magnitude of the system's response to this disturbance to the magnitude of the disturbance itself is the loop gain. Loop gain is a function of the frequency of the disturbance.

We use the Nyquist stability criterion to evaluate stability when a disturbance with a frequency ω is introduced. The Nyquist stability criterion gives two conditions which must be met for a system to be unstable: (1) The magnitude of the loop gain evaluated at the complex frequency $i\omega$ is at least 1. (2) The polar

angle of the loop gain evaluated at $i\omega$ is 180° . This angle is referred to as the phase lag.

To derive expressions for the loop gain and phase lag we apply a small perturbation such that the total response, $X(t)$, equals a steady state term, \bar{X} , plus the perturbation term, $\tilde{X}(t)$. We then take the Laplace transforms of the resulting equations. We denote the Laplace transform of $X(t)$ as $X(s)$. The Laplace transform of $X(t) = \tilde{X}(t) + \bar{X}$ is $X(s) = \tilde{X}(s) + \frac{1}{s}\bar{X}$. (Recall that the Laplace transform of $\frac{dX(t)}{dt}$ is $sX(s) - \bar{X}$.) We replace C_v and C_a with $K \cdot P_v$ and $K \cdot P_a$ where K is the slope of the dissociation curve at P_v or P_a . For equation 4.3 this gives:

$$\frac{dP_a}{dt} = \left(\frac{\dot{Q}K(P_v - P_a)}{V_L} \cdot 863\text{mmHg} + \frac{\dot{V}_A(P_I - P_a)}{V_L} \right)$$

$$\text{Let } T = \frac{V_L}{863\text{mmHg} \cdot \dot{Q} \cdot K}$$

At steady state equation 4.3 becomes $\frac{dP_a}{dt} = 0 = \frac{(\bar{P}_v - \bar{P}_a)}{T} + \frac{\bar{V}_A(P_I - \bar{P}_a)}{V_L}$, simplifying

gives:

$$\bar{P}_v - \bar{P}_a = -\frac{\bar{V}_A(P_I - \bar{P}_a)}{V_L} T \quad (4.19)$$

Similarly for equations 4.6 and 4.7, letting $T_T = \frac{V_t}{\dot{Q}}$, we have:

$$\overline{P}_a - \overline{P}_v = \mp \frac{MR}{KV_t} T_T \quad (4.20)$$

Taking the Laplace transform of equations 4.6 and 4.7 we have:

$$sP_v(s) - \overline{P}_v = \frac{(P_a(s) - P_v(s))}{T_T} \pm \frac{MR}{V_t K s}$$

Note that $sP_v(s) - \overline{P}_v = s\tilde{P}_v(s)$. Using equation 4.11:

$$\begin{aligned} s\tilde{P}_v(s) &= \frac{1}{T_T} \left(P_a(s) - P_v(s) - \frac{1}{s} (\overline{P}_a - \overline{P}_v) \right) = \frac{1}{T_T} (\tilde{P}_a(s) - \tilde{P}_v(s)) \\ \frac{\tilde{P}_v(s)}{\tilde{P}_a(s)} &= \frac{1}{1 + sT_T} \end{aligned} \quad (4.21)$$

We now turn our attention towards equation 4.3. We replace the term $\dot{V}_A P_a$ with a Taylor expansion keeping only lower order terms, $\overline{V}_A P_a + \dot{V}_A \overline{P}_a - \overline{V}_A \overline{P}_a$. Then, taking the Laplace transform we have:

$$sP_a(s) - \overline{P}_a = \left(\frac{1}{T} (P_v(s) - P_a(s)) + \frac{P_a}{V_L} \dot{V}_A(s) - \frac{1}{V_L} \left(\overline{P}_a \dot{V}_A(s) + \overline{V}_A P_a(s) - \frac{\overline{V}_A \overline{P}_a}{s} \right) \right)$$

Further simplification gives:

$$\tilde{P}_a(s) T \left(s + \frac{\overline{V}_A}{V_L} \right) = \tilde{P}_v(s) - \tilde{P}_a(s) + (\overline{P}_v - \overline{P}_a) \left(\frac{1}{s} - \frac{\dot{V}_A(s)}{\overline{V}_A} \right)$$

Then we substitute using equations 4.19 and 4.21:

$$\tilde{P}_a(s) T \left(s + \frac{\overline{V}_A}{V_L} \right) = \tilde{P}_a(s) \left(\frac{1}{1 + sT_T} - 1 \right) - \left(\frac{\overline{V}_A (P_t - \overline{P}_a)}{V_L} T \right) \left(\frac{1}{s} - \frac{\dot{V}_A(s)}{\overline{V}_A} \right)$$

$$\begin{aligned} \tilde{P}_a(s) \left(sT + \frac{\bar{V}_A}{V_L} T + \frac{sT_T}{1+sT_T} \right) &= - \left(\frac{(P_l - \bar{P}_a)}{V_L} T \right) \left(\frac{\bar{V}_A}{s} - \dot{V}_A(s) \right) = \frac{(P_l - \bar{P}_a)}{V_L} T \tilde{V}_A(s) \\ \frac{\tilde{P}_a(s)}{\tilde{V}_A(s)} &= \frac{(P_l - \bar{P}_a) T}{V_L \left(sT + \frac{\bar{V}_A}{V_L} T + \frac{sT_T}{1+sT_T} \right)} \end{aligned} \quad (4.22)$$

The Laplace transform of equation 4.8 is:

$$s\tilde{P}b_{CO_2}(s) = \frac{\dot{Q}b}{Vb} (P_{aCO_2}^C(s) - Pb_{CO_2}(s)) + \frac{MRb_{CO_2}}{sK_{CO_2}Vb}$$

with $Tb = \frac{Vb}{\dot{Q}b}$ and using equation 4.11:

$$s\tilde{P}b_{CO_2}(s) = \frac{1}{Tb} (P_{aCO_2}^C(s) - Pb_{CO_2}(s)) - \frac{1}{sTb} (\overline{P_{aCO_2}} - \overline{Pb_{CO_2}})$$

$$s\tilde{P}b_{CO_2}(s) = \frac{1}{Tb} (\widetilde{P_{aCO_2}^C}(s) - \widetilde{Pb_{CO_2}}(s))$$

$$\widetilde{P_{aCO_2}^C}(s) = (sTb + 1)\tilde{P}b_{CO_2}(s) \quad (4.23)$$

We come now to the control equations.

Equation 4.12 at steady state is:

$$\bar{V}_C = G_C (\overline{Pb_{CO_2}} - \frac{MRb_{CO_2}}{K_{CO_2}\dot{Q}b} - I_C)$$

thus:

$$I_C = \overline{Pb_{CO_2}} - \frac{MRb_{CO_2}}{K_{CO_2}\dot{Q}b} - \frac{\bar{V}_C}{G_C} \quad (4.24)$$

taking the Laplace transform gives:

$$\dot{V}_C(s) = G_C (Pb_{CO_2}(s) - \frac{MRb_{CO_2}}{sK_{CO_2}\dot{Q}b} - \frac{I_C}{s})$$

substituting equation 4.24:

$$\dot{V}_C(s) = G_C (Pb_{CO_2}(s) - \frac{\overline{Pb_{CO_2}}}{s}) + \frac{\overline{V}_C}{s}$$

$$\widetilde{V}_C(s) = G_C \widetilde{Pb_{CO_2}}(s)$$

using equation 4.23:

$$\widetilde{V}_C(s) = G_C \left(\frac{1}{1 + sTb} \right) \widetilde{P_{aCO_2}^C}(s)$$

For equation 4.9 we let $f_{O_2} = e^{-0.05\overline{P_{aO_2}}}$. Taking the Taylor expansion we get:

$$\dot{V}_P = \overline{V}_P - 0.05G_P f_{O_2} (\overline{P_{aCO_2}} - I_P) (\overline{P_{aO_2}^P} - \overline{P_{aO_2}}) + G_P f_{O_2} (\overline{P_{aCO_2}^P} - \overline{P_{aCO_2}})$$

then the Laplace transform is:

$$\dot{V}_P(s) = \frac{\overline{V}_P}{s} - 0.05G_P f_{O_2} (\overline{P_{aCO_2}} - I_P) \left(P_{aO_2}^P(s) - \frac{\overline{P_{aO_2}}}{s} \right) + G_P f_{O_2} \left(P_{aCO_2}^P(s) - \frac{\overline{P_{aCO_2}}}{s} \right)$$

$$\widetilde{V}_P(s) = -0.05G_P f_{O_2} (\overline{P_{aCO_2}} - I_P) \widetilde{P_{aO_2}^P}(s) + G_P f_{O_2} \widetilde{P_{aCO_2}^P}(s)$$

Let $\widetilde{V}_{PCO_2}(s) = G_P f_{O_2} \widetilde{P_{aCO_2}^P}(s)$ and $\widetilde{V}_{PO_2}(s) = -0.05G_P f_{O_2} (\overline{P_{aCO_2}} - I_P) \widetilde{P_{aO_2}^P}(s)$. Then

$$\widetilde{V}_E = \widetilde{V}_P + \widetilde{V}_C = \widetilde{V}_{PO_2} + \widetilde{V}_{PCO_2} + \widetilde{V}_C.$$

$$\frac{\widetilde{V}_{PO_2}(s)}{\widetilde{P_{aO_2}^P}(s)} = -0.05G_P f_{O_2} (\overline{P_{aCO_2}} - I_P)$$

$$\frac{\widetilde{V}_{PCO_2}(s)}{\widetilde{P_{aCO_2}^P}(s)} = G_P f_{O_2}$$

The loop gain as defined by Khoo et al. is $\frac{\widetilde{V}_E}{\widetilde{V}_A} = \frac{\widetilde{V}_{PCO_2}}{\widetilde{V}_A} + \frac{\widetilde{V}_{PO_2}}{\widetilde{V}_A} + \frac{\widetilde{V}_C}{\widetilde{V}_A}$.

We have three gain terms; one due to the peripheral response to carbon dioxide, one due to the peripheral response to oxygen, and one due to the central response to carbon dioxide.

The peripheral response to carbon dioxide is:
$$LG_{PCO_2} = \frac{\widetilde{V}_{PCO_2}(s) \widetilde{P}_{aCO_2}^P(s) \widetilde{P}_{aCO_2}(s)}{\widetilde{P}_{aCO_2}^P(s) \widetilde{P}_{aCO_2}(s) \widetilde{V}_A(s)}$$

The peripheral response to oxygen is:
$$LG_{PO_2} = \frac{\widetilde{V}_P(s) \widetilde{P}_{aO_2}^P(s) \widetilde{P}_{aO_2}(s)}{\widetilde{P}_{aO_2}^P(s) \widetilde{P}_{aO_2}(s) \widetilde{V}_A(s)}$$

The central response to carbon dioxide is:
$$LG_C = \frac{\widetilde{V}_C(s) \widetilde{P}_{aCO_2}^C(s) \widetilde{P}_{aCO_2}(s)}{\widetilde{P}_{aCO_2}^C(s) \widetilde{P}_{aCO_2}(s) \widetilde{V}_A(s)}$$

Our model includes time delay terms. These terms have a magnitude of one, and thus have no effect on the magnitude of the loop gain, they do however add a phase shift. The time delay terms are $\frac{\widetilde{P}_{aCO_2}^P(s)}{\widetilde{P}_{aCO_2}(s)} = e^{-\tau_p s}$, $\frac{\widetilde{P}_{aO_2}^P(s)}{\widetilde{P}_{aO_2}(s)} = e^{-\tau_p s}$, and

$\frac{\widetilde{P}_{aCO_2}^C(s)}{\widetilde{P}_{aCO_2}(s)} = e^{-\tau_b s}$, with polar angles $-\omega\tau_p$, $-\omega\tau_p$, and $-\omega\tau_b$ respectively.

Our three loop gain expressions are:

$$LG_{PCO_2} = \frac{\widetilde{V}_{PCO_2}(s) \widetilde{P}_{aCO_2}^P(s) \widetilde{P}_{aCO_2}(s)}{\widetilde{P}_{aCO_2}^P(s) \widetilde{P}_{aCO_2}(s) \widetilde{V}_A(s)} = G_P f_{O_2} \cdot e^{-\tau_p s} \cdot \frac{(P_{ICO_2} - \overline{P}_{aCO_2}) T_{CO_2}}{V_{LCO_2} \left(sT_{CO_2} + \frac{\overline{V}_A}{V_{LCO_2}} T_{CO_2} + \frac{sT_{T_{CO_2}}}{1 + sT_{T_{CO_2}}} \right)}$$

$$LG_{PO_2} = \frac{\widetilde{V}_P(s) \widetilde{P}_{aO_2}^P(s) \widetilde{P}_{aO_2}(s)}{\widetilde{P}_{aO_2}^P(s) \widetilde{P}_{aO_2}(s) \widetilde{V}_A(s)} = -0.05 G_P f_{O_2} (\overline{P}_{aCO_2} - I_P) \cdot e^{-\tau_p s} \cdot \frac{(P_{IO_2} - \overline{P}_{aO_2}) T_{O_2}}{V_{LO_2} \left(sT_{O_2} + \frac{\overline{V}_A}{V_{LO_2}} T_{O_2} + \frac{sT_{T_{O_2}}}{1 + sT_{T_{O_2}}} \right)}$$

$$LG_C = \frac{\widetilde{V}_C(s) \widetilde{P}_{aCO_2}^C(s) \widetilde{P}_{aCO_2}(s)}{\widetilde{P}_{aCO_2}^C(s) \widetilde{P}_{aCO_2}(s) \widetilde{V}_A(s)} = G_C \left(\frac{1}{1+sT_b} \right) \cdot e^{-\tau_b s} \cdot \frac{(P_{ICO_2} - \overline{P}_{aCO_2}) T_{CO_2}}{V_{LCO_2} \left(sT_{CO_2} + \frac{\widetilde{V}_A}{V_{LCO_2}} T_{CO_2} + \frac{sT_{TCO_2}}{1+sT_{TCO_2}} \right)}$$

The model and loop gain analysis is based on work by Khoo et al. and Batzel and Tran (Batzel, Tran 2000, Khoo et al. 1982). We used this theory to calculate loop gain based on estimated parameter values for an awake four month old infant (Batzel, Tran 2000). To evaluate the effect that each parameter has on the loop gain we changed parameter values one at a time and calculated the resulting loop gain. Changing only one parameter is not physiologically accurate. If one parameter changes it will cause some of the others to also change. For instance, raising the inspired partial pressure of oxygen would cause the arterial partial pressure of oxygen to rise also. Nevertheless, this analysis gives us an idea of the parameters that have the greatest effect on loop gain. The results are shown in Table 11. The parameters that had the greatest effect on the loop gain were (in decreasing order): P_{aO_2} , P_{aCO_2} , I_P , P_{IO_2} , T_P , G_P , V_{LO_2} , and τ_b . Central and peripheral control gains (G_C and G_P) can vary widely across individuals (Khoo et al. 1982). These results are typical of what is seen in periodic breathing modeling with excessive time delays, high gain factors, low lung volume, and large differences between inspired and arterial partial pressures all increasing loop gain and the peripheral chemoreceptors (G_P and I_P) having a much larger effect than the central chemoreceptors (G_C and I_C) (Edwards, Sands & Berger 2013, Khoo et al. 1982).

Table 11: Change in loop gain (parameter values for awake 4 month old)

parameter changed by:		-15%	-5%	5%	15%
parameter	original value	change in loop gain (from 0.16 at original values)			
G_p	2 liters/min/mmHg	-13%	-4%	4%	13%
G_c	0.1 liters/min/mmHg	-0.4%	-0.1%	0.1%	0.2%
I_p	26 mmHg	34%	11%	-11%	-33%
I_c	26 mmHg	-5%	-2%	2%	4%
τ_p	3 seconds	-18%	-6%	6%	16%
τ_b	4 seconds	5%	2%	-2%	-6%
\dot{Q}	1.16 liters/min	5%	2%	-1%	-4%
V_{LCO_2}	0.11 liters	-1%	-0.3%	0.2%	1%
V_{LO_2}	0.92 liters	12%	4%	-3%	-9%
P_{IO_2}	150 mmHg	-29%	-10%	10%	30%
P_{aCO_2}	34 mmHg	-46%	-15%	14%	38%
P_{aO_2}	96 mmHg	132%	32%	-24%	-53%
\dot{V}_D	0.54 liters/min	-1%	-0.4%	0.3%	1%

In all cases: $\dot{Q}_b = 0.24$ liters/min, $V_b = 0.10$ liters, $P_{Ico_2} = 0$ mmHg, $V_{Ico_2} = 1.05$ liters, $V_{IO_2} = 0.24$ liters. Parameter values from Batzel and Tran (Batzel, Tran 2000).

During sleep P_{aO_2} , \dot{Q} , and \dot{Q}_b are lower. In the asleep 1 case in Table 12 these parameter values are changed, with \dot{Q} and \dot{Q}_b 5% lower than the awake 1 case and $P_{aO_2} = 79$ mmHg (Batzel, Tran 2000). In the asleep 1 case loop gain is higher but still less than one. Also shown in Table 12 are both an awake and an asleep case in which periodic breathing could arise. The parameter values for the awake 2 and the asleep 2 cases are based on changes that are seen for awake and asleep cases in adults in Khoo et al. (Khoo et al. 1982).

Table 12: Parameter values for loop gain analysis

parameter	unit	awake 1	awake 2	asleep 1	asleep 2
G_p	liters/min/mmHg	2	2	2	2
I_p	mmHg	26	26	26	26
G_c	liters/min/mmHg	0.1	0.1	0.1	0.1
I_c	mmHg	26	26	26	32*
τ_p	seconds	3	3	3	3.5*
τ_b	seconds	4	4	4	4.5*
\dot{Q}	liters/min	1.16	1.16	1.10*	1.10
V_{LCO_2}	liters	0.11	0.11	0.11	0.08*
V_{LO_2}	liters	0.092	0.092	0.092	0.07*
P_{IO_2}	mmHg	150	150	150	150
P_{aCO_2}	mmHg	34	34	34	40*
P_{aO_2}	mmHg	96	62*	79*	77*
\dot{V}_D	liters/min	0.54	0.54	0.54	0.42*
\dot{Q}_b	liters/min	0.24	0.24	0.228*	0.228
loop gain		0.16	1.2	0.44	1.04

* indicates a change from the preceding column

We have presented a model of periodic breathing in infants and analyzed stability in the model. Comparing the loop gain at 180° in the awake 1 case to the loop gain in the asleep 1 case, where the values of P_{aO_2} , \dot{Q} , and \dot{Q}_b have been decreased, shows that the loop gain increases from 0.16 to 0.44, bringing the loop gain closer to 1 where the system is unstable and periodic breathing could arise. In the awake 2 and the asleep 2 case the loop gain is greater than 1. Periodic breathing may arise in both while the infant is awake while the infant is asleep. Measurements of parameter values could help to determine infants who are more likely to have periodic breathing.

Chapter 5

Clinical Correlates of Excessive Periodic Breathing

The periodic breathing detection algorithm was applied to the entire dataset. Our goals were to quantify periodic breathing in preterm infants throughout their stay in the NICU, and to identify clinical correlations with excessive periodic breathing. We focused our study of clinical correlations to infants who were <35 weeks' gestation. 1372 infants <35 weeks' gestation were admitted to the UVa NICU from 2009-2014. Data was available for periodic breathing analysis in 1268 of these infants. 1196 of them (94%) had some detected periodic breathing Figure 29.

When the periodic breathing detection algorithm was applied to the dataset the start time and duration of every detected event was recorded. At all times when data was available for analysis the percent of periodic breathing, defined as the time spent in periodic breathing divided by the amount of data available for analysis, was calculated. Time during which the infant was on a ventilator was excluded, as this prevents periodic breathing. We evaluated the amount of periodic breathing that infants had by gestational age. Figure 30 shows the amount of periodic breathing by PMA and GA. We found that infants who were born at around 32 weeks gestation had the most periodic breathing.

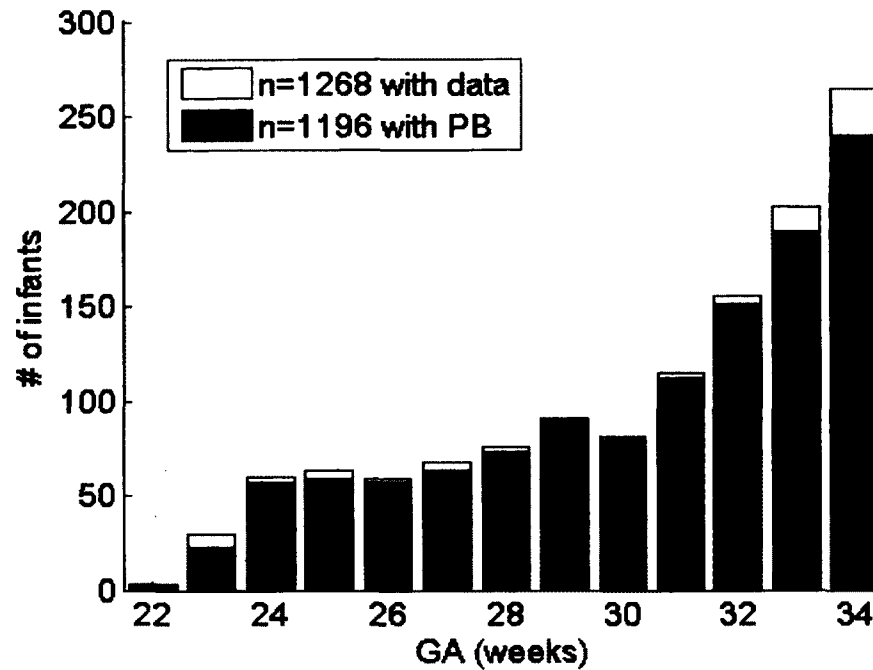


Figure 29: Infants with data available for analysis and with periodic breathing detected by gestational age (GA).

For gestational ages from 23 to 32 weeks periodic breathing increases with gestational age. Additionally, it was seen that periodic breathing typically peaks at about 2-4 weeks after birth. Figure 31 compares the percent of periodic breathing to the number of ABD10s per day. Periodic breathing peaks at a postmenstrual age of 34 to 35 weeks, while ABD10s peaks earlier.

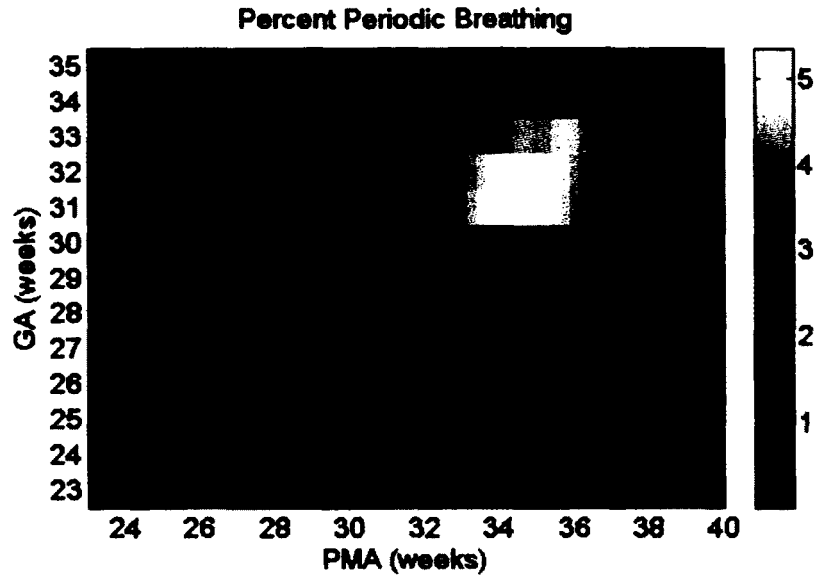


Figure 30: Mean percent of time in periodic breathing for infants based on gestational age and postmenstrual age

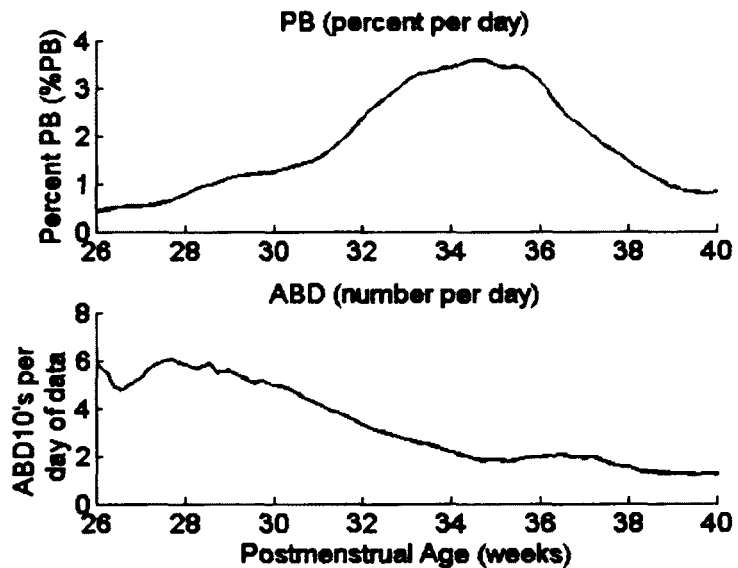


Figure 31: Percent of periodic breathing and number of ABD10s per day by postmenstrual age. Periodic breathing peaks at a later postmenstrual age than ABD10s.

The results of our quantification of periodic breathing in our population of infants allowed us to establish what is a normal amount of periodic breathing. We used these results to find cases of excessive periodic breathing. We defined

excessive periodic breathing as a z-score greater than 6 (more than 6 standard deviations above the mean for that GA and PMA) and at least 10% periodic breathing during a 12 hour period in which there was at least 6 hours of data available for analysis. By this definition extreme periodic breathing was identified in 76 infants. The clinical records of the 76 infants with excessive periodic breathing and the 1192 infants who had no excessive periodic breathing were examined. Table 13 compares the clinical characteristics in these two groups.

Table 13: Clinical characteristics of infants with and without excessive periodic breathing (PB)

Demographics and clinical events	Excessive PB (n=76) median (25th-75th%) or n (%)	No Extreme PB (n=1192) median (25th-75th%) or n (%)
Gestational age (weeks)	28 (25-30)	32 (28-33)
Birthweight	1075 (833-1440)	1603 (1120-2060)
Late onset sepsis	9 (11.8%)	81 (6.8%)
NEC	9 (11.6%)	33 (2.8%)
Severe IVH	6 (7.9%)	45 (3.8%)
BPD	20 (26%)	223 (19%)
Death prior to NICU discharge	3 (3.9%)	47 (3.9%)

The clinical records of patients with excessive periodic breathing were also examined for clinical events that occurred within 24 hours of the 12 hour period when periodic breathing was the highest. In Table 14 it is shown that 34 infants (45%) had some clinical event occurring within 24 hours of excessive periodic breathing. One infant died suddenly (of presumed sepsis) while in the NICU. This infant had excessive periodic breathing in the hours preceding death. Of the 42 infants for which there was no clinical event within 24 hours of the excessive periodic breathing episode, 4 had severe IVH and one died of SIDS

five weeks after being discharged from the NICU. This is the only known case of SIDS after discharge from the UVa NICU.

Table 14: Clinical events near the time of excessive periodic breathing

Event	Number
Late onset sepsis \pm 24h	1
NEC \pm 24h	1
Suspected infection or NEC \pm 24h	8
Death within 24h	1
Surgery <24h prior	3
Immunization <24h prior	9
Caffeine stopped <8 days prior	11
No event identified	42
TOTAL	76

The patient who died of SIDS had periodic breathing almost continuously during her 2 week stay in the NICU and spent 40% of the time in periodic breathing from day 7 to 14 after birth (Figure 32). This patient was still spending 36% of the time in periodic breathing at discharge. This patient was a twin. The twin of the infant who died of SIDS spent 15% of the time in periodic breathing during the second week of life. Other infants born at the same gestational age, 32 weeks, spent on average 5% of the time in periodic breathing during the second week of life. The patient who died of SIDS had no evidence of neurologic, cardiovascular, or other pathology based on her clinical course in the NICU or on autopsy. It was only on retrospective review of the patient's data that the excessive amounts of periodic breathing were revealed.

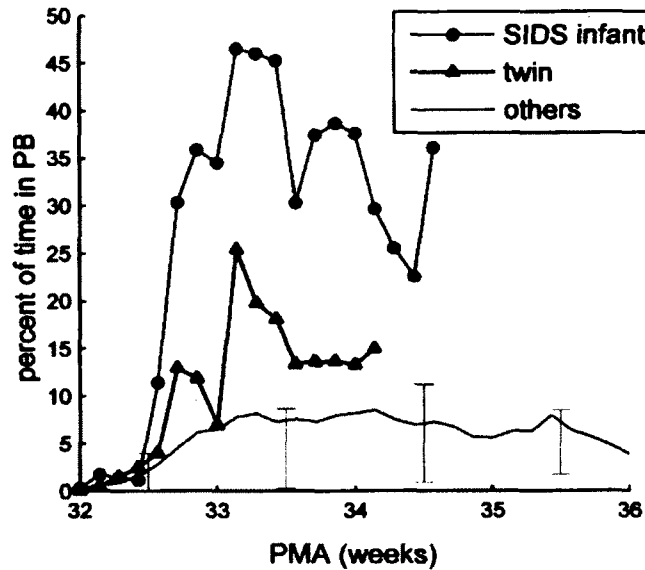


Figure 32: Percent of periodic breathing for SIDS infant and gestational age-matched infants. The percent of time spent in periodic breathing (time periodic breathing index ≥ 0.6 / time data available) is shown based on post-menstrual age (PMA) for the infant that died of SIDS 2 weeks after NICU discharge, her twin sister, and all other infants born at 32 weeks' gestation ($n=68$). The 25th and 75th percentiles every week for all other infants of 32 weeks' gestation are indicated with error bars ($n=35-62$). (Reproduced from Mohr et al. 2015a.)

Our analysis of extreme periodic breathing suggested an association between periodic breathing and necrotizing enterocolitis (NEC) and also periodic breathing and late onset sepsis (LOS). We identified all cases of NEC and LOS in the 1268 infants <35 weeks' gestation with data available for periodic breathing analysis. Periodic breathing was evaluated in the 72 hours before diagnosis. We required that data was available for at least 50% of the time and excluded cases where infants were on a ventilator. There were 20 cases of NEC and 28 cases of LOS. Periodic breathing in the 24 hours before diagnosis was compared to the baseline value of periodic in the 78 to 24 hours before diagnosis. In 26 cases of LOS, periodic breathing increased in 11 cases. The increase was greater than

two-fold in 9 cases. The Wilcoxon sign rank test was used to test whether there was a significant increase in periodic breathing in the 24 hours before diagnosis compared to the 24-72 hours before diagnosis. The p-value was >0.1 , indicating that periodic breathing might often rise before LOS, but our data does not establish such a relationship to within the desired p-value of 0.05. In 20 cases of NEC, periodic breathing increased in 14 cases. In 8 cases of NEC the increase was greater than two-fold. The Wilcoxon sign rank test gives a p-value of 0.02, indicating that there may be a significant rise in the amount of periodic breathing before diagnosis of NEC.

The infant that died of presumed sepsis had over a 10-fold increase in periodic breathing in the 18 hours before death. Aside from this exceptional case, the correlation between increased periodic breathing seems to be greater with NEC than with sepsis. Figures 33 and 34 show increases in periodic breathing in cases of sepsis and NEC.

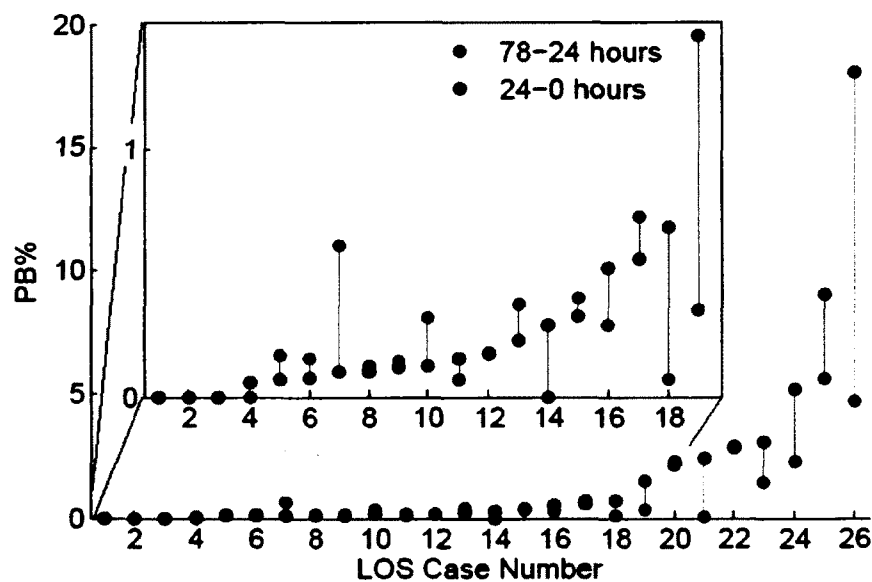


Figure 33: Percent of periodic breathing (PB%) in the 78 hours before diagnosis of LOS.

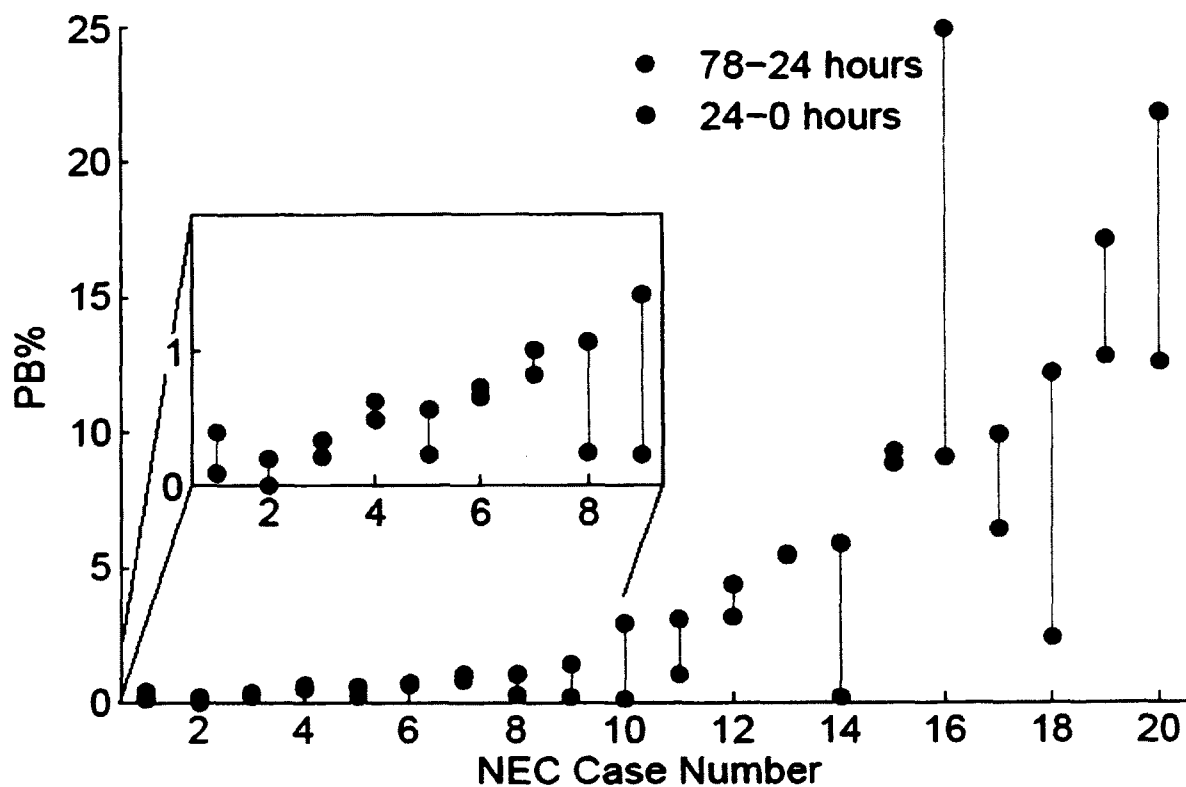


Figure 34: Percent of periodic breathing (PB%) in the 78 hours before diagnosis of NEC.

Summary

A new method of detecting periodic breathing was presented. This method allowed us to quantify periodic breathing in a large number of infants over a long period of time. We found that periodic breathing increases with gestational age up to 32 weeks gestation, infants born at this age have the most periodic breathing. We identified infants that had excessive periodic breathing. Clinical correlations were analyzed in these infants. The clinical records of these infants were examined throughout their entire stay and after discharge. Correlations within 24 hours of the highest 12 hour period of periodic breathing were also

analyzed. The results of these examination suggested possible correlations between periodic breathing and LOS or NEC. We studied 26 cases of LOS and 20 cases of NEC. Periodic breathing increased before 11 cases of sepsis and 14 cases of NEC. The correlation between increased periodic breathing and NEC appears to be strong among the study cohort. Real time analysis of periodic breathing in the NICU may result in earlier detection of some cases of NEC. Two infants who had excessive periodic breathing later died. One had high amounts of periodic breathing throughout her NICU course and died of SIDS after discharge. The other had excessive periodic breathing in the 18 hours before death of presumed sepsis. Excessive periodic breathing may be an indication of an immediate or future illness.

Chapter 6

Future Directions

The data collected from the University of Virginia's NICU over the past five years has allowed us to make advances in the detection of apnea and periodic breathing. Currently this detection is only taking place on the data after it is collected and stored. In the future we would like this detection to take place in real-time at the patient's bedside. Our goal is to find new ways of predictive monitoring. Reliable detection of apnea and periodic breathing at the bedside is the next step in putting our findings into practice.

The study of very long apneas in infants led us to develop and test a theory of the rate of decrease of SpO₂ in those events. The theory gives a good account of observations of averages of many events, and it works just as well for short events as for long events. We have not yet applied the theory to individual cases. This is potentially a very valuable thing to do. The theory could be used to fit the rate of decline of SpO₂ to individual events in individual infants. Such a fit involves two parameters, the coefficient C in equation 2.2 (which is primarily related to cardiac output) and S_v , the venous oxygen saturation (which is affected by the respiration rate and the metabolism rate). Such fits might provide a means for monitoring those physiological parameters, which otherwise cannot be measured non-invasively.

Turning now to periodic breathing, in the past, even large amounts of periodic breathing in NICU patients has largely gone unnoticed and unrecorded. Our work has raised awareness among the clinicians at University of Virginia and they now pay closer attention to periodic breathing. Running the periodic breathing detector real-time in the NICU would allow clinicians to see how much time an infant is been spending in periodic breathing and alert them to cases of excessive periodic breathing. It is reasonable to hope that real-time detection of periodic breathing could lead leads to early warning of NEC.

Fitting the model of periodic breathing to an individual infant's data may allow us to determine the values of the parameters that are used in the periodic breathing model. Future studies could explore whether parameter values differ in infants who have excessive periodic breathing. It is possible that the infant who died of SIDS had abnormal parameter values that put the infant at risk for SIDS.

Future studies could also explore possible differences in the appearance of periodic breathing. We have not yet explored whether the cycle length is different in excessive periodic breathing. It would also be of interest to look at the breathing spells. These spells sometimes show a "spindle" pattern analogous to the "crescendo-diminuendo" pattern of Cheyn-Stokes breathing, and in other cases begin with a sudden deep breath that is larger in amplitude than those that follow. It is not known whether such distinctive patterns have clinical or physiological significance.

Real-time detection of apnea events and of periodic breathing in the NICU, together with the application of mathematical models, may help us to uncover new knowledge of the physiology of infants, and may allow early warning of pathology and therefore earlier and more effective treatment.

Appendix A

Table 15: Infant IDs, start times, and durations of VLAs. Start time is given as seconds from midnight. Days are measured continuously over the entire dataset. Duration is weighted apnea duration (WAD), area under probability of apnea signal divided by duration of apnea. (See page 18 for definitions.)

ID	WAD	Day	Start
1132	72	40	11348
1145	81	76	65708
1145	64	76	65925
1145	72	76	66064
1147	61	41	78682
1147	90	42	26769
1148	88	60	45101
1148	90	60	74766
1153	119	47	78341
1153	80	47	79819
1153	80	55	59302
1154	61	57	10327
1154	89	69	85629
1154	80	71	53899
1154	88	73	61938
1154	71	86	48683
1202	85	115	76317
1231	87	105	50852
1231	67	106	69566
1231	86	107	2457
1231	65	107	22152
1231	80	107	49305
1231	62	113	22446
1231	94	114	1720
1231	67	115	49848
1231	101	115	74516
1231	68	116	75890
1231	61	117	58296
1231	67	118	67560
1231	91	119	35901
1231	80	120	9907
1231	71	122	52983
1231	84	123	10063
1231	75	126	2665
1231	78	126	70351
1231	63	127	9573
1232	72	99	27516
1253	71	170	73168
1269	98	128	45080
1339	78	182	59465
1339	63	182	80014
1339	87	183	15970
1339	67	187	60791

ID	WAD	Day	Start
1339	77	189	2222
1339	64	189	5853
1339	72	189	15734
1339	69	190	3963
1339	88	190	8152
1339	130	190	8683
1339	97	190	9429
1339	96	190	10351
1341	85	185	46446
1341	92	185	53230
1341	74	185	58246
1344	70	192	53031
1451	65	243	60025
1251	88	126	58901
1251	96	126	85973
1251	71	127	49219
1509	78	279	84136
1509	68	280	8787
1509	88	280	13706
1509	78	280	20481
1859	61	535	5236
1859	66	539	1358
1979	63	577	32891
2050	86	613	49057
2110	69	649	56573
2110	81	661	47811
2122	97	659	10460
2123	74	650	52350
2123	67	652	19641
2123	104	652	26778
2123	62	689	14444
2150	62	665	8912
2150	70	686	13998
2166	73	678	21918
2172	67	674	83095
2275	75	771	72912
2275	72	771	78434
2275	64	776	59849
2307	64	790	27627
2307	70	791	10922
2307	118	791	47112
2308	95	788	13884
2308	62	789	4648

Appendix B

Table 16: Mean percent of time in periodic breathing (%) by gestational age and postmenstrual age

		Gestational age (weeks)												
		23	24	25	26	27	28	29	30	31	32	33	34	35
Postmenstrual age (weeks)	24	0.4	0.4	-	-	-	-	-	-	-	-	-	-	-
	25	0.3	0.4	0.4	-	-	-	-	-	-	-	-	-	-
	26	0.3	0.4	0.4	0.4	-	-	-	-	-	-	-	-	-
	27	0.4	0.6	0.5	0.5	0.4	-	-	-	-	-	-	-	-
	28	0.6	0.8	0.8	0.7	0.7	0.8	-	-	-	-	-	-	-
	29	1	1	1	1	1.2	1.2	1.3	-	-	-	-	-	-
	30	1.2	1.1	1.1	1	1.4	1.4	1.4	1.1	-	-	-	-	-
	31	1.2	1.2	1.1	1.1	1.5	1.8	2	1.7	1.5	-	-	-	-
	32	1.5	1.5	1.3	1.4	1.9	2.5	2.9	2.8	2.7	2.6	-	-	-
	33	1.7	1.6	1.3	1.6	2.3	3.1	3.4	3.8	4.2	3.8	3.6	-	-
	34	1.6	1.7	1.4	1.9	2.3	2.9	3.2	3.9	5.2	4.9	4	3	-
	35	1.4	1.5	1.3	1.8	2	2.5	2.6	3.8	5.1	5.4	4.4	3.4	2.6
	36	1.5	1.4	1.1	1.3	1.6	2.1	2.3	3.3	4.3	4.5	4.7	3.4	2.7
	37	1.6	1.4	1.1	1	1.4	2	2.3	2.5	3.1	3.3	3.5	3.1	2.3
	38	1.1	1	0.8	0.8	1.3	2.1	2.1	1.8	2	2.2	2.2	2.3	2.1
39	0.8	0.7	0.6	0.7	1.1	1.5	1.4	1	0.8	0.8	0.9	1.6	1.3	
40	0.9	0.7	0.7	0.6	0.9	1.2	1.2	0.9	0.6	0.6	0.6	1.3	1	

Table 17: Infant IDs and diagnosis times for infants with late onset sepsis. Diagnosis time is given as seconds from midnight. Days are measured continuously over the entire dataset.

ID	Case #	Day	Diagnosis time
1089	16	46	55560
1132	23	40	31860
1138	7	102	71100
1147	22	56	6300
1315	11	193	83580
1331	1	238	900
1341	10	244	0
1394	4	236	63840
1837	26	489	5760
1927	2	555	39600
1977	8	590	80100
1977	13	601	65340
2148	21	723	7200
2154	6	669	50400
2672	24	1030	7740
2690	3	1092	77160
2690	14	1142	48600
2945	17	1198	36660
2964	25	1223	60720
3183	20	1365	69180
3296	12	1434	0
3482	9	1550	55260
3598	18	1624	84540
3804	15	1730	39540
3837	19	1733	53280
3979	5	1840	71520

Table 18: Infant IDs and diagnosis times for infants with necrotizing enterocolitis. Diagnosis time is given as seconds from midnight. Days are measured continuously over the entire dataset.

ID	Case #	Day	Diagnosis time
1181	16	88	61020
1209	14	106	45120
1209	15	122	31020
1210	17	89	67020
1241	5	134	6480
1241	8	170	76980
1262	19	130	11760
1837	12	493	1860
2122	13	695	1920
2204	20	725	22020
2291	10	762	52260
2308	4	802	70560
2495	2	891	900
2957	7	1239	24960
3002	6	1235	25560
3076	18	1293	54300
3097	9	1306	51960
3187	1	1359	3000
3296	3	1434	49380
3385	11	1495	38100

References

- Ainslie, P.N., Lucas, S.J. & Burgess, K.R. 2013, "Breathing and sleep at high altitude", *Respiratory physiology & neurobiology*, vol. 188, no. 3, pp. 233-256.
- Al-Matary, A., Kutbi, I., Qurashi, M., Khalil, M., Alvaro, R., Kwiatkowski, K., Cates, D. & Rigatto, H. 2004, "Increased peripheral chemoreceptor activity may be critical in destabilizing breathing in neonates", *Seminars in perinatology*, vol. 28, no. 4, pp. 264-272.
- Anderson, P., Kleinman, C., Lister, G. & Talner, N. 1998, "Cardiovascular Function During Normal Fetal and Neonatal Development and with Hypoxic Stress" in *Fetal and neonatal physiology*, eds. R.A. Polin & W.W. Fox, Elsevier, , pp. 837.
- Barrington, K.J. & Finer, N.N. 1990, "Periodic breathing and apnea in preterm infants", *Pediatric research*, vol. 27, no. 2, pp. 118-121.
- Batzel, J. & Tran, H. 2000, "Modeling instability in the control system for human respiration: applications to infant non-REM sleep", *Applied mathematics and computation*, vol. 110, no. 1, pp. 1-51.
- Ben-Tal, A. & Smith, J.C. 2010, "Control of breathing: two types of delays studied in an integrated model of the respiratory system", *Respiratory physiology & neurobiology*, vol. 170, no. 1, pp. 103-112.
- Berger, K.I., Ayappa, I., Sorkin, I.B., Norman, R.G., Rapoport, D.M. & Goldring, R.M. 2000, "CO(2) homeostasis during periodic breathing in obstructive sleep apnea", *Journal of applied physiology (Bethesda, Md.: 1985)*, vol. 88, no. 1, pp. 257-264.
- Carley, D.W. & Shannon, D.C. 1988, "A minimal mathematical model of human periodic breathing", *Journal of applied physiology (Bethesda, Md.: 1985)*, vol. 65, no. 3, pp. 1400-1409.
- Cherniack, N.S. & Longobardo, G.S. 2006, "Mathematical models of periodic breathing and their usefulness in understanding cardiovascular and respiratory disorders", *Experimental physiology*, vol. 91, no. 2, pp. 295-305.
- Cherniack, N., Longobardo, G. & Evangelista, C. 2005, "Causes of Cheyne-stokes respiration", *Neurocritical care*, vol. 3, no. 3, pp. 271-279.
- Darnall, R.A., Kattwinkel, J., Nattie, C. & Robinson, M. 1997, "Margin of safety for discharge after apnea in preterm infants", *Pediatrics*, vol. 100, no. 5, pp. 795-801.
- Delivoria-Papadopoulos, M. & McGowan, J. 2011, "Oxygen transport and delivery" in *Fetal and neonatal physiology*, eds. R.A. Polin, W.W. Fox & S. Abman, Elsevier-Saunders, , pp. 970.
- Delivoria-Papadopoulos, M., Roncevic, N.P. & Oski, F.A. 1971, "Postnatal changes in oxygen transport of term, premature, and sick infants: the role of red cell 2, 3-diphosphoglycerate and adult hemoglobin", *Pediatric research*, vol. 5, no. 6, pp. 235-245.
- Dowell, A.R., Buckley, C.E., Cohen, R., Whalen, R.E. & Sieker, H.O. 1971, "Cheyne-Stokes respiration: a review of clinical manifestations and critique of physiological mechanisms", *Archives of Internal Medicine*, vol. 127, no. 4, pp. 712-726.

- Edwards, B.A., Sands, S.A. & Berger, P.J. 2013, "Postnatal maturation of breathing stability and loop gain: the role of carotid chemoreceptor development", *Respiratory physiology & neurobiology*, vol. 185, no. 1, pp. 144-155.
- Eichenwald, E.C., Aina, A. & Stark, A.R. 1997, "Apnea frequently persists beyond term gestation in infants delivered at 24 to 28 weeks", *Pediatrics*, vol. 100, no. 3 Pt 1, pp. 354-359.
- Finer, N.N., Higgins, R., Kattwinkel, J. & Martin, R.J. 2006, "Summary proceedings from the apnea-of-prematurity group", *Pediatrics*, vol. 117, no. Supplement 1, pp. S47-S51.
- Fowler, A.C. & Kalamangalam, G.P. 2002, "Periodic breathing at high altitude", *IMA journal of mathematics applied in medicine and biology*, vol. 19, no. 4, pp. 293-313.
- Fowler, A.C. & Kalamangalam, G.P. 2000, "The role of the central chemoreceptor in causing periodic breathing", *IMA journal of mathematics applied in medicine and biology*, vol. 17, no. 2, pp. 147-167.
- Francis, D.P., Willson, K., Davies, L.C., Coats, A.J. & Piepoli, M. 2000, "Quantitative general theory for periodic breathing in chronic heart failure and its clinical implications", *Circulation*, vol. 102, no. 18, pp. 2214-2221.
- Girling, D.J. 1972, "Changes in heart rate, blood pressure, and pulse pressure during apnoeic attacks in newborn babies", *Archives of Disease in Childhood*, vol. 47, no. 253, pp. 405-410.
- Glotzbach, S., Tansey, P., Baldwin, R. & Ariagno, R. 1989, "Periodic breathing cycle duration in preterm infants", *Pediatric research*, vol. 25, no. 3, pp. 258-261.
- Grodins, F.S., Gray, J.S., Schroeder, K.S., Norins, A.L. & Jones, R.W. 1954, "Respiratory Responses to CO₂ Inhalation. A Theoretical Study of a Nonlinear Biological Regulator", *Journal of applied physiology*, vol. 7, pp. 283.
- Hall, J.E. & Guyton, A.C. 2011, *Guyton and Hall Textbook of Medical Physiology*, 12th edn, Saunders/Elsevier, Philadelphia, PA.
- Hermann, D.M., Siccoli, M., Kirov, P., Gugger, M. & Bassetti, C.L. 2007, "Central periodic breathing during sleep in acute ischemic stroke", *Stroke; a journal of cerebral circulation*, vol. 38, no. 3, pp. 1082-1084.
- Hill, A. 1910, "The possible effects of the aggregation of the molecules of haemoglobin on its dissociation curves", *Journal of Physiology*, vol. 40, pp. iv.
- Kaiser, G. 1994, *A Friendly Guide to Wavelets*, Birkhäuser.
- Kelly, D.H. & Shannon, D.C. 1979, "Periodic breathing in infants with near-miss sudden infant death syndrome", *Pediatrics*, vol. 63, no. 3, pp. 355-360.
- Kelly, D.H., Walker, A.M., Cahen, L. & Shannon, D.C. 1980, "Periodic breathing in siblings of sudden infant death syndrome victims", *Pediatrics*, vol. 66, no. 4, pp. 515-520.
- Khan, A., Qurashi, M., Kwiatkowski, K., Cates, D. & Rigatto, H. 2005, "Measurement of the CO₂ apneic threshold in newborn infants: possible relevance for periodic breathing and apnea", *Journal of applied physiology (Bethesda, Md.: 1985)*, vol. 98, no. 4, pp. 1171-1176.

- Khoo, M., Kronauer, R.E., Strohl, K.P. & Slutsky, A.S. 1982, "Factors inducing periodic breathing in humans: a general model", *Journal of applied physiology*, vol. 53, no. 3, pp. 644-659.
- Kirkpatrick, S.E., Pitlick, P.T., Naliboff, J. & Friedman, W.F. 1976, "Frank-Starling relationship as an important determinant of fetal cardiac output", *The American Journal of Physiology*, vol. 231, no. 2, pp. 495-500.
- Lange, R.L. & Hecht, H.H. 1962, "The mechanism of Cheyne-Stokes respiration", *The Journal of clinical investigation*, vol. 41, pp. 42-52.
- Lee, H., Rusin, C.G., Lake, D.E., Clark, M.T., Guin, L., Smoot, T.J., Paget-Brown, A.O., Vergales, B.D., Kattwinkel, J., Moorman, J.R. & Delos, J.B. 2012, "A new algorithm for detecting central apnea in neonates", *Physiological Measurement*, vol. 33, no. 1, pp. 1-17.
- Levine, M., Hathorn, M. & Cleave, J. 2004, "Mathematical methods in the study of respiration in newborn babies", *Cardiovascular Engineering: An International Journal*, vol. 4, no. 2, pp. 133-138.
- Lieber, C. & Mohsenin, V. 1992, "Cheyne-Stokes respiration in congestive heart failure", *The Yale journal of biology and medicine*, vol. 65, no. 1, pp. 39-50.
- Manisty, C.H., Willson, K., Wensel, R., Whinnett, Z.I., Davies, J.E., Oldfield, W.L., Mayet, J. & Francis, D.P. 2006, "Development of respiratory control instability in heart failure: a novel approach to dissect the pathophysiological mechanisms", *The Journal of physiology*, vol. 577, no. 1, pp. 387-401.
- Martin, R.J., Abu-Shaweesh, J.M. & Baird, T.M. 2004, "Apnoea of prematurity", *Paediatric respiratory reviews*, vol. 5, pp. S377-S382.
- Milhorn, H.T. & Guyton, A. 1965, "An analog computer analysis of Cheyne-Stokes breathing", *Journal of applied physiology*, vol. 20, no. 2, pp. 328-333.
- Mohr, M.A., Fairchild, K.D., Patel, M., Sinkin, R.A., Clark, M.T., Moorman, J.R., Lake, D.E., Kattwinkel, J. & Delos, J.B. 2015a, "Quantification of periodic breathing in premature infants", *Physiological Measurement*, vol. 36, no. 7, pp. 1415.
- Mohr, M.A., Vergales, B.D., Lee, H., Clark, M.T., Lake, D.E., Mennen, A.C., Kattwinkel, J., Sinkin, R.A., Moorman, J.R., Fairchild, K.D. & Delos, J.B. 2015b, "Very long apnea events in preterm infants", *Journal of applied physiology* (Bethesda, Md.: 1985), vol. 118, no. 5, pp. 558-568.
- Neu, J. & Walker, W.A. 2011, "Necrotizing enterocolitis", *New England Journal of Medicine*, vol. 364, no. 3, pp. 255-264.
- Norman, R.G., Goldring, R.M., Clain, J.M., Oppenheimer, B.W., Charney, A.N., Rapoport, D.M. & Berger, K.I. 2006, "Transition from acute to chronic hypercapnia in patients with periodic breathing: predictions from a computer model", *Journal of applied physiology* (Bethesda, Md.: 1985), vol. 100, no. 5, pp. 1733-1741.
- Oken, E., Kleinman, K.P., Rich-Edwards, J. & Gillman, M.W. 2003, "A nearly continuous measure of birth weight for gestational age using a United States national reference", *BMC pediatrics*, vol. 3, pp. 6.
- Oliveira, A.J., Nunes, M.L., Fojo-Olmos, A., Reis, F.M. & da Costa, J.C. 2004, "Clinical correlates of periodic breathing in neonatal polysomnography", *Clinical neurophysiology*, vol. 115, no. 10, pp. 2247-2251.

- Pereira, M., Reis, F., Landriault, L., Cates, D. & Rigatto, H. 1995, "Profile of alveolar gases during periodic and regular breathing in preterm infants", *Neonatology*, vol. 67, no. 5, pp. 322-329.
- Poets, C.F. & Southall, D.P. 1991, "Patterns of oxygenation during periodic breathing in preterm infants", *Early human development*, vol. 26, no. 1, pp. 1-12.
- Price, J.F. 2011, "Unique aspects of heart failure in the neonate" in *Heart Failure in Congenital Heart Disease*: Springer, , pp. 21-42.
- Rapoport, D.M., Norman, R.G. & Goldring, R.M. 1993, "CO₂ homeostasis during periodic breathing: predictions from a computer model", *Journal of applied physiology (Bethesda, Md.: 1985)*, vol. 75, no. 5, pp. 2302-2309.
- Razi, N.M., DeLauter, M. & Pandit, P.B. 2002, "Periodic breathing and oxygen saturation in preterm infants at discharge", *Journal of perinatology : official journal of the California Perinatal Association*, vol. 22, no. 6, pp. 442-444.
- Rebuck, A., Slutsky, A. & Mahutte, C. 1977, "A mathematical expression to describe the ventilatory response to hypoxia and hypercapnia", *Respiration physiology*, vol. 31, no. 1, pp. 107-116.
- Richerson, G.B. & Boron, W.F. 2005, "Control of Ventilation" in *Medical Physiology*, eds. W.F. Boron & E.L. Boulpaep, 2nd edn, Elsevier Health Sciences, , pp. 716.
- Rigatto, H. 2003, "Periodic Breathing" in *Respiratory Controls and Disorders In The Newborn*, ed. O.P. Mathew, CRC Press, , pp. 266.
- Sands, S.A., Edwards, B.A., Kelly, V.J., Davidson, M.R., Wilkinson, M.H. & Berger, P.J. 2009, "A model analysis of arterial oxygen desaturation during apnea in preterm infants", .
- Schnabl, K.L., Van Aerde, J.E., Thomson, A.B. & Clandinin, M.T. 2008, "Necrotizing enterocolitis: a multifactorial disease with no cure", *World journal of gastroenterology : WJG*, vol. 14, no. 14, pp. 2142-2161.
- Severinghaus, J. & Crawford, R. 1978, "Regulation of respiration.", *Acta Anaesthesiol Scand Suppl.*, .
- Severinghaus, J.W. 1979, "Simple, accurate equations for human blood O₂ dissociation computations", *Journal of applied physiology: respiratory, environmental and exercise physiology*, vol. 46, no. 3, pp. 599-602.
- Simakajornboon, N., Beckerman, R.C., Mack, C., Sharon, D. & Gozal, D. 2002, "Effect of supplemental oxygen on sleep architecture and cardiorespiratory events in preterm infants", *Pediatrics*, vol. 110, no. 5, pp. 884-888.
- Southall, D., Levitt, G., Richards, J., Jones, R., Kong, C., Farndon, P., Alexander, J. & Wilson, A. 1983, "Undetected episodes of prolonged apnea and severe bradycardia in preterm infants", *Pediatrics*, vol. 72, no. 4, pp. 541-551.
- Stoll, B.J., Hansen, N., Fanaroff, A.A., Wright, L.L., Carlo, W.A., Ehrenkranz, R.A., Lemons, J.A., Donovan, E.F., Stark, A.R. & Tyson, J.E. 2002, "Late-onset sepsis in very low birth weight neonates: the experience of the NICHD Neonatal Research Network", *Pediatrics*, vol. 110, no. 2, pp. 285-291.
- Strueby, L. & Thebaud, B. 2014, "Advances in bronchopulmonary dysplasia", *Expert review of respiratory medicine*, vol. 8, no. 3, pp. 327-338.

- Takahashi, E. & Doi, K. 1993, "Destabilization of the respiratory control by hypoxic ventilatory depressions: a model analysis.", *The Japanese journal of physiology*, vol. 43, no. 5, pp. 599-612.
- Tehrani, F.T. 1997, "A model study of periodic breathing, stability of the neonatal respiratory system, and causes of sudden infant death syndrome", *Medical engineering & physics*, vol. 19, no. 6, pp. 547-555.
- Vergales, B.D., Paget-Brown, A.O., Lee, H., Guin, L.E., Smoot, T.J., Rusin, C.G., Clark, M.T., Delos, J.B., Fairchild, K.D., Lake, D.E., Moorman, R. & Kattwinkel, J. 2014, "Accurate automated apnea analysis in preterm infants", *American Journal of Perinatology*, vol. 31, no. 2, pp. 157-162.
- Verma, V.K., Katiyar, V. & Singh, M. 2009, "Study of periodic breathing and human respiratory system", *International Journal of Medicine and Medical Sciences*, vol. 1, no. 8, pp. 330-333.
- Vielle, B. & Chauvet, G. 1993a, "Cyclic model of respiration applied to asymmetrical ventilation and periodic breathing", *Journal of Biomedical Engineering*, vol. 15, no. 3, pp. 251-256.
- Vielle, B. & Chauvet, G. 1998, "Delay equation analysis of human respiratory stability", *Mathematical biosciences*, vol. 152, no. 2, pp. 105-122.
- Vielle, B. & Chauvet, G. 1993b, "Mathematical study of periodic breathing as an instability of the respiratory system", *Mathematical biosciences*, vol. 114, no. 2, pp. 149-172.
- Weintraub, Z., Alvaro, R., Kwiatkowski, K., Cates, D. & Rigatto, H. 1992, "Effects of inhaled oxygen (up to 40%) on periodic breathing and apnea in preterm infants", *J Appl Physiol*, vol. 72, no. 1, pp. 116-120.
- Wijdicks, E.F. 2007, "Biot's breathing", *Journal of neurology, neurosurgery, and psychiatry*, vol. 78, no. 5, pp. 512-513.
- Wilkinson, M., Cranage, S., Berger, P., Blanch, N. & Adamson, T. 1995, "Changes in the temporal structure of periodic breathing with postnatal development in preterm infants", *Pediatric research*, vol. 38, no. 4, pp. 533-538.